# Thyroid Hormone Receptor Nucleocytoplasmic Transport

Jibo Zhang
Williamsburg, VA

Bachelor of Science, Department of Biology
Florida Institute of Technology, 2013

A Thesis Presented to the Graduate Faculty
of the College of William and Mary in Candidacy for the Degree of

Master of Science

Department of Biology

The College of William and Mary
August, 2016

# APPROVAL PAGE

The thesis is submitted in partial fulfillment of the requirements for the degree of

Master of Science

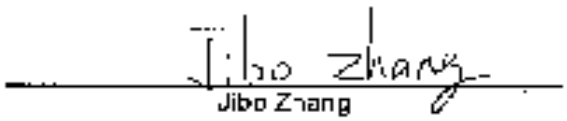

Jibo Zhang

Approved by the Committee, August 2016

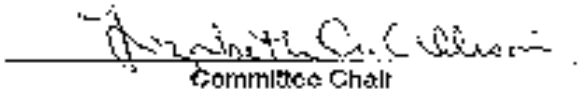

Committee Chair
Professor Lizabeth A. Allison, Biology
The College of William and Mary

Professor Patty Zwollo, Biology
The College of William and Mary

Professor Diane Shakes, Biology
The College of William and Mary

# COMPLIANCE PAGE

Research approved by:

Institutional Biosafety Committee

Protocol number: IBC-2014-01-10-9227-laalli

Date(s) of approval: 01-30-2014

01-30-2015

01-30-2016

# ABSTRACT

The thyroid hormone receptor α1 (TRα1) and the thyroid hormone receptor β1 (TRβ1) are transcription factors that modulate the expression of target genes that are important in metabolism and development in response to thyroid hormone. Although primarily localized to the nucleus, prior studies have shown that TRα1 and TRβ1 shuttle rapidly between the nucleus and cytoplasm, and that nuclear import of TR$\alpha$1 is directed by two nuclear localization signal (NLS) motifs: NLS-1 in the hinge domain, and NLS-2 in the N-terminal A/B domain. In contrast, TR$\beta$1 lacks NLS-2. Previous studies also characterized two nuclear export signal (NES) motifs, NES-H3/H6 and NES-H12, that reside in the ligand-binding domain and mediate TR nuclear export. Here, we investigated which importins mediate nuclear import of TR$\alpha$1 using a combined approach of shRNA-mediated knockdown and coimmunoprecipitation assays in HeLa (human) cells. Among all the importins we tested in transient transfection assays (importins 4, 5, 6, 7, 8, 9, 13, importin β1, and adaptor importin α variants), only importin 7, importin β1, and adaptor importin α1 knockdown experiments resulted in a significant localization pattern change from primarily nuclear to a more cytosolic distribution of TRα1. To demonstrate direct interaction between TRα1 or TRβ1 and the importins, “GFP-trap” co-immunoprecipitation assays were performed. Importin 7, importin β1, and adaptor importin α1 were shown to interact with TRα1, while importin 4 as a negative control, did not. Our data show that nuclear entry of TR$\alpha$1 in HeLa cells is facilitated by both importin 7, likely through interactions with NLS-2, and importin $\beta$1 and the adapter importin $\alpha$1 interacting with NLS-1 and NLS-2. In contrast, TR$\beta$1 nuclear import is facilitated only by importin $\alpha$1/$\beta$1 interacting with NLS-1. Prior results from knockdown and overexpression studies provided evidence that multiple exportins influence TR localization. Here, we investigated which exportins serve as a direct carrier for each of the multiple NES motifs in TR$\alpha$1, using GFP-trap assays. Consistent with our prior studies, results show protein-protein interactions between TRα1 and exportin4, exportin5, and exportin7, but not with exportin6. Taken together, our findings highlight a fine balance of nuclear import, retention, and export that modulates TR function.

# TABLE OF CONTENTS

# ACKNOWLEDGEMENTS

I have always wondered why my thesis advisor Dr. Lizabeth Allison accepted me three years ago, since my undergraduate GPA was not outstanding and I did not have any research experience by then. After I passed my comprehensive exam in May 2014, she finally revealed her reason “because I saw the potential. I was willing to take the chance, and I haven’t regretted it ever since”. Dr. Allison gave me a chance that no one else would ever do. She lightened my future and helped me realize how much I love science. From an insecure undergraduate international student to a confident PhD candidate, this amazing transition would never happen without Dr. Allison’s selflessness and complete trust.

I would also like to thank Dr. Diane Shakes and Dr. Patty Zwollo for all their advice and long term support as my committee members. Thanks to Dr. Shantá Hinton and Dr. William Buchser for being great friends and helping me along my way to success. Last but not least, I would like to thank all my wonderful lab mates, especially Cyril Anyetei-Anum and Yazdi Doshi for providing such a great research environment. A big shout out to Vinny Roggero and Rose Dziedzic. You are my family who I learned everything from.

# LIST OF TABLES

# LIST OF FIGURES

## Chapters 1 and 2 Figures



## Chapter 3 Figures

## Chapter 1: General Introduction

Thyroid hormones (THs) affect a wide variety of tissues, and have major influences on metabolic efficiency, thermogenesis and energy expenditure (Yeshuda-Shnaidman et al., 2013). THs also play a role in the development of muscles, liver tissue, brain tissue, and others (Chavez et al., 1998). It is safe to say that every single cell in our body is, or has been, influenced by THs.

Thyroid hormone regulates gene expression by binding with the thyroid hormone receptor (TR), a ligand-dependent transcription factor. TR is expressed as different variants (TRα1, TRα2, TRα3, TRβ1, TRβ2, TRβ3) in different tissues (Schapira et al., 2003). These variants are closely related to each other. TRα1, TRα3 and TRα3 are the results of alternative splicing of TRα mRNA which is encoded on chromosome 17. TRβ1, TRβ2 and TRβ3, on the other hand, are encoded by a separate gene on chromosome 3, and result from alternative promoter usage (Wood et al., 1994). Each isoform can form either homodimers or heterodimers with retinoid X receptors on thyroid hormone response elements (TREs) to repress gene expression when TH is absent. When cells are exposed to TH, TRs (except for TRα2 which does not bind ligand) bind with TH, and promote gene expression by recruiting coactivators. Unlike steroid hormone receptors which are sequestered in the cytosol and translocate to the nucleus in response to ligand, TRs are primarily nuclear localized both in the presence and absence of ligand. An interesting phenomenon, discovered by Bunn et al. (2001) is that TRα1 shuttles between the nucleus and the cytoplasm. Since the molecular weight of TRα1 is about 46 kD, which is larger than the limit for diffusion through the nuclear pore complexes (NPCs), the process of TRα1 crossing the nuclear envelope must be mediated by transport factors,

called karyopherins (Steward, 2007). Karyopherins that transport proteins into the nucleus are called importins, while those that transport proteins back to the cytoplasm are called exportins.

The National Center for Biotechnology Information (NCBI) indicates that more than 18 importins and 6 exportins are encoded in the human genome (Okada et al., 2008). Each of them overlaps in function, meaning a cargo can be transported by multiple importins or exportins. Elucidating the specific transport factors that are responsible for the shuttling of TR is of fundamental importance because of the receptor's direct influence on thyroid hormone regulatory functions. Another important factor is the "signals" that determine the interaction between TR and importins and exportins. In this case, prior studies have shown that TRα1 has two nuclear localization signals (NLSs) and least three nuclear export signals (NESs) for importin and exportin recognition, respectively (Mavinakere et al., 2012). In contrast, TRβ1 only has one NLS Therefore, it is of interest to determine which NLS or NES of TR interacts specifically with which importin(s) or exportin(s).

The main goal of this thesis research was to determine which importins directly mediate the nuclear import process of TR. Additional work addressed which exportins directly mediate TRα1's nuclear export. RNA interference (RNAi)-based knockdown of specific importins, analysis of TR distribution by fluorescence microscopy, and "GFP-trap" coimmunoprecipitation assays were the main approaches used in the thesis. A detailed review of the literature on THs, TRs, transport factors, and the main experimental approaches are provided in the following sections and in Chapter 2.

## Thyroid Hormone & Thyroid Hormone Receptors

## Thyroid Hormone (TH)

Thyroid hormones (THs) have major influences on development, growth, metabolic efficiency, thermogenesis and energy expenditure, and are involved in cross-talk with other hormones (Hikunguwo et al., 2007). TH disorders not only cause irregular development of brain tissues, muscles, bone structures and neuronal activity (Yeshuda-Shnaidman et al., 2013), but also are involved in the development of certain diseases like breast cancer (Onde et al., 2006). Without a doubt, THs influence every cell in our body.

Production of TH follows a tightly regulated positive feedback pathway from the hypothalamus to the pituitary to the thyroid gland (Furumoto et al., 2005) (Figure 1). The signal starts with the secretion of thyrotropin-releasing hormone (TRH) by the hypothalamus into the blood (Klieverik et al., 2009). TRH eventually travels to the pituitary gland and upregulates the secretion of thyroid stimulating hormone (TSH) (Wolf, 2002). TSH binds with the thyroid stimulating hormone receptor (a G protein-coupled receptor) on the thyroid gland epithelial cells, which contributes to the secretion of thyroglobulin—the precursor of THs (Linke et al., 2002). Thyroglobulin gets iodinated by a protein called thyroperoxidase (Haddow et al., 2010). The iodinated thyroglobulin includes two types of molecules, thyroglobulin with one iodine bound is called monoiodotyrosine (MIT), while thyroglobulin with two iodines is called diiodotyrosine (DIT) (Mansourian, 2011). The combination of one MIT and one DIT yields one molecule of triiodothyronine (T3), and a combination of two DIT produces one molecule of thyroxine (T4) (Dunn, 2001). Interestingly, T4 is entirely synthesized within the thyroid gland, while only a few percent of the total hormone produced by the thyroid gland is T3 (Senese et al., 2014). Based on

the fact that T3's activity is 10 times higher than T4's activity (Wawrzynska et al., 2003), and a large amount of T4 will be de-iodinated to T3 in tissues other than the thyroid (Braverman et al., 1970), T4 is viewed as the "pro-hormone" of T3. T4 also has a longer half-life time, meaning it is more stable than T3. In the circulatory system, 99.97% of total T4 and 99.7% of total T3 are bound with three different thyroid hormone carrying proteins—thyroxine-binding globulin (TBG), transthyretin (TTR), and human serum albumin (HAS) (Pappa et al., 2015). As the name indicates, TBG has the highest binding affinity to T4 in serum. Cell membrane transporters are essential for THs to enter the cytoplasm because of the cell membrane's relative impermeability towards THs (Cheng, et al., 2010). In addition, literature published by Yen (2001) and Bassett (2003) suggested the existence of a cell membrane receptor for TH (Davis et al., 2005). Recently, integrin αVβ3 was identified as a cell membrane receptor for TH (Bergh et al., 2005). Integrin αVβ3 is also known for regulating signal transduction pathways such as MAPK (D'Arezzo, et al., 2004), which means TH not only has genomic regulatory functions (performed through binding its nuclear receptor, TR) but also possesses non-genomic regulatory functions of activating cell signaling pathways.

As mentioned earlier, most T4 will be de-iodinated to T3 after it enters a target cell. This TH deiodination process is regulated by several deiodinase isoforms: deiodinase 1 (D1), deiodinase 2 (D2), and deiodinase 3 (D3) (Bianco et al., 2002). D1 and D2 are the enzymes that convert T4 to T3. The main difference between them is that they are expressed in different tissues. For example, D1 is expressed more in liver and kidney tissues and D2 activity is present in different muscles, brain, and brown adipose tissues

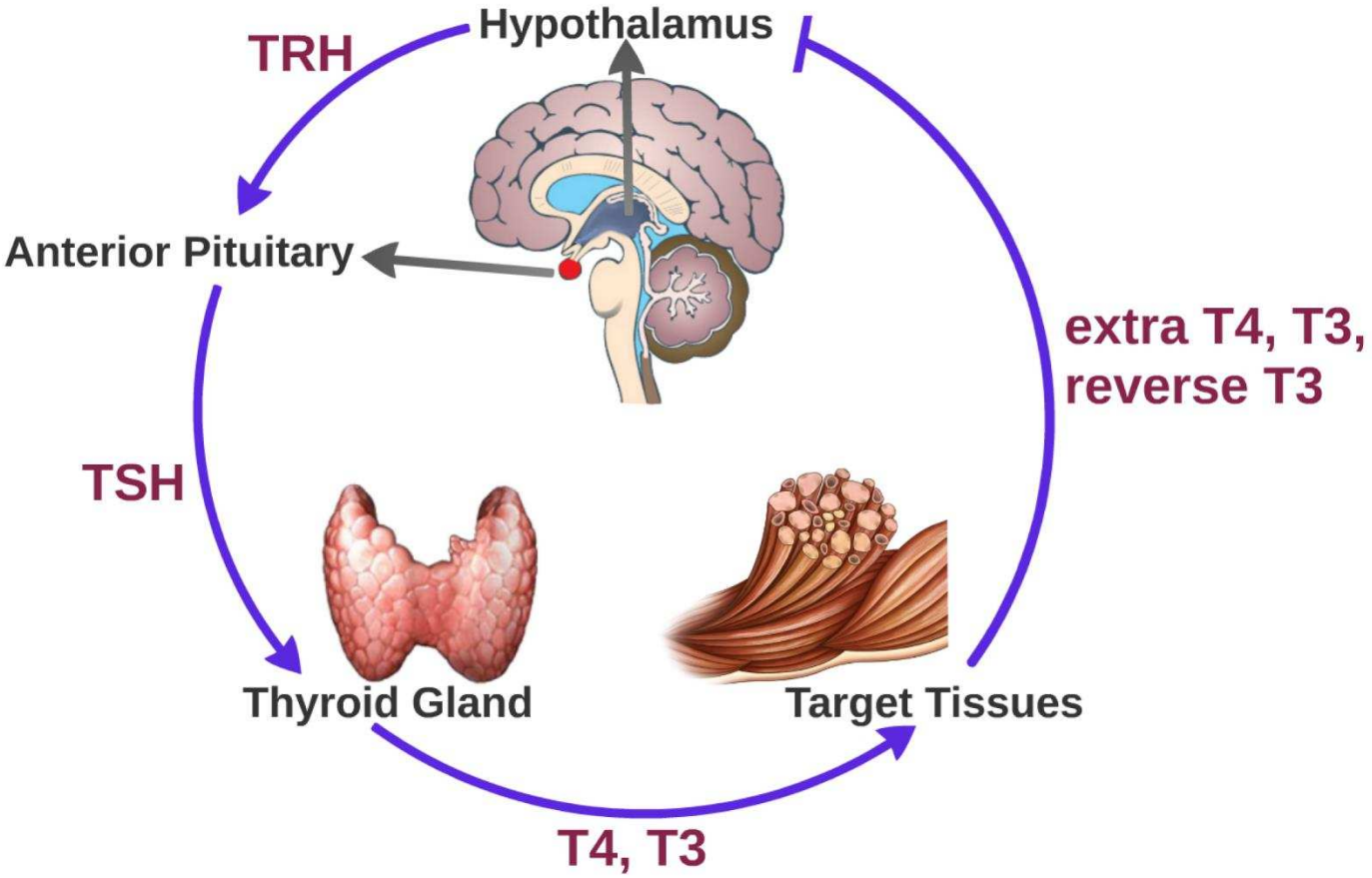


**Figure 1. Thyroid hormone regulation pathway.** The hypothalamus releases thyrotropin-releasing hormone (TRH) which has a positive influence on the anterior pituitary gland. The stimulation causes the synthesis of thyroid stimulating hormone (TSH). TSH acts on the thyroid gland which produces the thyroid hormones, T4 and T3. The amount of free thyroid hormone and T3's inactive form, reverse T3, give negative feedback to the anterior pituitary to downregulate this pathway (adapted from Razani, 2010).

(Pilo et al., 1990). D3, on the other hand, converts T3 to an inactive form termed reverse T3 (r-T3), which in turn maintains T3 homeostasis by downregulating its production (Bianco, 2011). It is interesting to note that both TH genomic and non-genomic functions are turned on and off by maintaining the T3/r-T3 balance via D3 deiodination (Gereben et al., 2008). It is safe to assert, however, that the TH pathway involves an extremely complicated and organized system, at the crux of which lies the thyroid hormone receptor.

## Nuclear Receptors

Outside of the nuclear receptor field, there is a common misconception that nuclear receptors and cell membrane receptors are similar. As a matter of fact, cell membrane receptors and nuclear receptors belong to a common receptor category but are totally different in their mechanism of action. The term “receptor” describes a protein that triggers a response when binding of a signal molecule causes the receptor to undergo a conformational change (Purves et al., 2001). For signal molecules that are impermeable to the membrane, cell membrane receptors will interact with them on the extracellular surface and activate a downstream signaling transduction cascade. When signal molecules are permeable to the cell membrane, or have specific transporter proteins, they cross the membrane and bind with intracellular receptors, called nuclear receptors, that are able to shuttle between the nucleus and cytoplasm. The nucleocytoplasmic shuttling property of nuclear receptors allows direct ligand-dependent gene regulation (Purves et al., 2001). Nuclear receptors are a superfamily of ligand-regulated transcription factors that are activated by steroid hormones (e.g., androgen, estrogen, progesterone), or other

ligands such as vitamin D and thyroid hormone (Sever and Glass, 2013). Four subtypes of nuclear receptors have been discovered so far. Receptors like androgen receptors and estrogen receptors are type 1 receptors. They are usually protected and anchored by chaperones in the cytoplasm (Echeverria and Picard, 2010). When the correct ligand binds with a type 1 receptor, the conformational change will cause the release of chaperones and then the exposure of a nuclear localization signal (NLS). The exposed NLS recruits importins to transport the ligand-receptor complex into the nucleus to activate gene transcription (Glass and Rosenfeld, 2000). In contrast, type 2 receptors, such as thyroid hormone receptors (TRs), are primarily located in the nucleus. When there is no ligand, they form either homodimers, or heterodimers with retinoid X receptor (RXR), on their DNA response elements to repress target gene transcription. Corepressors like NCoR and SMRT are recruited and help with the repressive function (Chen and Evans, 1995). The homodimers or heterodimers of type 2 receptors are dissociated from the corepressors in the presence of ligand, and coactivators are recruited by the ligand-receptor complex to promote gene transcription. Type 3 receptors have a similar function as type 1; type 4 receptors bind to half-site hormone response elements as monomers (Mangelsdorf et al., 1995). This thesis focuses on one group of type 2 receptors, the thyroid hormone receptors.

## Thyroid Hormone Receptors

As mentioned in the nuclear receptor section, in most cases, unliganded TRs repress target gene transcription while liganded TRs do the opposite (Chassande et al., 2003). The reason TRs are referred to as a group is because they are encoded by two separate genes: the α c-*erb*A gene on chromosome 17 encodes TRα; the β c-*erb*A gene

on chromosome 3 encodes TRβ (Lazar, 1993; Brent, 1994). Moreover, TRα and TRβ each has multiple isoforms (Figure 2). TRα's three isoforms (TRα1, TRα2, and TRα3) are generated by alternative splicing of the primary transcript of the α c-*erb*A gene (Hahm et al., 2014). Only TRα1 shows high affinity for T3, whereas TRα2 and TRα3 do not interact with any form of TH (Moran et al., 2014). TRβ isoforms (TRβ1, TRβ2, and TRβ3) are the result of alternative promoter usage within the β c-*erb*A gene (Williams, 2000; Tagami et al., 1998). These three isoforms' sequences are highly conserved, especially their DNA binding domain and ligand binding domain (Navarrete-Ramírez et al., 2014). Although TRα1 and TRβ1 are both ubiquitously present, the ratio of their expression in different tissues tends to vary (Sadow et al., 2003). For example, TRα1 is expressed dominantly in different muscle, bone and adipose tissues while TRβ1 is more expressed in liver, kidney, and brain tissues (Pascual and Aranda, 2013). A more detailed list of TRs' roles in different cell types is provided in Table 1. Although this thesis research primarily focused on TRα1, experiments on TRβ1 are also presented.

## Thyroid Hormone Response Elements

Since the critical importance of TH has been emphasized multiple times, it is not surprising that at least 100 genes in humans are TH responsive (Feng et al., 2000). TH-responsive genes have TH response elements (TREs) that function as enhancers or silencers. TREs are the DNA sequences to which TRs bind, and are usually located within the non-coding regions on the target DNA (Yen et al., 2006). There are a number of different TRE sequence motifs, which might explain how TR differentily modulates

transcription in various tissues (Hartong et al., 1994). Whether TR activates or represses gene transcription depends on the property of the TRE (Wu and Koenig, 2000). At a positive TRE, unliganded TR represses transcription but switches to activating transcription when T3 binds to it. At a negative TRE, unliganded TR promotes transcription whereas T3-bound TR is repressive.

## TRα1 Structure and Regulatory Activity

Much research has been conducted on the impact of different TR variants using TR knockout mice (Ribeiro et al., 2001). For example, TRα1 mostly regulates thermogenesis, while TRβ1 turns out to be essential for cholesterol metabolism (Wikstrom et al., 1998). However, the functional and expression level differences in various tissues do not mean that TR isoforms work in isolation. According to Tinnikov and coworkers' 2002 paper, both expression and activity of TRα1 arise after TRβ1 suppression, meaning there is interplay between the two dominant variants. TRα, TRβ and their isoforms share a common protein structure (Figure 2a). This common structure includes multiple functional regions: a less-conserved N-terminal A/B region, a highly conserved DNA binding domain, a short hinge region and a C-terminal ligand binding domain. The N-terminal A/B domain (NTD) contains a constitutive autonomous activation function 1 domian (AF-1), which is used to regulate transcription. Compared to the other domains, the NTD is the most divergent and less well-characterized (Thuestad et al., 2000). The NTD, however, contributes to transcriptional activation significantly through AF-1.

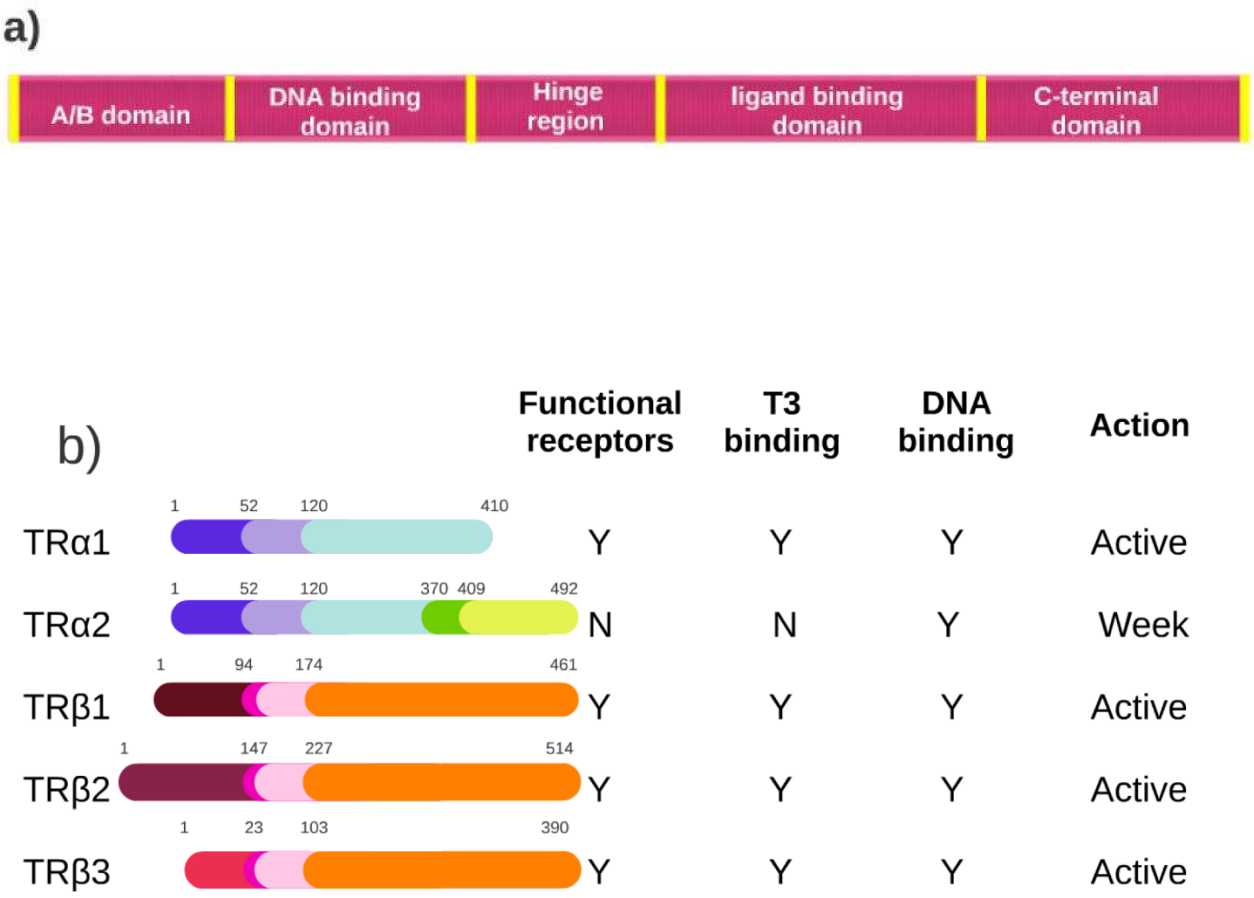


**Figure 2. TR isoforms and their general structure.** The general structure of thyroid hormone receptor's four functional domains is represented in a). Different TRα and TRβ isoforms are listed in b) (adapted from Bassett, 2003). Numbers indicate amino acid residues.

## Table 1. The role of TR in the development of selected cell types

| Cell type | Main receptor | Proliferation | Signaling pathways involved | Biological response |
|---|---|---|---|---|
| **Hepatocytes** | TRβ | + | Cyclin D1 | Liver hyperplasia |
| **Hepatocarcinoma cells** | TRα, TRβ | _ | PTTG1 | Cellular invasion |
| **Pancreatic β-cells** | TRβ | + | Cyclin D1/CDK/E2F | Cell proliferation |
| **Cardiomyocytes** | TRα | + | ANF/SERCA2/AKT | Contractility<br>Heart rate<br>Cardiac hypertrophy |
| **Skeletal muscle cells** | TRα | _ | MyoD | Myoblast differentiation |
| **Keratinocytes** | TRα, TRβ | + | Cyclin D1/STAT | Skin carcinogenesis<br>Epidermal proliferation |
| **Oligodendrocyte Precursors** | | _ | Cyclin D1/c-Myc | Oligodendrocyte maturation |
| **Neuroblastoma cells** | TRβ | _ | Cyclin D1/c-Myc | Morphological differentiation |
| **Photoreceptors** | TRβ | | Opsins | Retinal development |
| **Cochlear cells** | TRβ | | | Auditory function |
| **Chondrocytes** | TRα, TRβ | _ | Wnt/β-catenin | Bone maturation<br>Mineralization |

(Adapted from Pascual, 2013)

Furthermore, it has been documented that the NTD also regulates transcription activation through interacting with the ligand binding domain (Huber et al., 2003; Tian et al., 2006). An extremely exciting property of the NTD that needs to be mentioned for the sake of this thesis is that a novel nuclear localization signal, NLS-2, is found in this domain in TRα1, meaning that the NTD is also involved in nuclear import (Mavinakere et al., 2012).

The DNA binding domain (DBD) of most nuclear receptors is highly conserved with regard to both structure and sequence (Chen and Young, 2010) (Figure 3). At least 40% of the sequence (66 amino acids) is identical among all nuclear receptors (Gronemeyer, 1995). There are two zinc-binding motifs and two α-helices in the main region sequence (two zinc fingers). Each zinc-binding motif contains four conserved cysteine residues (Lee et al., 1993). The first zinc finger contains a P box that regulates TRα1-DNA interaction by binding with phosphate groups of a TRE's major groove (Oetting and Yen, 2007), whereas the D box of the second zinc finger binds to a TRE's minor groove. A charged C-terminal extension region (CTE), following the second zinc finger, regulates the DBD's interactions with other proteins as well as DNA (Zilliacus et al., 1995). The CTE has a short T box region at the very beginning. This T box region facilitates the dimerization of the TRα1-RXR heterodimer, which represses gene transcription when T3 is absent (Rastinejad et al., 1995).

TRα1's hinge domain (D domain) is a short bridge between the DBD and ligand binding domain (LBD) (Nascimento et al., 2006). Originally, the hinge domain was considered to be no more than a flexible rotation "joint" between the DBD and LBD that helps different nuclear receptors to mediate their conformations to adapt to different

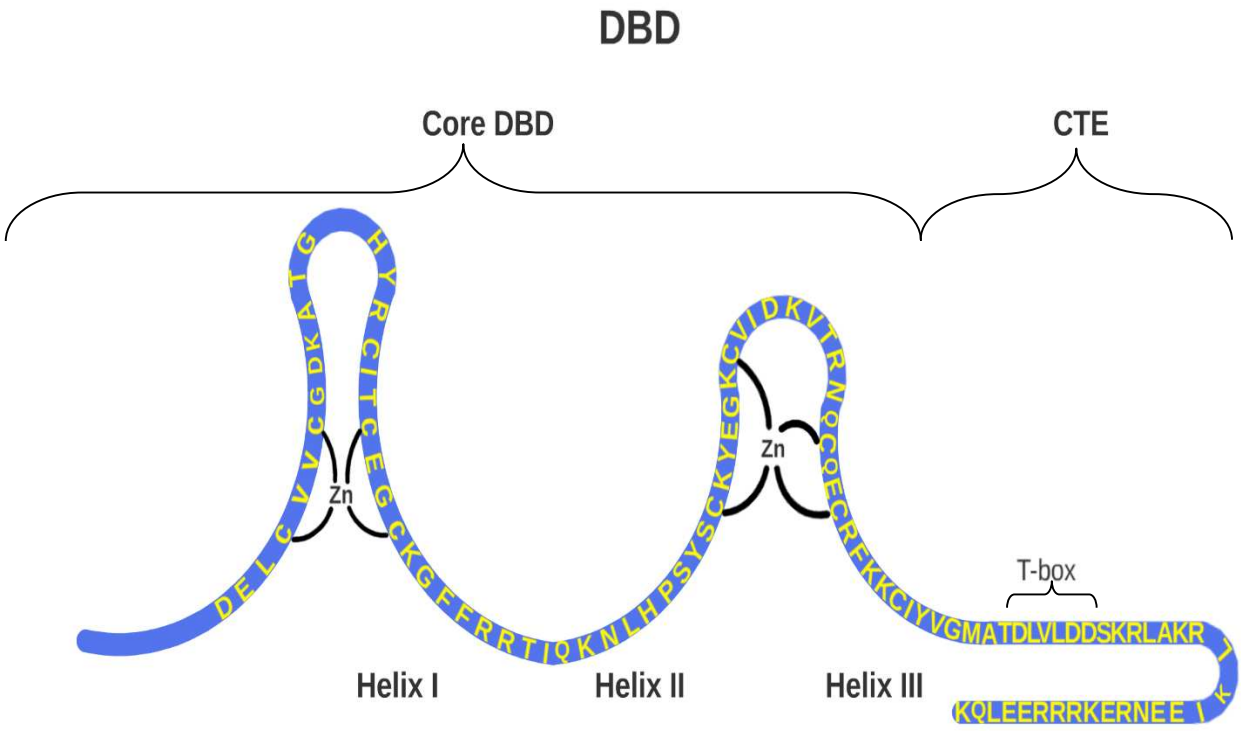


**Figure 3. TR DBD CTE structure.** A schematic diagram of the full-length TR and its DBD domain. The core sequence has two zinc-binding motifs and two α-helices. The C-terminal extension region (CTE) contains a T-box region (adapted from Chin, 2010).

response elements (Baniahmad et al., 1992).

However, more and more functional elements of the hinge domain have been proposed ever since. For example, Baniahmad et al.'s 1995 paper reported an activation element on TR's hinge domain, and a couple of sequences that appeared to be essential for efficient DNA binding. TR's hinge domain has also been suggested to be essential for TH-binding (Lin et al., 1991), and to have corepressor binding sites (Horlein et al., 1995). More importantly, the hinge domain contains a nuclear localization signal, NLS-1, that directs the nuclear import process (Mavinakere et al., 2012).

Recall that the AF-1 domain is located in the NTD. In addition, another ligand-dependent autonomous activation function domain, AF-2, is found in the C-terminal ligand binding domain (LBD) (Aranda et al., 2001). AF-2's crucial property of regulating transcriptional activation was confirmed by X-ray crystallography (Wurtz et al., 1996). TR's LBD is the most complex domain to study because of its various activities, including ligand binding, nuclear export, receptor dimerization and hormone-induced transcriptional activation or repression (Wu and Koenig, 2000). The LBD was suggested to have an essential role in mediating TR-RXR heterodimer or TR homodimer formation because of the conserved ninth heptad close to the C-terminus. The crystal structure of TRα1 revealed that the LBD contains twelve α-helices and a couple of β-turns, which is believed to fold into a hydrophobic binding pocket for ligand (Wagner et al., 1995). Among the twelve helices, helices 3 and 5 of unliganded TRα1 recruit corepressor proteins to suppress transcription (Bassett et al., 2003). The two major LBD recruited corepressors are nuclear receptor corepressor (NCoR) and silencing mediator of RAR and TR (SMRT). Besides their own inhibitory effects, NCoR and SMRT also recruit histone deacetylases,

which repress transcription by promoting chromatin condensation (Hu and Lazar, 1999). The TR-DNA-corepressor complex causes a non-permissive chromatin structure and inevitably inhibits the basal transcriptional machinery (Rosenfeld and Glass, 2001).

When T3 binds with the hydrophobic pocket, the LBD changes its conformation to rearrange the position of helix 12. This conformational change of helix 12, the AF-2 domain specifically, triggers the release of corepressors and generates a surface for coactivators to bind. One of the three nuclear export signals (NESs), NES-H12, overlaps with the AF-2 domain. SRC1 and p160, for example, are coactivators possessing histone acetyltransferase (HAT) activity that “opens” up chromatin for transcription. More coactivators that have HAT and histone demethylase activities will be recruited. Some crucial coactivators, such as TR associated proteins (TRAPs), might not possess HAT activity but are capable of regulating the binding of RNA polymerase II to a target gene’s promoter (Fondell et al., 1999). The existence of two distinct groups of coactivators (coactivators with HAT activity and coactivators without HAT activity) suggests that there are two steps for liganded TRα1 to promote transcription. First, the recruitment of coactivators with HAT activity (SRC1/p160) triggers chromatin modification. Second, after “opening up” DNA by chromatin remodeling, coactivators without HAT activity (TRAPs) are recruited to promote transcription by interacting with the basal transcription complex and RNA polymerase II. Although these two steps seem to be exclusive, the two groups of coactivators actually help each other like co-workers. For instance, other than remodeling chromosome structure by acetylating histones, HAT coactivators can also acetylate non-histone proteins such as the basal transcription factors TFIIE and TFIIF. This post-translational modification of TFIIE and TFIIF is crucial for the formation of the

basal transcription complex (Lee et al., 2003). Last, but not least, one of the LBD's activities that is related to this thesis is mediating TRα1 nuclear export. Multiple nuclear export signals have been discovered in the LBD of TRα1 (Mavinakere et al., 2012).

## Nucleocytoplasmic Transport

A eukaryotic cell has a nuclear envelope that serves as a defensive wall around the nucleus to maintain an intracellular compartmentalization. Important content such as DNA and nuclear proteins are strictly kept in the nucleus, while large cytoplasmic components are not allowed to freely enter. Proteins with a molecular mass of less than 40 kilodalton (kDa), however, can passively diffuse through the nuclear envelope, either from nucleus to cytoplasm or cytoplasm to nucleus (Cooper, 2000). Larger proteins that have important regulatory or structural functions in the nucleus need to be assisted to cross the nuclear envelope and, in some cases, to then return to the cytoplasm. This process is called nucleocytoplasmic transport. The following section provides a detailed review of each element involved in the nucleocytoplasmic transport pathway, including the nuclear envelope, nuclear pore complex, importins and exportins, and the energy source that drives the entire cycle.

## The "Wall" – The Nuclear Envelope

The nuclear envelope is a bilayer membrane made of phospholipids. The layer facing the cytoplasm is called the outer nuclear membrane (ONM), and the layer facing the nucleus is called the inner nuclear membrane (INM) (D'Angelo et al., 2006). The space between the membranes is called the perinuclear space, which is continuous with the rough endoplasmic reticulum (ER) through the ONM (Gerace and Burke, 1988). The

ONM provides binding sites for structural proteins in the cytoplasm, whereas the INM associates with the lamina and chromatin in the nucleus through membrane-associated proteins (Burke and Stewart, 2002). When you look at a eukaryotic cell, the nucleus is always positioned at a non-centered location. This specific location of the nucleus is essential for various cell activities, and is mediated by a conserved group of nuclear membrane proteins that are believed to be the ONM proteins (Padmakumar et al., 2004).

According to Murray and Davies's classic work in 1979, heterochromatin in the nucleus is tightly bound to the INM in mammalian cells. Much later evidence also established the existence of INM-associated regions of chromatin (Marshall, 2002). Studies have suggested that the INM is involved in the coordination of chromatin organization (Hochstrasser et al., 1986), which explains how chromosomes are separated from each other into their relatively "exclusive" territories (Razin et al., 2004). The lamina is a layer of intermediate filaments underneath the INM that maintains nuclear integrity (Holaska et al., 2003). The main component of the lamina is the lamin proteins, one of the three classes of proteins that interact with chromatin. The lamina layer functions as a "molecular shock absorber" (Dahl et al., 2004) that relieves the tension on the nuclear envelope (Hutchison et al., 2001) and, in turn, helps to maintain nuclear integrity.

## The "Gate" – The Nuclear Pore Complex

The nuclear envelope's two layers, the INM and ONM, are functionally different from each other but are linked by nuclear pore complexes (NPCs) as a whole. The NPC functions as the communicator between the cytoplasm and the nucleus (Sorokin et al.,

2007). The complex is about 60,000 kDa in vertebrates, and is an assembly of at least 30 different types of proteins called nucleoporins (D'angelo and Hetzer, 2006). Each type of nucleoporin has multiple copies, which brings the total protein number to 500-1000 per NPC (Cronshaw et al., 2002). The 30 types of nucleoporins can be divided into two classes: class one nucleoporins (usually form the NPC's cytoplasmic filaments) have FG repeats that are used to interact with transport factors; class two nucleoporins that lack FG repeats are the structural components of the NPC (Weis, 2002; Rout and Aitchison, 2001). Although the NPC is assembled from multiple copies of 30 types of nucleoporins encoded by a relatively small number of genes, each of them occupies multiple, distinct biochemical environments (Lin et al., 2016). The majority of the nucleoporins are distributed symmetrically, explaining the basket shape structure (Rout et al., 2001).

Nuclear receptors, soluble proteins, and RNAs are transported through the central channel of the NPC (Suntharalingam and Wente, 2003). When smaller proteins or ions passively diffuse through the NPC, they do not physically bind to the nucleoporins, and the diameter of the channel is only about 10 nm (Bustamante, 1993). Large proteins like TRα1 need to be brought to the NPC by transport factors. Cargo-bound transport factors interact with nucleoporins, which triggers the NPC channel to enlarge the diameter to 40 nm (Panté and Kann, 2002). This conformational change makes the transport process of large proteins much faster. Although it is possible for ions and smaller proteins to diffuse through the channel, most proteins are selectively blocked by the NPC. The selectivity could be explained by the presence of a group of hydrophobic nucleoporins lining the center of the NPC channel (Siebrasse and Peters, 2002). A very interesting fact about the NPC is that among all the nucleoporins there is no ATPase or GTPase. It means that

even though the NPC mediates the nucleocytoplasmic transport of large proteins, the energy for selective transport is neither provided by the transport factors nor by the NPC.

## The "Shuttle"—Transport Factors

As mentioned previously, small molecules and ions can passively diffuse though the NPC, but proteins bigger than 40 kDa need to be recognized and brought in to the nucleus by a group of cytosolic proteins called transport factors. Most of the macromolecules are transported by a group of evolutionarily conserved karyopherin-β family transport factors. Karyopherins that are in charge of importing cargo into the nucleus are called importins, whereas those that are in charge of exporting cargo back to the cytoplasm are exportins. Karyopherins have two major binding targets: they interact with macromolecular cargo, and they interact with nucleoporins (Soniat and Chook, 2015). Nuclear proteins that can be recognized by karyopherins contain nuclear localization signals (NLSs) and may also contain nuclear export signals (NESs). Those signals are within the protein's amino acid sequence. NLSs direct nuclear import by binding with importins while NESs direct nuclear export by interacting with exportins (Xu et al., 2010). Besides interacting with protein cargo, karyopherins also weakly bind to FG repeats in nucleoporins to bring the cargo to the NPC (Fung and Chook, 2014).

At least 20 β-family karyopherins have been identified in humans. They have similar molecular masses and all contain multiple HEAT repeats, but their sequences are 90% different from each other (O'Reilly et al., 2011). Each of them is able to transport a distinct group of cargo, but most proteins appear to utilize multiple karyopherins for transportation (Chook and Süel, 2011). This explains how such a small group of proteins

does the work of transporting millions of macromolecules. Among the 20 karyopherins, 11 are either importins that only import cargo into the nucleus or bidirectional transporters that also possess exportin function (Chook and Blobel, 2001). These karyopherins belong to the karyopherin-β family (Soniat and Chook, 2015), and mostly interact with their cargo directly. But some of them, importin β1 for example, require an adaptor protein called karyopherin-α (also known as importin α) to assist the cargo-recognizing process by binding with a classic NLS within the cargo polypeptide chain. Importin α acts as the mediator between karyopherin-β family importins and nuclear proteins, and is the most studied adapter importin (Conti et al., 1998). In the following content, all the importins will be referred to as "IPO + number." An interesting note is that although karyopherins shuttle proteins between the cytoplasmic and nuclear compartments, they do not necessarily determine the direction of transport. Which compartment the protein cargo stays in depends on the gradients of Ran GTP and Ran GDP.

## Karyopherin/Importinα (IPOα)

As an adaptor protein, IPOα interacts with IPOβ1 and recognizes protein cargo with a classical NLS to form the complete classical import complex. In other words, cargo that contains a classical NLS is imported by a IPOα-IPOβ1 heterodimer (Pemberton et al., 1998). Ever since the classical pathway was identified, many other different import pathways have been discovered. Compared to the classical NLS, which is made of one or two segments of basic residues (Pemberton et al., 1998), nonclassical NLSs directing other import pathways usually contain more diverse sequences and bind with other unidirectional karyopherin-β family importins directly. Although this indicates that IPOα

only works as a mediator for the indirect binding between cargo and IPOβ1, most proteins possess classical NLSs. Studies even suggest that IPOα and IPOβ1 have crucial regulatory functions in mitosis because they act as chaperones to protect the major factors involved (Gruss et al., 2001; Nachury et al., 2001; Wiese et al., 2001).

IPOα is composed of three structural units: a positively charged N-terminal domain that binds IPOβ1 (IBB domain), a central NLS-binding domain with 10 ARM repeats that recognizes a variety of classical NLSs, and a hydrophilic C-terminal domain (Chook and Blobel, 2001). IPOα's affinity for substrates is regulated by binding to IPOβ1 (Fanara et al., 2000). According to Moroianu et al. (1996), when IPOα is not binding with IPOβ1, a classical NLS-like sequence in the positively charged N-terminal domain binds to the ARM repeats of the NLS-binding domain which auto-inhibits the interaction with substrates. IPOβ1 binding to IPOα's N-terminal releases the ARM repeats, which explains why the IPOα-IPOβ1 heterodimer has a higher affinity for NLSs. When IPOα is released from IPOβ1 and cargo in the nucleus, a karyopherin-β family exportin called CAS (cellular apoptosis susceptibility) binds to the tenth ARM repeat and exports the free IPOα under a high Ran GTP concentration (Kutay et al., 1997). This export pathway is part of the IPOα-cargo dissociation mechanism since CAS binding and NLS binding are mutually exclusive (Herold et al., 1998).

Karyopherin-β family members are encoded by separate genes in all eukaryotes, whereas IPOα has at least seven family members (Pumroy and Cingolani, 2015). Human IPOα family members have more than 40% conservation and 26% identity in their sequences (Henikoff and Henikoff, 1992). The IPOα family is divided into three subfamilies, based on karyopherin nomenclature (Figure 4): α1 subfamily including IPOα1

and IPOα8; α2 subfamily including IPOα3 and IPOα4; and α3 subfamily including IPOα5, IPOα6, and IPOα7 (Pumroy and Cingolani, 2015). IPOα1 and IPOα8 of the α1 subfamily share 55% identity (Weis, et al., 1995). IPOα1, also known as SRP1 or Rch1, is considered to be the general adaptor importin for classical NLS containing cargo. Its mouse homologue, IPOα2, sharing 99.2% similarity to IPOα1, has been used in a variety of studies (Kobe, 1999). Since the other α1 subfamily member, IPOα8, was just recently discovered, only a little is known about it, besides being overexpressed in prostate cancer (Kelley et al., 2010; Laurila et al., 2014).

A year after the discovery of IPOα1, the α2 subfamily's two members, IPOα3 and IPOα4, were identified and put in the same group for their 86% identity (Takeda et al., 1997). However, even though these two proteins are almost identical, only IPOα3's crystal structure has been revealed very recently (Pumroy et al., 2015). Both IPOα3 and IPOα4 are known for their capacity of transporting important substrates like RCC1 (regulator of chromosome condensation 1) (Köhler et al., 1999), RanBP3, and transcription factor NF-κB (p50/p65) (Fagerlund et al., 2005). The last subfamily, including IPOα5, IPOα6, and IPOα7, is believed to be the earliest branched off group in evolution due to its yeast homologs (Mason et al., 2009). The three subfamily members share 74% identity, which makes it difficult to distinguish their functions. The only difference within the subfamily is that IPOα6 is strictly expressed in the testis (Köhler et al., 1997). Although determining their distinct cargo has not been realistic, important regulatory factors, such as phosphorylated STAT1 (signal transducer and activator of transcription 1), have been reported to use IPOα3 subfamily isoforms (Sekimoto et al., 1997).

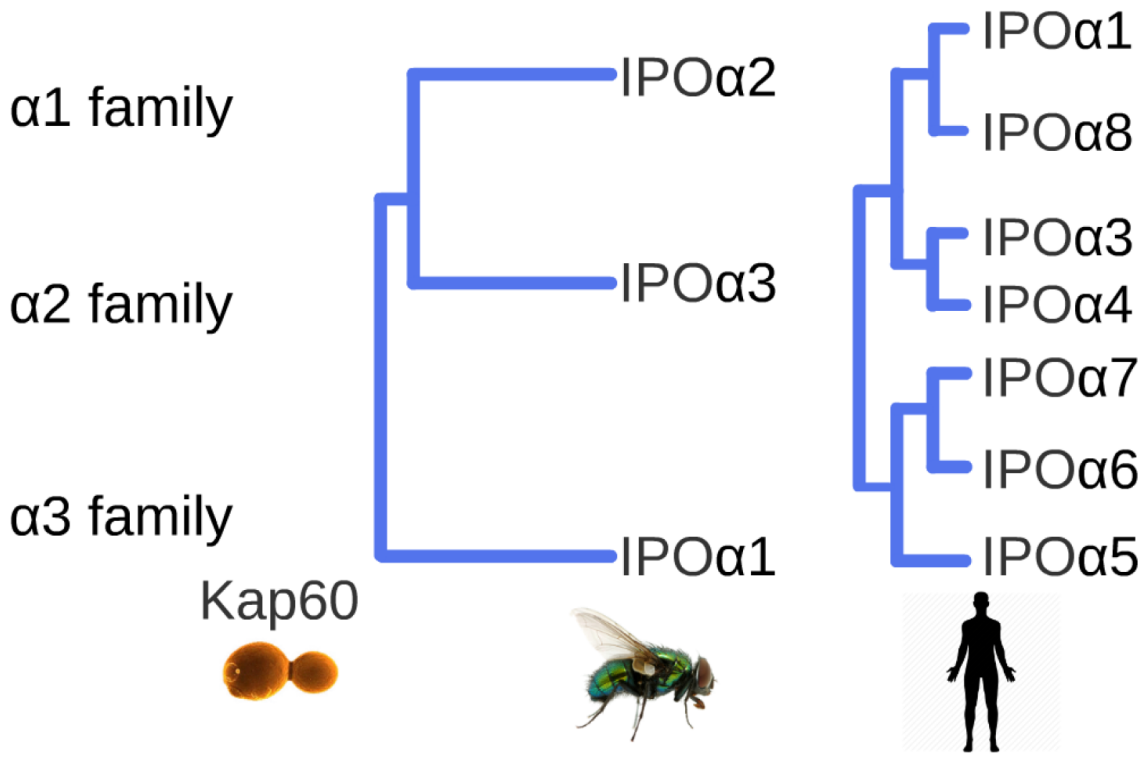


**Figure 4. Evolution of importin α.** The IPOα family is divided into three subfamilies: α1 subfamily including IPOα1 and IPOα8; α2 subfamily including IPOα3 and IPOα4; and α3 subfamily including IPOα5, IPOα6 and IPOα7. From left to right is a schematic diagram of the evolution of the importinα family in *Saccharomyces cerevisiae*, *Drosophila* sp. and *Homo sapiens* (adapted from Pumroy, 2015).

## Table 2. Alternative names of importin α isoforms.

| Subfamily | Protein names | Other names | Gene name |
|---|---|---|---|
| **α1** | IPOα1 | Karyopherin α2, Qip2, NPI-3 | KPNA2 |
| | IPOα8 | Karyopherin α7 | KPNA7 |
| **α2** | IPOα3 | Karyopherin α4, Qip1 | KPNA4 |
| | IPOα4 | Karyopherin α3, Qip2 | KPNA3 |
| **α3** | IPOα5 | Karyopherin α1, NPI-1 | KPNA1 |
| | IPOα6 | Karyopherin α5 | KPNA5 |
| | IPOα7 | Karyopherin α6, NPI-2 | KPNA6 |

## Table 3. Selected cellular cargoes specific to importin α isoforms.

| Import Cargoes | IPOα1 | IPOα3 | IPOα4 | IPOα5 | IPOα6 | IPOα7 | Import Cargoes | IPOα1 | IPOα3 | IPOα4 | IPOα5 | IPOα6 | IPOα7 |
|---|---|---|---|---|---|---|---|---|---|---|---|---|---|
| ADAR2 | - | | ++ | ++ | | | **Keap1** | - | - | - | - | - | ++ |
| ADAR2R | ++ | | - | - | | | **Kir** | - | - | - | ++ | - | - |
| ADAR3 | ++ | | - | - | | | **LSD1** | - | - | + | ++ | | ++ |
| AIRE | + | ++ | | ++ | | + | **Mycd** | - | - | | ++ | | |
| ARHI | ++ | ++ | | - | ++ | ++ | **NBS1** | ++ | - | | - | | |
| Arx | - | ++ | | ++ | - | - | **P50** | - | ++ | ++ | ++ | ++ | - |
| BRCA1 | ++ | | | | | | **P65** | ++ | - | - | - | - | - |
| BRMS1 | - | - | | | ++ | | **c-Rel** | - | - | - | ++ | ++ | ++ |
| Brn2 | - | - | | ++ | | | **P52** | - | ++ | ++ | ++ | ++ | - |
| Cby | + | ++ | | ++ | ++ | | **RelB** | - | - | - | ++ | ++ | ++ |
| CIC | - | - | ++ | - | - | - | **Notch** | - | ++ | ++ | - | - | ++ |
| CREB2 | - | - | - | ++ | | ++ | **NUCKS** | - | ++ | | ++ | | |
| Daxx | - | ++ | - | - | - | - | **Oct6** | - | ++ | | ++ | | |
| DGK | - | ++ | | ++ | | | **Orc6** | - | - | - | | | |
| DNA Helicase | ++ | ++ | | + | | | **P27** | - | ++ | | ++ | | |
| DYRK4 | - | ++ | | ++ | | | **P53** | - | ++ | | - | - | - |
| E47 | ++ | ++ | - | - | | | **PABPC** | - | | | | | |
| Endostatin | ++ | - | | - | | - | **Par3** | - | - | ++ | - | | - |
| FGF1 | | | | | | | **PARP-2** | + | ++ | | + | | |
| GLUT2 | ++ | | | - | | | **PKM2** | - | - | - | ++ | | - |
| GlyR | | ++ | ++ | | | | **RAC3** | - | ++ | - | - | - | - |
| hnRNP | - | ++ | ++ | ++ | ++ | ++ | **RanBP3** | - | ++ | ++ | - | - | - |
| HuR | ++ | - | - | - | | - | **Rcc1** | - | ++ | ++ | - | - | - |
| IRF-1 | ++ | | | | | | **RNA helicase** | ++ | ++ | - | - | - | - |
| IRF-9 | - | ++ | ++ | - | - | + | **SET** | - | ++ | + | - | - | - |
| Itk | ++ | | | | - | | **Pstat1** | - | | | ++ | | |
| JNK1 | ++ | - | | - | | | **Pstat2** | - | - | | ++ | | - |

(Adapted from Pumroy, 2015)

## Karyopherin-β family

Twenty β family karyopherins have been identified in humans. All β karyopherins' molecular masses are between 90 to 150 kDa. They share low sequence identity but the helical HEAT repeats are conserved (Chook and Süel, 2011). As mentioned earlier, 11 out of the 20 human β family karyopherins can import proteins into the nucleus. They are either unidirectional importins (IPOβ1, IPOβ2, IPO4, IPO5, IPO7, IPO8, IPO9, IPO11, IPO13) that each serves a specific set of cargos, or bidirectional transporters (Trn-SR and exportin 4) possessing export function. Besides IPOβ1 which requires the adaptor protein IPOα to import cargos, the rest of the unidirectional IPOs bind to their cargo's nonclassical NLS directly without forming heterodimers with IPOα, due to their Ran-binding domains (Kortvely et al., 2005).

IPOβ2 is the only importin that requires simultaneous binding with both nucleoporins and cargo (Bonifaci et al., 1997). Numerous mRNA binding proteins and nuclear proteins are imported by IPOβ2 specifically (Lee et al., 2006), which indicates that IPOβ2 recognizes a diverse set of non-classical NLSs. The term PY-NLS was given to all the NLSs that bind IPOβ2, based on the fact that they share common biochemical and structural characteristics while being completely different from each other (Lee et al., 2006). Since a PY-NLS contains either a N-terminal hydrophobic motif or a N-terminal basic motif, PY-NLSs are divided into hydrophobic or basic subclasses. This explains how IPOβ2 is able to recognize the basic and hydrophobic cargos that are chemically diverse (Cansizoglu et al., 2007).

Compared to the divergent cargo imported by IPOβ2, IPO4's target set is relatively unexplored. Only four protein cargos have been identified so far: ribosomal protein (rPS3a), vitamin D receptor (VDR), hypoxia-inducible factor (HIF1-α), and transition protein 2. The common property is that they are all basic proteins (Chachami et al., 2009; Jäkel et al., 2002). Since the mechanism of binding between IPO4 and cargo is unclear, it is highly possible that these four proteins use other importins for transport as well. For example, Chachami and coworkers' 2009 paper indicates that IPO7 is also involved in the import of HIF1-α. The yeast homolog of IPO4, Kap123p, is the second choice for many cargos that are originally imported by yeast Kap121p (Quan et al., 2008), whereas some proteins that are Kap123p-specific use Kap121p as a backup plan. Yeast Kap121p is the homolog of human IPO5's homolog in human (Leslie et al., 2004). Therefore, it is possible that IPO4 and IPO5 have similar characteristics, and might have overlap with each other's cargo sets. Like its yeast homolog, IPO5 also imports core histone proteins (Mühlhäusser et al., 2001). Twenty different types of cargo have been reported but only a few of them are IPO5 specific, such as transcription regulator PGC7/Stella (Heese et al., 2004; Nakamura et al., 2007).

IPO7 caught scientists' attention not only because of its tremendous cargo pool but also for the fact that it is so far the only known β-family karyopherin that can import cargos by interacting with another karyopherin, IPOβ1. The IPO7-IPOβ1 heterodimer has been reported to import cargos such as linker histone H1 (Jäkel et al., 2002), human immunodeficiency virus 1 (HIV-1) integrase (Zaitseva et al., 2002), and Adenovirus core protein pVII (Wodrich et al., 2006).

There is a large number of proteins that are primarily transported by IPO7, such as the zinc finger protein (EZI) (Saijou et al., 2007), ERK-2 kinase, Smad3 (Chuderland et al., 2008), histone core proteins (Mühlhäusser et al., 2001), HIV-1 reverse transcription complex (RTC) (Zaitseva et al., 2002), and proline-rich homeodomain (PRH) (Ploski et al., 2004). IPO7 not only recognizes various conformational epitopes such as certain zinc fingers, PAS domains (Chachami et al., 2009) and leucine-zipper domains (Waldmann et al., 2007), but also interacts with diverse linear recognition epitopes. Moreover, the fact that IPO7 imports the HIV-1 RTC supports the idea that eukaryotic cells use IPO7-dependent transport pathway to uptake endogenous and exogenous DNA (Dhanoya et al., 2013).

IPO8 is quite similar to IPO7. They share 68% identity, which makes them the most identical relative to other karyopherin pairs (Chook and Süel, 2011). IPO8 has not yet been extensively explored. No NLS specific for IPO8 recognition has been determined yet. Although proteins such as Smad3, Smad4, Argonaut protein 2 (Ago2) (Weinmann et al., 2009), and Signal recognition particle protein 19 (SRP19) (Dean et al., 2001) can to be imported by IPO8, most of them are primarily imported by other importins.

IPO9 is also responsible for importing a large number of cargos. Examples are hepatocellular carcinoma-associated protein (Jäkel et al., 2002), Aristaless (Arx) (Lin et al., 2009), c-Jun (Waldmann et al., 2007), PP2A (Lubert and Sarge, 2003), and the histone core proteins H2A, H2B, H3, and H4 (Baake et al., 2001). Although the NLSs of IPO9's cargos appear to be quite different from each other, the common characteristic

## Table 4. Nuclear import cargos of IPO4, IPO5, IPO7, IPO 7/β1, IPO8, IPO9, IPO11, and IPO13

| IPO 4 Cargo | NLS Location | Other importins that could also be used | IPO 5 Cargo | NLS Location | Other importins that could also be used |
|---|---|---|---|---|---|
| Vitamin D receptor | Residues 4-232 | | P60TRP | | |
| TP2 | Residues 87-95 | | Rag-2 | Residues 439-527 | |
| HIF1-α | | IPO7 | PGC7/Stella | | |
| Rps3A | | IPO β1/7; IPO 5 | Apolipoprotein A-1 | Residues 149-243 | |
| | | | Influenza A PB1-PA | | |
| **IPO 7/β1 Cargo** | **NLS Location** | **Other importins that could also be used** | RL13 | | |
| HIV-1 Integrase | Residues 4–232 | IPO α1/β1 | HPV16/18 L2 | N-terminal basic | IPO α1/β1 |
| Adenovirus core protein pVII | Residues 82–198 | IPO α1/β1; IPO 7; IPO β1 | CDK5 activator p35 | Residues 31-98 | IPO 7; IPO β1 |
| H1 | Full length protein | | C-Jun | Residues 250-334 | IPO 7; IPO β1; IPO 9 |
| rPL6 | | IPO β1; IPO 9; IPO 7 | HIV-1 Rev | Residues 35-46 | IPO β1 |
| rPS3a | | IPO 4; IPO5 | Rps7 Rpl5 Rps3a | | IPO α1/β1; IPO 7; IPO β1 |
| | | | H2A, H2B, H3, H4 | | IPO α1/β1 |
| **IPO 8 Cargo** | **NLS Location** | **Other importins that could also be used** | **IPO 11 Cargo** | **NLS Location** | **Other importins that could also be used** |
| NPM-ALK | | IPO β2 | UbcM2, UbcH6 | Ubiquitin-charged catalytic domain | |
| SRP19 | | IPO β1; IPO β2; IPO5 | rPL12 | | |
| Smad4 | Includes residues 1–63 | | Gag (RSV) | MA domain | IPO β1 |
| Smad1 | | | Rps7 Rpl5 Rps3a | | IPO α1/β1; IPO 7; IPO β1 |
| Ago2 | | | H2A, H2B, H3, H4 | | IPO α1/β1 |

| IPO 7 Cargo | NLS Location | Other importins that could also be used | IPO 9 Cargo | NLS Location | Other importins that could also be used |
|---|---|---|---|---|---|
| Proline-rich homeodomain | Homeodomain | | HSP27 | | |
| ZEI | Zinc fingers 9–12 | | Hepatocellular carcinomaassociated protein | | |
| dpERK | | | rPS3, rPS9, rPL19 | | |
| ERK2 | 10-residue SPS region | | Aristaless (Arx) | Homeodomain | IPO β1; IPO 13 |
| MEK1 | SPS region | | PP2A (PR65) | Residues 205–589 | IPO β1 |
| P60TRP | SPS region | | c-Jun | Residues 250–334 | IPO β1; IPO 5; IPO 7 |
| Rag-2 | Residues 439-527 | | rPL18a | | IPO β1 |
| HIV-1 Integrase | Residues 212–288 | IPO α1/β1 | H2A, H2B, H3, H4 | | IPO β1; IPO β2 |
| CDK5 activator p35 | | IPO β1; IPO 5 | rPS7 | Residues 98–120 | IPO β1; IPO β2; IPO 5 |
| HIF1-α | PAS domain | IPO 4 | | | |
| Glucocorticoid receptor | | IPO α1/β1 | **IPO 13 Cargo** | **NLS Location** | **Other importins that could also be used** |
| HPV16/18 L2 | N-terminal basic | | NF-YB/NF-YC | Heterodimer of histone fold domains | |
| H2A, H2B, H3, H4 | Residues 31-98 | IPO α1/β1; IPO 9 | NC2α/NC2β | Heterodimer of histone fold domains | IPO α1/β1 |
| C-Jun | Residues 250-334 | IPO α1/β1; IPO 9 | Myopodin | 360–698 | |
| HIV-1 Rev | Residues 35-46 | IPO β1 | glucocorticoid receptor | | IPO α1/β1; IPO 7 |
| rPS7, rPL5 | | IPO α1/β1; IPO 5 | Y14-Mago | Entire heterodimer | |
| | | | p12/CHRAC-17 | | |
| | | | PAX6 | Residues 208–288 | |
| | | | Aristaless (Arx) | Homeodomain | IPO α1/β1; IPO 9 |
| | | | Crx | Homeodomain | |
| | | | rPL5 | | IPO α1/β1; IPO 5 |

(Adapted from Pumroy, 2015)

shared by all the NLSs is their positively charged sequences. IPO9's yeast homolog Kap114 also has a large cargo pool. In addition to transporting important proteins like histone chaperone Nap1p (Mosammaparast et al., 2005), in yeast, Kap114 also appears to mediate the assembly of the transcription initiation complex due to its interaction with both TFIIB and the TBP domain (Kim et al., 1993; Liu et al., 2010). IPO9's ability to interact with such a large group of cargo is impressive, but what truly makes it outstanding is its cytoplasmic chaperone function (Kortvely et al., 2005). Compared to the IPOα-IPOβ1 heterodimer's weak chaperone function, IPO9 effectively shields basic cargo proteins from degradation and aggregation (Jäkel et al., 2002).

IPO11's cargo pool includes ubiquitin-charged class III E2 Ub conjugating enzymes UbcM2, UbcH6, UBE2E2 (Plafker et al., 2004), ribosomal protein L12 (rpL12) (Plafker and Macara, 2002) and Gag polyprotein of Rous Sarcoma Virus (Gudleski et al., 2010). The three E2 Ub conjugating enzymes are primarily imported by IPO11, but the fact that only multiprotein complexes of the E2 enzymes can be recognized by IPO11 makes it nearly impossible to identify the NLSs. Meanwhile, the NLS of rpL12 has not been explored, although IPO11 appears to be rpL12's only transporter. The very first identified NLS of IPO11 cargo is the 5-helix MA domain located in the N-terminal of Gag (RSV) (McDonnell et al., 1998).

Among all the β family importins that were investigated in this thesis, IPO13 is the only bidirectional karyopherin that mediates both import and export of certain cargos (Grünwald et al., 2013). Proteins that are imported by IPO13 are paired-type homeodomain transcription factors PAX 3 and PAX 6 (Ploski et al., 2004), core exon junction complex components Mago-Y14 (Bono et al., 2010), Aristaless (Arx) (Lin et al.,

2010), glucocorticoid receptor (GR) (Tao et al., 2006) and five other proteins. The characterized IPO13 recognition sites are predominantly folded domains; for example, both Arx and PAX 6 bind IPO13 through small helical homeodomains (Ploski et al., 2004). The large non-overlapping surfaces explain, in part, how IPO13 recognizes so many different cargos, and subsequently leads to a different releasing mechanism for the cargos. Initially, IPO13 was defined as an importin. However, the first export cargo of IPO13, eukaryotic initiation factor 1A (eIF1A), was discovered by Mingot et al. in 2001. eIF1A, along with other translation factors, is directly involved in the forming of the translational pre-initiation complex through interacting with the small ribosomal subunit (Jackson et al., 2010). But due to its small size (18 kDa), an active export pathway is required to maintain the cytoplasmic localization of eIF1A. The structure of the RanGTP-IPO13-eIF1A complex illustrates that eIF1A binds to the inner surface of IPO13's C-terminal arch. The binding of RanGTP to IPO13 stabilizes eIF1A rather than competing with the cargo, since their binding sites do not overlap (Grünwald et al., 2013). This cargo stabilizing function, which does the opposite of the unidirectional importins, allows IPO13 to perform double duty (Mingot et al., 2001). The IPO13 transport cycle allows two cargos to be transported in opposite directions by consuming only one GTP molecule. After eIF1A is exported out of the nucleus, import substrates bind IPO13, which triggers the cytoplasmic release of eIF1A.

## Ran-dependent Directional Transport

Although karyopherins are the "shuttles" that import and export cargo, they do not control the transport direction. Whether a karyopherin transports cargo from the cytoplasm to the nucleus (importins) or does the opposite (exportins) is driven by the Ras-

related small GTPase (Ran) system (Moore and Blobel, 1993). Ran has two forms: GTP-bound and GDP-bound. RanGTP hydrolysis is activated by the cytoplasmic GTPase activating protein (RanGAP) to RanGDP, whereas the GDP (guanosine diphosphate) on RanGDP will be exchanged for a GTP (guanosine triphosphate) in the nucleus by the guanine nucleotide exchange factor (RanGEF) (Cavazza and Vernos, 2015). The fact that RanGAP and RanGEF (also known as RCC1) are strictly located in different compartments leads to a high concentration of RanGTP in the nucleus and a high concentration of RanGDP in the cytoplasm (Görlich et al., 2003). It is the gradient difference of RanGTP and RanGDP between the two compartments that determines where importins and exportins bind or release their cargos. After an importin-cargo complex enters the nucleus through the NPC, RanGTP, which has high affinity for importins, binds tightly to the importin. The binding of RanGTP causes a conformational change in the importin that lowers its affinity for and displaces the cargo. The RanGTP-importin complex then translocates back to the cytoplasm, where GTPase is activated and RanGTP is hydrolyzed to RanGDP. The switch from RanGTP to RanGDP drastically decreases Ran's affinity for importins. Therefore, the importin is released and starts the next round of cargo import. On the other hand, the export pathway regulated by the Ran system is rather different, or even opposite. In contrast to the importin pathway, exportins bind cargo after binding RanGTP and displace cargo when RanGDP-bound.

## The Nucleocytoplasmic Transport Pathway of TR

From the "shuttle" karyopherins to the "cargo" TR that regulates TH genomic function, all the machinery that is involved in the process of TR nucleocytoplasmic transport has now been introduced. Figure 5 illustrates the entire nucleocytoplasmic

transport pathway of TR. The story starts with a cytoplasmic TR that needs to be imported into the nucleus. Under a high RanGDP concentration, TR binds to specific importins with high affinity. Two possible binding products might occur: a classical NLS directed TR-IPOα1-IPOβ1 complex or a nonclassical NLS directed TR-β family importin complex. Both complexes interact with the FG repeats on the cytoplasmic filaments of NPC embedded in the nuclear envelope. The TR-importin complex passes through the NPC and translocates into the nucleus where there is a high concentration of RanGTP. RanGTP then binds to the importin in the complex, causing a conformational change that lowers importin's affinity for TR. Subsequently, TR is released in the nucleus and represses target gene transcription by forming homodimers or heterodimers when TH is absent.

The importin-RanGTP complex will then exit through the NPC. The hydrolysis of RanGTP is activated shortly after the importin-RanGTP complex interacts with the RanGAP associated with cytoplasmic nucleoporins. RanGDP no longer occupies the importin, allowing the free importin to start another round of TR nuclear import. In order to maintain a high nuclear RanGTP concentration, presumably all RanGDP molecules need to be transported back to the nucleus for RanGTP conversion. A different transporter called nuclear transport factor 2 (NTF2) delivers RanGDP into the nucleus, where RanGDP is converted to RanGTP by RanGEF.

Since TR shuttles between the nucleus and cytoplasm, some TR eventually will be sent back to the cytoplasm through the NPC by specific exportins. The high concentration of nuclear RanGTP increases exportins' affinity for any free TR. TR bound exportin interacts with the FG-repeats of certain nucleoporins on the nuclear side of the NPC (Askjaer et al., 1999), which allows the TR-exportin complex to pass through the NPC

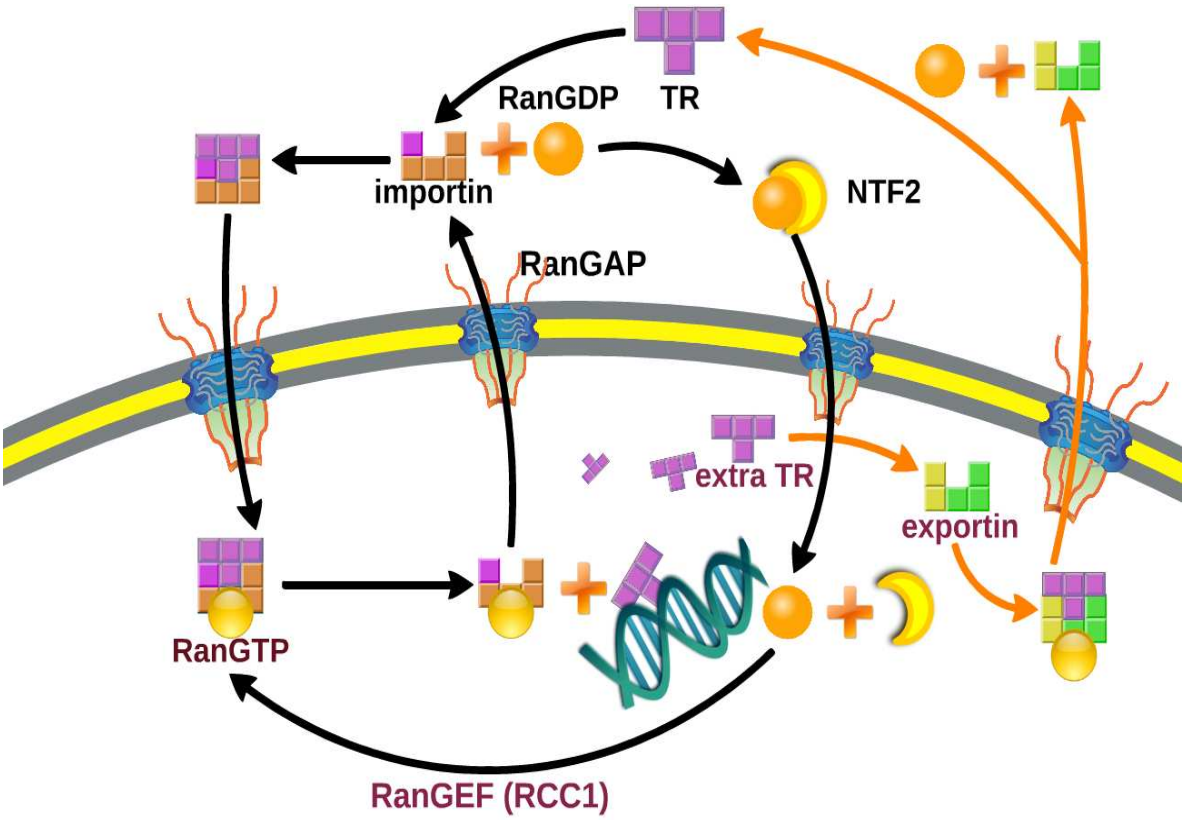


**Figure 5. TRα1 nucleocytoplasmic transport pathway**. TR binds to specific importins under a high RanGDP concentration. The TR-importin complex passes through the NPC and translocates into the nucleus where there is a high concentration of RanGTP. RanGTP then binds to the importin, causing a conformational change that lowers importin's affinity for TR. The new dual importin-RanGTP complex will exit through the NPC. The hydrolysis of RanGTP causes importin dissociation, allowing the free importin to start another round of TR nuclear import. Nuclear transport factor 2 (NTF2) delivers RanGDP into the nucleus, where RanGDP is converted to RanGTP by RanGEF. Free TR will be sent back to the cytoplasm by specific exportins.

and translocate to the cytoplasm. Finally, the exportin dissociates from the TR due to its decreased affinity under high cytoplasmic RanGDP concentration, allowing the free TR to enter the next cycle of nucleocytoplasmic transport. Although the overall pathway is clear, many aspects of the mechanism still need to be explored. For example, among all the 20 characterized karyopherins, which importin(s) and exportin(s) are responsible for TR's nucleocytoplasmic transport? Furthermore, since TRα1 has multiple NLSs and NESs, which ones are recognized by which specific importin(s) or exportin(s), respectively? The story of TR nucleocytoplasmic transport pathway cannot be fully understood without these missing pieces.

## What's Known and Unknown

Ever since TRα1 was discovered to undergo nucleocytoplasmic shuttling, using a signal-mediated pathway in mammalian cells (Bunn et al., 2001), researchers started paying more attention to the TRα1 transport mechanism. TRα1 nucleocytoplasmic shuttling requires energy, physiological temperature, and soluble factors (Grespin et al., 2008; Roggero et al., 2016). Due to the large number of characterized karyopherins and the evidence that they have overlapping cargo sets, a detailed investigation of which of the importins/exportins are used to import or export TRα1 is crucial for a greater understanding of the TRα1 nucleocytoplasmic transport mechanism. Previous studies have targeted the possible importins and exportins that are involved in the transport of TRα1, including the use of both IPOβ1/IPOα1-mediated classical pathways and other importin-mediated non-classical import pathways (Mavinakere et al., 2012; Roggero et

al., 2016), as well as the use of both CRM1/calreticulin mediated and other exportin-mediated export pathways (Grespin et al., 2008; Subramanian et al., 2015). However, all these possible candidates could not be confirmed without evidence of direct, physical protein-protein interaction between them and TRα1. Chapter 3 of this thesis presents our recently published article (Roggero et al., 2016) that provides an in-depth explanation of how those interactions were determined. Since this thesis mainly focuses on TRα1 nuclear import, the additional work done for the exportins is presented in Chapter 5. Therefore, the first question that is addressed in this thesis is which importins, when down-regulated by RNAi, have a strong impact on TRα1 nuclear localization *in vivo*, and also interact with TRα1 directly in coimmunoprecipitation assays.

As mentioned earlier in the introduction, two NLSs have been identified in TRα1 so far. The first classical bipartite NLS, named NLS-1, is located in the hinge region (Bunn et al., 2001; Mavinakere et al., 2012). The overall basic amino acid sequence KRVAKRKLIEQNRERRRK (Lysine-Arginine-Valine-Alanine-Lysine-Arginine-Lysine-Leucine-Isoleucine-Glutamic Acid-Glutamine-Asparagine-Arginine-Glutamic Acid-Arginine-Arginine-Arginine-Lysine) meets with the requirement for interacting with karyopherins. Mavinakere et al.'s work in 2012 demonstrated that NLS-1 is sufficient to import the G3 protein (a cytoplasmic-localized fusion protein consisting of GFP-GST-GFP) into the nucleus when G3 is fused with the hinge region. This classical bipartite NLS-1 is conserved in TRβ1. Since NLS-1 is classical, it's logical to predict that the IPOβ1-IPOα1 heterodimer mediates nuclear import. However, there is a high possibility that other β-family importins could take part in the import process as well. On the other hand, NLS-1 in the hinge region was shown to only partially target TRα1 into the nucleus

(Picard and Yamamoto, 1987), indicating the existence of a second NLS. With the help of the program PSORT II (Nakai and Horton, 1999), Mavinakere et al. (2012) identified the second NLS (NLS-2) located in the A/B domain. They performed the same experiment in which G3 was fused with either TRα1's or TR β1's A/B domain to examine if there were sufficient sequences to target the cytoplasmic protein into the nucleus. The result showed a non-classical, novel, and monopartite 8-amino acid sequence PDGKRKRK that only exists in TRα1, not in TRβ1, that successfully targets G3 into the nucleus. This points to the possibility of TRα1 using multiple importins other than the classical import pathway. At the same time, studying which importin recognizes which NLS also helps to gain a better knowledge of the TRα1 import mechanism. Therefore, the second research question addressed in this thesis is which importins interact with TRα1's NLSs.

## RNA Interference-Induced Importin Knockdown

RNAi is one of the most important discoveries in biology over the past decade. It totally changed how scientists value RNA as a regulatory molecule, as opposed to simply an information carrier. Researchers found out that RNA-induced RNAi is a process of down-regulating mRNA expression, therefore consequently knocking down the corresponding proteins. If that is not impressive enough, this mechanism has become the heart of scientific research as well as medical treatment of certain diseases. But who would have ever thought this revolution all started with cultivating a purple petunia. In 1986, Dr. Richard Jorgensen was asked to create a dazzling flower to attract investors. Since the genetic engineering techniques in 1986 were lacking in sophistication, the

experiment was done in petunia which was easier to introduce genes into at the time. Jorgensen and coworkers attempted to make a very purple petunia by introducing more copies of the purple pigment gene. Logically, the flowers would be more purple, but instead they harvested white flowers with no purple pigmentation. This completely unexpected result caused a huge debate in the scientific field. Scientists tried to map out the mechanism by working on different organisms, but it wasn't understood until 1998.

In 1998, Dr. Craig Mello and Dr. Andrew Fire discovered an interesting phenomenon when they were studying the *C. elegans* muscle protein unc-22. After they injected unc-22 double stranded RNA (dsRNA) into *C. elegans*, the unc-22 gene was specifically silenced which lead to decreased unc-22 production. This phenotype caused by the dsRNA precisely mimicked the unc-22 mutations (Fire et al., 1998). What was realized by this discovery is that scientists would be able to artificially silence specific genes without mutating the DNA sequence. Furthermore, the post-translational silencing effects could be passed on to the next generation. Fire and Mello named this mechanism RNAi. For this amazing discovery, they were awarded the Nobel Prize in Medicine at 2006. So, how does RNAi interfere with protein production and how was it used in our TRα1 nuclear import research?

Soon after 1998, many laboratories began developing strategies to silence genes by triggering RNAi, either through introducing long dsRNA or constructing plasmids that encode the small interfering RNA (siRNA) of interest (Clemens et al., 2000). However, the problem was that not only were those strategies not efficient in mammalian cells but they also triggered innate immune responses (Stark et al., 1998). Ever since the discovery that RNAi is triggered by 21 nucleotide RNAs with phosphorylated 5' ends and

hydroxylated 3' ends was reported (Elbashir et al., 2001), introducing 21 base pair dsRNAs to knockdown gene expression has become practical (Zamore et al., 2000). This technique was demonstrated to be efficient in both mammalian cells and *Drosophila* without causing innate immune responses (Elbashir, et al., 2001). Now, two ways to trigger RNAi are widely used, introducing dsRNAs directly or plasmid vectors that encode short hairpin RNAs (shRNA) which are eventually processed to siRNAs. Either way, selecting a siRNA that has the highest knockdown potency among a few designed siRNAs ensures the siRNA's specificity towards the target mRNA. The most important benefit of using plasmid vectors to introduce dsRNA is that it maintains high siRNA levels for a long period of time in the cells, since siRNA degrades more quickly (Grimm, 2009).

Of relevance to this thesis research, the half-life of importins is typically 12 hours, which indicates the requirement of a long term supply of siRNA. In this thesis, all importin knockdown experiments were conducted by introducing shRNA plasmid sets into HeLa cells using a lipid-based transfection reagent called Lipofectamine 2000. These positively charged lipid molecules are attracted to the negatively charged plasmids to form liposomes which fuse with the plasma membrane and allow plasmids to enter the cell. The plasmids then enter the nucleus by an unknown mechanism and are transcribed to dsRNAs with short hairpins by utilizing the cell's RNA polymerase II system. Shortly after being transcribed, dsRNAs are exported out of the nucleus through NPCs. When dsRNA or shRNA locates in the cytoplasm, it is cut by the protein Dicer into a siRNA. The siRNA then interacts with the RNA-induced silencing complex (RISC). RISC is activated after incorporating with one of the two RNA strands, whereas the other strand is degraded. The activated RISC-single strand RNA complex binds with complementary target mRNA

and cleaves it through action of the endonuclease Slicer. Consequently, the loss of mRNA directly suppresses target protein translation.

RISC is the heart of the entire RNAi-induced knockdown pathway. It has many critical functions, such as recognizing siRNA, unwinding siRNA, incorporating with the template RNA strand, and cutting the target mRNA strand. All those jobs are done by a group of proteins called Argonaute proteins (AGO). Among the 8 human AGO proteins, only AGO2 assists the silencing process (Hutvagner and Simard, 2008). AGO2 has three domains, Piwi-Argonaute-Zwille (PAZ) domain, middle (MID) domain, and PIWI domain, each of them possesses specific duties. The 5' monophosphate group of the template strand tucks in between the PIWI and MID domains, whereas the PAZ domain recognizes the 3' dinucleotide end. This orientation allows the PIWI domain, which has an RNase H fold, to cut the target mRNA strand by base pairing to the "seed region" of the template strand (Liu et al., 2004; Song et al., 2004).

After going through this RNAi-induced knockdown process, in the experiments presented in this thesis, each endogenous importin was partially depleted individually due to the lack of corresponding mRNA and its impact on TRα1's nuclear import could then be tested. Figure 6 illustrates the procedure of RNAi-induced protein knockdown. Although RNAi's popularity was gained from its specificity, some nonspecific off-target effects have been reported. Due to shRNAs' similarities with microRNAs (miRNA), unintended RNAi could happen via shRNA causing miRNA-like binding in the 3' UTRs (Birmingham et al., 2006). Moreover, since both shRNA and miRNA are exported by exportin 5 (XPO 5), long term expression of shRNA could compete with miRNA, which causes saturation and represses the natural miRNA machinery (Wang et al., 2011).

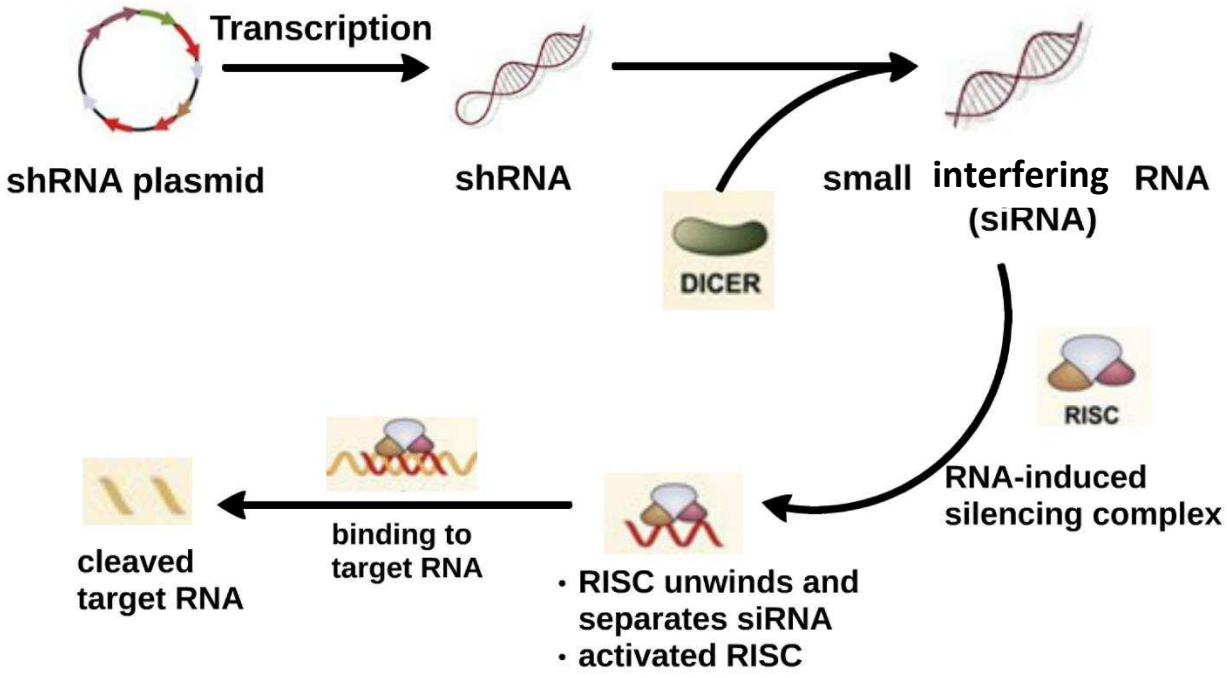


**Figure 6. RNAi induced protein knockdown mechanism.** A brief illustration of RNAi induced protein knockdown used in this thesis research. shRNA plasmids are introduced to HeLa cells. After shRNA is transcribed, it gets exported into the cytoplasm where DICER cuts it to siRNA. RISC complex unwinds and separates siRNA. The activated RISC-single strand RNA complex will bind with complementary target mRNA and cut it into small pieces. Consequently, the loss of mRNA directly suppresses target protein translation.

# Chapter 2: Materials and Methods

## RNA interference

Pre-designed SureSilencing™ shRNA plasmid sets, including plasmids of a scrambled negative control, IPOβ1, IPOα1, IPO4, IPO5, IPO7, IPO8, IPO9, IPO11, and IPO13 were used to knockdown importins. Each of the sets came with four types of target-specific plasmids (named as “Red”, “Yellow”, “Blue”, and “Green”) that can produce functional designed siRNAs. Instead of selecting the one that has the highest knockdown potency, we adjusted the concentrations of the four types to the same level (1 μg/1μl) and combined them together for transfection.

## Transient Transfection and Fluorescence Microscopy

Human (HeLa, ATTC CCL-2) cells were used as the model system. They were cultured in Minimum Essential Medium (MEM) supplemented with 10% fetal bovine serum (FBS) (Life Technologies) at 37°C under 5% CO2 and 98% humidity. Twenty-four hours before transfecting HeLa cells with importin shRNA coded plasmids, as well as GFP-tagged TRα1 plasmids, cells were seeded on 22mm coverslips in 6-well culture dishes at a density of 2.2 x $10^5$ cells per well with fresh MEM containing 10% FBS. Since experiments were performed in 6-well culture dishes, three different treatments could be tested in every trial with two technical replicates for each. The three treatments were negative control (1 μg scrambled sequence shRNA plasmid + 1 μg GFP-TRα1 expression plasmid), TRα1-only control (1 μg GFP-TRα1 expression plasmid only), and experimental

group (1 μg appropriate importin shRNA plasmid + 1 μg GFP-TRα1 expression plasmid). All the plasmids were contained in 2ml MEM supplemented with 10% FBS along with 3 μl Lipofectamine 2000 (Invitrogen). Right before the transfection, cells were washed with 1x Dulbecco's phosphate buffered saline (1x DPBS). 8 hours after transfection, the transfection media was replaced with 2 ml fresh MEM supplemented with 10% FBS. 26-hours post-transfection, cells were washed with 1x DPBS three times, and fixed in 3.7% formaldehyde for 7 min. The fixation was followed by three more washes (5 min each time) with 1x DPBS. The last step was to mount the coverslips on microscope slides using 8 μl Fluoro-Gel II containing DAPI (0.5 μg/ml). The slides were analyzed by fluorescence microscopy to determine the localization pattern of GFP-TRα1.

Each slide was viewed under fluorescence microscopy and 200 cells were scored into three categories (Figure 7) based on the overall localization pattern of fluorescence (performed blind). The first category was nuclear only (N). Cells in this category showed an almost completely nuclear localization pattern of GFP-TRα1. The second category was nuclear greater than cytoplasmic (N>C). Cells of this category still showed a strong nuclear fluorescence but there was also a distinct cytoplasmic fluorescence pattern. As long as the nucleus still could be distinguished from the cytoplasm through the bright edge of the nuclear envelope, the cell was put into this group. The last category was whole cell (N=C). The fluorescence localization of cells in this group was spread out; the nucleus could not be distinguished from the cytoplasm due to the even distribution of fluorescence. At least three independent, biologically separated replicates (with 2 technical replicates each) were included in the Microsoft Excel data analysis.

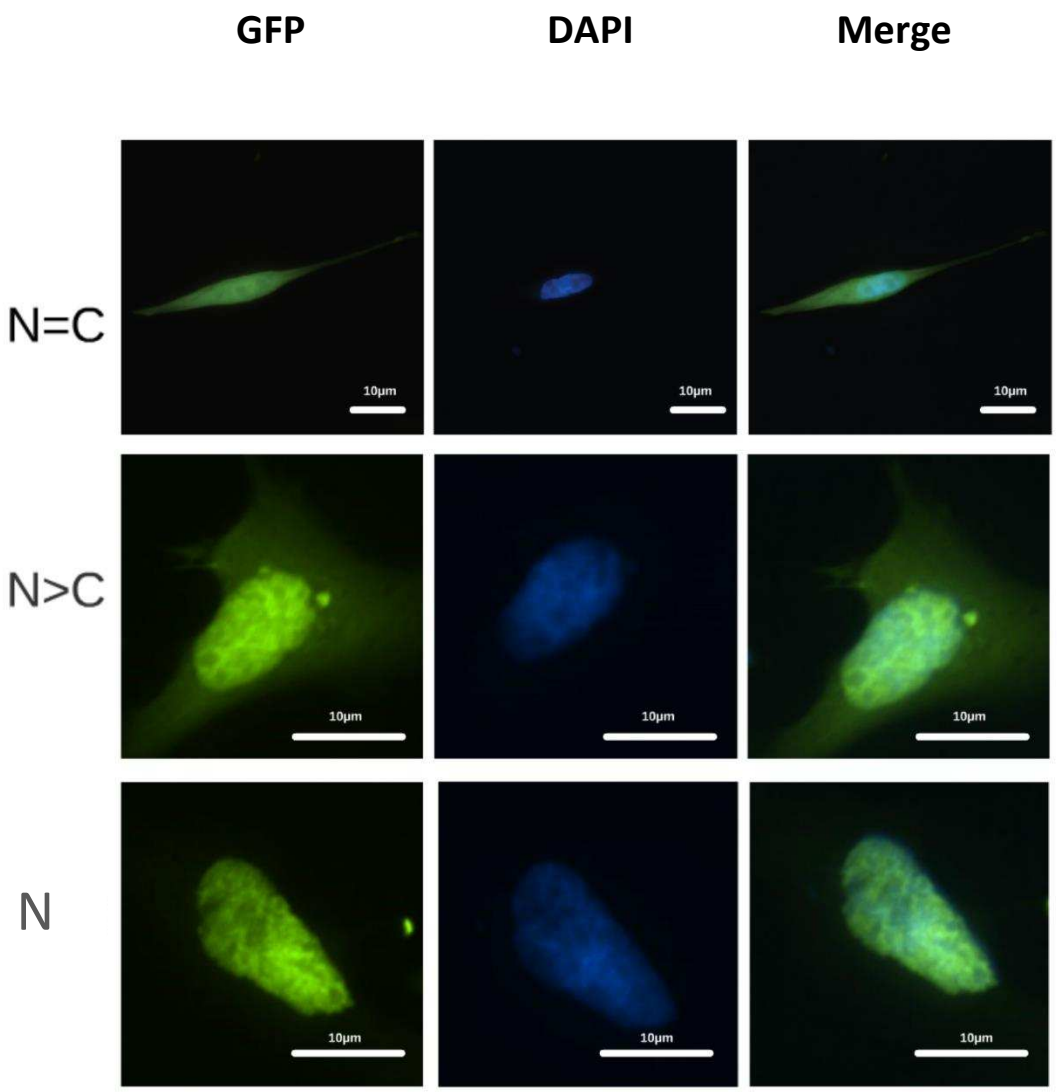


## Figure 7. Scoring categories for TRα1 localization.

GFP-TRα1 localization pattern was scored as one of the three categories: cells that showed almost complete nuclear localization pattern of GFP-TRα1 were categorized as nuclear only (N); cells that had a nuclear GFP-TRα1 localization and less intense cytoplasmic distribution were categorized as nuclear greater than cytoplasmic (N>C); cells that had almost equal GFP-TRα1 distribution among the nucleus and cytoplasm were categorized as whole cell (N=C).

## Western Blotting (Immunoblotting)

To ensure that any visualized GFP-TRα1 localization change was directly linked to the decrease of an importin, the knockdown efficiency needed to be confirmed. Therefore, the second major approach used in this thesis to test importin knockdown efficiency was immunoblotting, or Western Blotting (WB) (Figure 8). Western Blotting has been widely used to detect specific proteins from cell extracts. The results of chemiluminescent detection show up on exposed X-ray films as dark bands that have different densities. According to the presence and the density of a band, WB generally answers two questions: 1) is the targeted protein expressed or present? and 2) is the expression of the targeted protein in a treatment group increased or decreased relative to a control? Clearly, the first question could be answered by checking if a band was present, whereas the second question is answered by comparing the densities of different bands under different treatments.

The first step here, was to knockdown the targeted importin by transfecting HeLa cells with the desired shRNA plasmid. Cells were seeded in 100 mm vented plates at a concentration of 9 x $10^5$ cells per plate and transfected with 10μg plasmid DNA. All conditions including temperature (37ºC), $CO_2$ (5%), humidity (98%), and incubation timing were kept the same as for the 6-well plate transfection described above. eight h post-transfection, the transfection medium was replaced with fresh MEM containing 10% FBS. Cell lysates were extracted after 26 h of transfection. Protein concentration was estimated by a NanoDrop® ND-1000 full-spectrum UV/Vis Spectrophotometer both to prevent protein over-load and ensure the same amount of protein was used. SDS-PAGE sample buffer was then added to lysate samples and they were boiled for 10 min to denature the

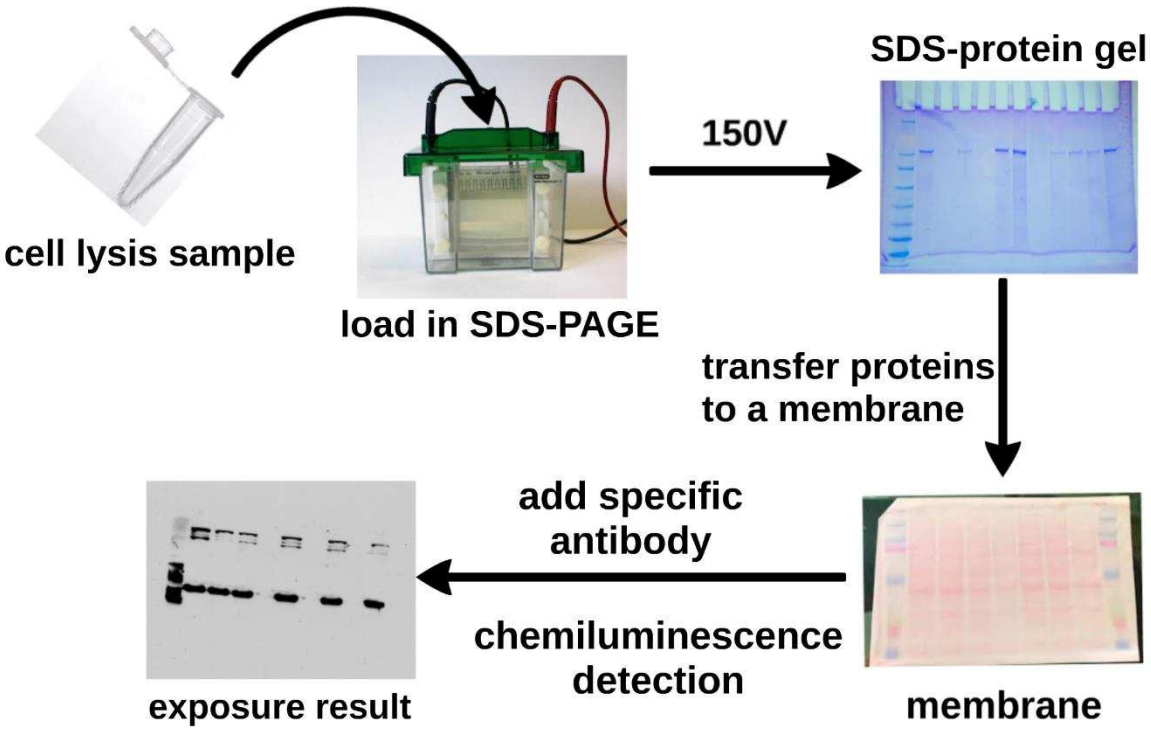


**Figure 8. Western blotting.** Cell protein lysate is extracted before loading the same amount of protein to each lane for SDS-PAGE. Proteins are separated based on their sizes after running at 150 volts for 45 min. Proteins are then transferred from the polyacrylamide gel to a special PDVF membrane with the same separation pattern. Then, the membrane is incubated with primary antibody and secondary antibody respectively with washes in between. After a chemiluminescent incubation step, the membrane is exposed to an X-ray film.

proteins (Algenäs et al., 2014). During denaturation, proteins are not only linearized but also negatively charged due to sodium dodecyl sulfate (SDS). This process ensures that proteins migrate towards the positive electrode. After the proteins were separated based on their sizes (shorter amino acid sequences run faster), they were transferred from the polyacrylamide gel to a special PVDF membrane with the same separation pattern. Then, the membrane was incubated with, for example, anti-IPO7 primary antibody and anti-rabbit secondary antibody, with washes (0.1 M Tris–HCl, 0.5 M NaCl, 0.1% Tween) in between. The secondary antibody is linked to Horseradish Peroxidase (HRP). After adding in the chemiluminescent substrate, the position that locates the importin band will show chemiluminescence due to the substrates' oxidation by HRP. The last step is to expose the membrane to an X-ray film in the dark room. If the target importin, for example IPO7, was expressed in the cells, then an exposed dark band was found on the film. Using NIH ImageJ software to perform densitometry on a scanned film, the densities of the IPO7 bands under different treatments could be measured as digital data for EXCEL input and compared for the fold difference.

Therefore, if the knockdown importin band's density was significantly lighter than the band from no treatment, while the loading control GAPDH (Glyceraldehyde 3-phosphate dehydrogenase) bands of both groups had a similar density, then the importin knockdown was efficient. In order to have non-overexpressed bands on X-ray films, multiple exposure times (e.g., 10 sec, 30 sec, 2 min) were taken for each trial and the best-exposed result was picked for publication. Meanwhile, an appropriate dilution of both primary and secondary antibodies was critical both to prevent extra signal which causes background subtraction and to ensure the interaction between antigen and antibody was

specific. The concentration of antibodies used in this thesis were as follows: anti-IPOβ1 (Santa Cruz), 1:2000; anti-IPOα1 (Santa Cruz), 1:2000; anti-IPO4 (Santa Cruz), 1:333; anti-IPO5 (Santa Cruz), 1: 10,000; anti-IPO7 (Abcam, Cambridge, MA), 1:1000; anti-IPO8 (Abcam), 1:250; anti-IPO9 (Abcam), 1:250; anti-IPO11 (Abcam), 1:333; anti-IPO13 (Santa Cruz), 1:100; anti-GAPDH (Santa Cruz Biotechnology Inc, Dallas, TX), 1:5000; horseradish peroxidase (HRP)-conjugated donkey anti-rabbit IgG (GE Healthcare Life Sciences), 1:25,000; HRP-sheep anti-mouse IgG (GE Healthcare Life Sciences), 1:25,000. Pre-Stained Kaleidoscope Protein Standards (Bio-Rad, Hercules, CA) were used as the ladder to confirm protein sizes. At least 3 knockdown replicates were performed for each importin.

## GFP-Trap Coimmunoprecipitation

When a research question asks whether one protein has influence on another, the final step always comes down to showing their physical interaction. Scientists have thus developed many technologies to this end, including yeast two-hybrid, Tandem affinity purification, Bimolecular fluorescence complementation, and the one that played a central role in this thesis, coimmunoprecipitation (CoIP). CoIP has been considered as the gold standard assay for testing protein physical interactions. Its benefits include that it is relatively easily performed, can be tested with endogenous proteins, and is highly specific due to antibody selection. The standard procedure of CoIP (Figure 9) contains three steps: first, proteins are extracted from the cells (cell lysate preparation); second, the protein of interest gets isolated by the specific antibody (IP); third, proteins interacting

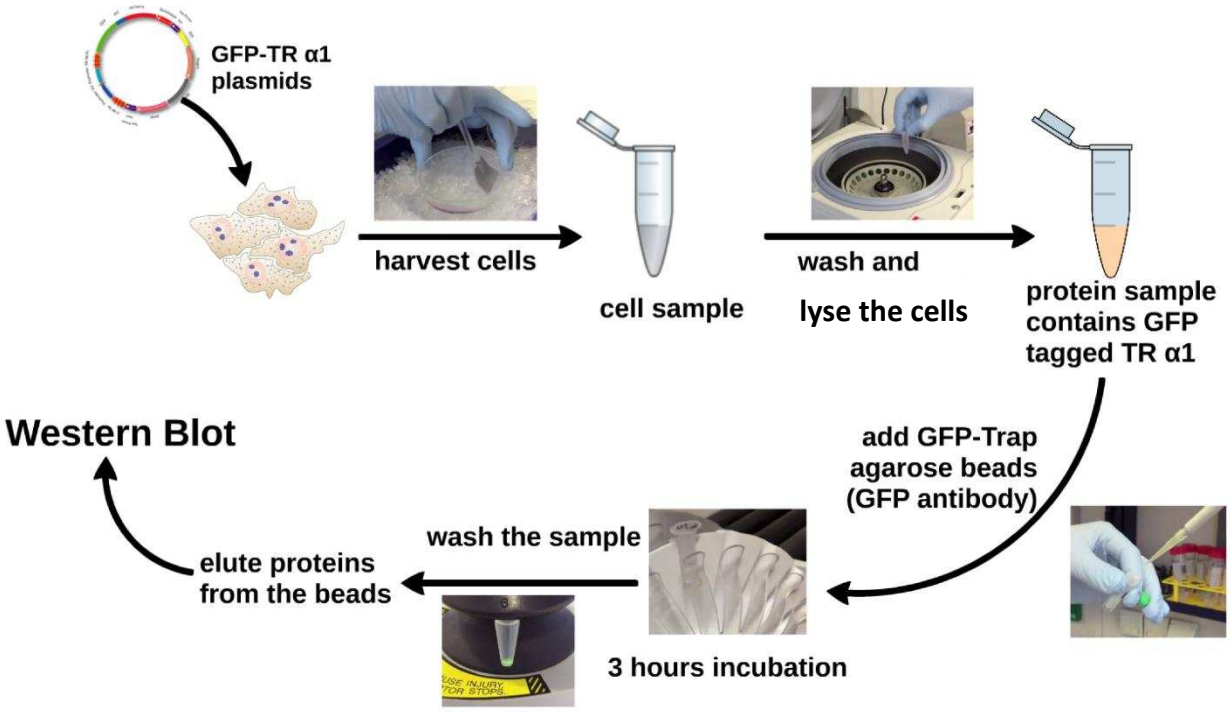


**Figure 9. "GFP-trap" coimmunoprecipitation.** Proteins are extracted from the cells. After being washed with 1 X DPBS several times, the protein extract is incubated with anti-GFP antibody embedded agarose beads. Proteins that are tagged with GFP will be trapped by the agarose beads, and the proteins of interest are coimmunoprecipitated. Elution buffer is used to elute the proteins from the beads and identify the protein of interest with Western blotting.

with the protein of interest are identified by WB (binding partner identification). The CoIP procedure used in this thesis is called “GFP-trap”. Recall that the protein of interest, TRα1, is tagged with GFP. When a cell lysate containing GFP-TRα1 is incubated with anti-GFP antibody embedded agarose beads, GFP-TRα1 will be “trapped” by the agarose beads. After a couple of washes with the dilution/washing buffer (2mM Tris-HCl, pH7.5, 30 mM NaCl, 0.1mM EDTA), proteins that could not bind with the beads are washed off, and GFP-TRα1 is specifically separated. Meanwhile, any proteins interacting with the TRα1 portion of the fusion protein would be subsequently “trapped” or coimmunoprecipitated. Finally, western blotting is performed to identify the importins that had interactions with GFP-TRα1.

Since the “GFP-trap” CoIP was one of the most important methods developed in this thesis as a new technique in the Allison lab, a detailed step-by-step explanation is provided. GFP-trap CoIP starts with transfecting HeLa cells with GFP-TRα1 expression plasmids. Cells were seeded at a concentration of at least $9\times10^5$ cells per 100mm plate. 24 hours after seeding, cells were transfected with 10 μg GFP-TRα1 expression plasmids with 20 μl Lipofectamine 2000. The transfection media was replaced with fresh MEM containing 10% fetal bovine serum after 8 h post-transfection. 26 h post-transfection, the transfection efficiency was determined by ZOE image analysis. The following GFP-trap procedure only continued when at least 80% of the cells were successfully transfected and healthy. The plates were brought back to the tissue culture hood and rinsed once with 10 ml of 1x DPBS. Cells were treated with 0.7 ml of 0.25% trypsin (Life Technologies) for no longer than 3 min, and then collected in 1.0 ml MEM supplemented with 10% FBS. After being transferred to 2.0 ml microcentrifuge tubes, cells were washed twice with

centrifugation at 1000rpm, room temperature for 1 minute between washes. The washed cells were incubated on ice for 30 min with 200 µl of Lysis Buffer (10 mM Tris-HCl, pH 7.2, 150 mM NaCl, 0.5 mM EDTA) containing 0.5% IGEPAL$^{R}$ (NP-40 equivalent, Sigma-Aldrich) and 2 µl 100X Halt Protease Inhibitor Cocktail (Thermo Scientific). The lysate was mixed through pipetting every 10 min. After the 30 min of incubation, the lysate was cleared by centrifugation at 4°C, 16,000 x g for 10 min, and the supernatant was transferred to a pre-cooled 1.5ml microcentrifuge tube and diluted with 300 µl of dilution/washing buffer containing 3 µl 100X Halt Protease Inhibitor Cocktail, to yield a final concentration of 0.2% IGEPAL. During the 30 min, 15 µl GFP-trap agarose beads (GFP-Trap$^{R}$_A, Chromotek GmbH, Planegg-Martinsried, Germany) were pre-equilibrated by washing three times with 500 µl Dilution/Washing Buffer in the uncapped filtration column, centrifuged at 4°C, 3000xg for 1 min between washes. A tip here is that agarose beads are concentrated at the bottom of the container. Therefore, to extract the same amount of beads for each sample, the bead slurry needs to be mixed completely by tapping the container. The next step was to add the diluted supernatant into the capped filtration columns, followed by a 2 h incubation in the 4°C cold room with end-over-end rotation. After the incubation, the uncapped filtration columns were centrifuged at 4°C, 3000 x g for 1 min, and a 60 µl sample of the flow-through was collected labeled as “unbound” and resuspended with an equal volume of 2X Sample Buffer (2% SDS, 10% glycerol, 250 mM Tris-HCl, pH 6.8, 0.01% bromophenol blue, 20 mM DTT). The beads in the uncapped filtration columns were washed 4 times with 500 µl dilution/washing buffer and centrifuged at 4°C, 3000xg for 1 min between washes. The last step was to dissociate the “trapped proteins” from the beads. 50 µl 0.2 M glycine, pH 2.5, was added to the

columns and incubated with the beads for 5 min followed by centrifugation at 4°C, 3000 x g for 1 min. Proteins that bound to GFP-TRα1 would be eluted to a new set of tubes labeled as “bound”. To neutralize the extremely acidic elution buffer, 5 µl 1M Tris base pH 10.4 was added to the final “bound” products. After adding 65 µl of 2X SDS Sample Buffer, the “bound” samples, along with the “unbound” samples, were analyzed by WB. The importins tested by GFP-trap were IPOα1, IPOβ1, and IPO7, due to the fact that their knockdown results showed significant TRα1 localization change. Among the rest of the importins that showed no impact on TRα1 localization, IPO4 was chosen as the negative control. A GFP transfected cell group was also included as a negative control to test for any nonspecific trapping. Antibodies were used at the following concentrations: anti-GFP (Santa Cruz), 1:2000; anti-IPO4 (Abcam), 1:1250; anti-IPOα1 (Abcam), 1:1000; anti-IPOβ1 (Santa Cruz), 1:1000; anti-IPO7 (Abcam), 1:1000; HRP-conjugated donkey anti-rabbit IgG (GE Healthcare Life Sciences), 1: 25,000.

GFP-trap coimmunoprecipitation helped to confirm the physical interactions between TRα1 and the importins that are responsible for its nuclear transport. As for the second research question, the same coimmunoprecipitation was performed but with the segments of TRα1 that contained either NLS1 or NLS2 to test which one of them recognizes which importin. Chapter 3 is the published paper that presents all the results.

## Chapter 3: Manuscript from Thesis Research

# Nuclear Import of the Thyroid Hormone Receptor α1 is Mediated by Importin 7, Importin β1, and Adaptor Importin α1

**Vincent R. Roggero[a], Jibo Zhang[a], Laura E. Parente[a], Yazdi Doshi[a], Rose C. Dziedzic[a], Emma L. McGregor[a], Arev D. Varjabedian[a], Sara E. Schad[a], Cornelius Bondzi[b], Lizabeth A. Allison[a*]**

[a]Department of Biology, College of William and Mary, Williamsburg, Virginia, 23185, USA
[b]Department of Biological Sciences, Hampton University, Hampton, Virginia, 23668, USA

*Corresponding author. Department of Biology, College of William and Mary, 540 Landrum Dr., ISC 2117, Williamsburg, Virginia 23185, USA. Tel.: +1 757 221-2232; Fax: +1 757 221-6483; E-mail address: laalli@wm.edu (L. A. Allison)

## Statement of Candidate's Contribution Towards Paper Completion

The work which was completed in preparation for the following manuscript was performed by several members of the Allison lab and their collaborators. The MS candidate contributed significantly in a number of capacities to the completion of this manuscript. The candidate, as the second author, also accounted for a substantial amount of the data collected throughout the course of this research. The following is a summary of the candidate's contribution towards the work involved in generating each individual figure which is presented in the following pages.

**Figure 1.** – The candidate did not collect the data presented in Figure 1

**Figure 2.** – The candidate was responsible for collection of the data presented in this figure, as well as for performing all relevant techniques and technical skills required for data acquisition, including maintaining cell cultures, protein lysate preparation, SDS page, and Western Blot.

**Figure 3.** – The candidate did not collect the data presented in Figure 3

**Figure 4.** – The candidate did not collect the data presented in Figure 4

**Figure 5.** – The candidate did not collect the data presented in Figure 5

**Figure 6.** – The candidate was responsible for collection of the data presented in this figure and for all relevant associated techniques including maintaining cell cultures, plasmids preparation, fluorescence microscopy, lysate preparation, SDS PAGE, and Western blotting.

**Figure 7.** – The candidate did not collect the data presented in Figure 7

**Figure 8A, 8B.**--The candidate was responsible for collection of the data presented in this figure and for all relevant associated techniques including maintaining cell cultures, plasmid preparation, lysate preparation, SDS PAGE, GFP-trap coimmunoprecipitation and Western blotting.

**Figure 8C, 8D.** – The candidate was not directly involved in the collection of the data presented in this figure, but the lab members that collected the data were mentored by the candidate.

## Abstract

The thyroid hormone receptor α1 (TRα1) is a nuclear receptor for thyroid hormone that shuttles rapidly between the nucleus and cytoplasm. Our prior studies showed that nuclear import of TRα1 is directed by two nuclear localization signals, one in the N-terminal A/B domain and the other in the hinge domain. Here, we showed using *in vitro* nuclear import assays that TRα1 nuclear localization is temperature and energy-dependent and can be reconstituted by the addition of cytosol. In HeLa cells expressing green fluorescent protein (GFP)-tagged TRα1, knockdown of importin7, importinβ1 and importinα1 by RNA interference, or treatment with an importinβ1-specific inhibitor, significantly reduced nuclear localization of TRα1, while knockdown of other importins had no effect. Coimmunoprecipitation assays confirmed that TRα1 interacts with importin 7, as well as importinβ1 and the adapter importinα1, suggesting that TRα1 trafficking into the nucleus is mediated by two distinct pathways.

## Abbreviations

The abbreviations used are: TRα1, thyroid hormone receptor α1; TRα1, thyroid hormone receptor α1; NPCs, nuclear pore complexes; NLS, nuclear localization signal; RNAi, RNA interference; GFP, green fluorescent protein; GST, Glutathione-S-transferase; shRNA, short hairpin RNA; RT-qPCR, real-time quantitative PCR; FITC, fluorescein isothiocyanate; RRL, rabbit reticulocyte lysate; TRE, thyroid hormone response element; T3, 3,3′,5-triiodo-L-thyronine (thyroid hormone).

## Introduction

The thyroid hormone receptor α1 (TRα1) is a transcription factor in the nuclear receptor superfamily that either activates or represses transcription of thyroid hormone-responsive genes, depending on its liganded state. TRα1 carries out its function through binding target genes in the nucleus; however, our previous research has shown that TRα1 shuttles back and forth between the nucleus and the cytoplasm (Bunn et al., 2001; Grespin et al., 2008). An important aspect of nucleocytoplasmic shuttling, and for the role of TRα1 as a transcription factor, is the process by which TRα1 is imported into the nucleus from the cytoplasm by crossing the nuclear envelope. The nuclear envelope creates an intracellular compartment that enables spatial regulation of gene expression and plays a key role in signal transduction pathways, in gene activation or repression, and in the regulation of major cellular processes (Lange et al., 2010; Sekimoto and Yoneda, 2012; Stewart, 2007; Tran et al., 2014).

Nuclear proteins cross the nuclear envelope via large protein assemblages approximately 100 MDa in size called nuclear pore complexes (NPCs) (Adams and Wente, 2013). Nuclear import of small molecules, including small proteins (less than 40 kDa), can occur by passive diffusion through the central channel of the NPCs; however, in most cases, both small and large proteins enter the nucleus by an energy-dependent, signal-mediated pathway (Gorlich and Kutay, 1999; Gorlich and Mattaj, 1996; Grossman et al., 2012; Stewart, 2007; Tetenbaum-Novatt and Rout, 2010). Signal-mediated transport requires soluble factors collectively called karyopherins, or importins, to facilitate translocation into the nucleus (Pemberton and Paschal, 2005; Sekimoto and Yoneda, 2012; Stewart, 2007), and also relies on an asymmetrical cellular distribution of the small

GTPase Ran in either its GTP or GDP bound state. A high nuclear RanGTP concentration is required for dissociation of import complexes that have successfully passed through the NPC (Fried and Kutay, 2003; Gorlich et al., 1997; Gorlich et al., 1996; Tetenbaum-Novatt and Rout, 2010; Wente and Rout, 2010). Adding to the complexity of mechanisms for nuclear entry, a recent report suggests that an importin-dependent nuclear import pathway can be accessed by proteins with conserved ankyrin repeats (Lu et al., 2014). Importins bind to a cargo protein by recognizing a short lysine or arginine-rich amino acid motif on the cargo protein known as a nuclear localization signal (NLS). Two NLSs in TRα1 have been fully characterized: NLS-1, a classical bipartite NLS in the hinge region (Baumann et al., 2001; Casas et al., 2006; Lee and Mahdavi, 1993; Maruvada et al., 2003; Mavinakere et al., 2012; Zhu et al., 1998) and, more recently, NLS-2, a novel, monopartite NLS in the N-terminal A/B domain (Mavinakere et al., 2012).

The karyopherin-β family is responsible for the majority of nuclear transport pathways, with each member performing a distinct nuclear import, export, or bi-directional transport function (Cook et al., 2007; Macara, 2001; Strom and Weis, 2001; Xu et al., 2010). Members of this family involved in nuclear import are characterized by their ability to either bind NLS-bearing cargo directly or indirectly via an adaptor importin (Cingolani et al., 2002; Lott and Cingolani, 2011; Palmeri and Malim, 1999). Importinβ1 is the best-studied member of the karyopherin-β1 family, which includes 10 other known family members that can mediate import of proteins into the nucleus (Lange et al., 2007; Mosammaparast and Pemberton, 2004; Pemberton and Paschal, 2005; Stewart, 2007; Strom and Weis, 2001). Most nuclear import occurs via direct binding of a karyopherin-β receptor to a cargo protein. In the classical nuclear import model, however, importinα acts

as an adaptor protein that recognizes and binds to a specific NLS motif on the cargo, and then binds importinα1 (Lange et al., 2007; Riddick and Macara, 2005, 2007). The human genome encodes at least six importinα isoforms: α1, α3, α4, α5, α6, and α7 (Friedrich et al., 2006). Each importinα isoform is responsible for binding to and facilitating import of several different cargo proteins in conjunction with importinβ1 (Cook et al., 2007; Goldfarb et al., 2004; Lange et al., 2010; Lange et al., 2007).

In the present study, we sought to characterize the general mechanism for TRα1 transport, using in vitro nuclear import assays. Additionally, we used RNA interference (RNAi), treatment with importazole, an importinβ1-specific inhibitor, and coimmunoprecipitation assays in HeLa cells to identify which importins mediate nuclear import of TRα1. Taken together, our *in vitro* and *in vivo* data suggest that TRα1 can follow two distinct temperature and energy-dependent, signal-mediated import pathways, with importin7, importinβ1, and the adapter importinα1 acting as major players in localizing TRα1 to the nucleus.

## Methods

### *Plasmids and recombinant proteins*

pGFP-TRα1 is an expression plasmid for functional green fluorescent protein (GFP)-tagged rat TRα1 (Bunn et al., 2001), and the expression vector for enhanced GFP, EGFP-C1, was obtained from Clontech Laboratories, Inc. (Mountain View, CA). The plasmid GFP-TRα1 encodes GFP-tagged human TRα1 (Mavinakere et al., 2012). The GFP-Glutathione-S-transferase (GST)-GFP (G3) expression vector, G3- A/BD

(containing NLS-2) expression plasmid, and G3-Hinge (containing NLS-1) expression plasmid were previously described (Mavinakere et al., 2012). The plasmid hTERT-GFP was a gift from R. H. Kehlenbach (University of Göttingen) and encodes GFP-tagged human telomerase reverse transcriptase (Frohnert et al., 2014). pGST-GFP-NLS was a gift from R. J.G. Haché (University of Ottawa) and expresses a fusion protein comprised of GST and GFP with the sequence of the simian virus 40 (SV40) T-antigen NLS (PKKKRKV) at the C terminus (Walther et al., 2003). pGEX-2T-T3Rα was a gift from M. Privalsky (University of California) and encodes GST-tagged TRα1 (Tzagarakis-Foster and Privalsky, 1998). Pre-designed SureSilencing™ short hairpin RNA (shRNA) plasmid sets, consisting of four different shRNA expression plasmids for each target mRNA, were purchased from SABioscience (Frederick, MD) for human importinα1 (KPNA2), importinα3 (KPNA4), importinα4 (KPNA3), importinα5 (KPNA1), importinα7 (KPNA6), importinβ1 (KPNB1), importin4 (IPO4), importin5 (IPO5), importin7 (IPO7), importin8 (IPO8), importin9 (IPO9), importin11 (IPO11), importin13 (IPO13), and a scrambled sequence negative control. The sequences of all shRNAs are provided as supplementary information (Table S1). 2xDR4-SV40-Luc was a gift from J. L. Jameson (Northwestern University), and consists of two copies of a positive, direct repeat TRE (DR+4) in the firefly luciferase vector pGL3. The plasmid pGL4.74 encodes Renilla luciferase (Promega, Madison, WI).

## *Protein purification and FITC labeling*

Recombinant GST-tagged TRα1 was bacterially expressed and purified by binding and elution from Glutathione-Sepharose 4B resin (GE Healthcare Life Sciences, Pittsburgh, PA), as described (Grespin et al., 2008). Protein samples were analyzed by

8% or 12% SDS-PAGE and protein concentration was estimated using a NanoDrop® ND-1000 full-spectrum UV/Vis Spectrophotometer. Samples were stored at -80ºC. For import assays, purified GST-TRα1 was labeled with fluorescein isothiocyanate (FITC) using a FluoReporter® Protein Labeling Kit (Life Technologies, Grand Island, NY), according to the manufacturer's instructions. The labeled sample was dialyzed against PBS overnight at 4ºC, and concentrated using Micron Ultracel YM-30 Centrifugal Filter Devices (Millipore, Bedford, MA). Samples were stored at -80ºC.

## *Permeabilized cell nuclear import assays*

HeLa cells (American Type Culture Collection [ATCC], #CCL-2) were cultured in Minimum Essential Medium (MEM) supplemented with 10% fetal bovine serum (FBS) (Life Technologies) at 37ºC under 5% $CO^2$ and 98% humidity. HeLa cells were seeded on 22 mm Coverslips for Cell Growth™ (Fisher Scientific, Pittsburgh, PA) in 6 well culture dishes at a density of 2-3 x $10^5$ cells per well. Sixteen to 24 h hours post-seeding the medium in each well was replaced with fresh MEM supplemented with 10% FBS. After 4 h, cells were washed 2X with 2 ml per well cold Import Buffer (20 mM HEPES, pH 7.3, 110 mM KOAc, 5 mM NaOAc, 2 mM Mg[OAc]2), then permeabilized with 50 µg/ml digitonin (Calbiochem, San Diego, CA) in Import Buffer for 4 min at room temperature. Cells were rinsed 1X with 2 ml per well cold Import Buffer for 10 min, and coverslips were then inverted over 50 µl drops of Import Reaction Mix (energy regeneration system composed of 5 mM creatine phosphate, 20 U/ml creatine phosphokinase, 0.5 mM ATP, and 0.5 mM GTP in Import Buffer; 0.67 mM FITC-labeled GST-TRα1; and 25 µl rabbit reticulocyte lysate or Import Buffer) on parafilm in a moist chamber for 30 min at 30ºC. For energy depletion, the energy regeneration system was replaced with apyrase (Grade

VIII, 100 U/ml, Sigma-Aldrich, St. Louis, MO). Subsequently, cells were fixed in 3.7% formaldehyde (Fisher Scientific) for 10 min, followed by a 5 min wash with Import Buffer. Coverslips were mounted on slides with Fluoro-Gel II mounting medium (Electron Microscopy Sciences, Hatfield, PA) containing the DNA counter stain 4′,6-diamidino-2′-phenylindole dihydrochloride (DAPI, 0.5 µg/ml). Cells were analyzed for nuclear localization of FITC-GST-TR α1 by fluorescence microscopy.

## *Importazole treatment*

HeLa cells were seeded on coverslips in 6 well culture dishes at a density of 2.0-2.5 x $10^5$ cells per well. Twenty-four hours post-seeding, cells were transfected with 2 µg of GFP-TRα1 or GFP-TRα1 expression plasmid using Lipofectamine 2000 (Life Technologies). The transfection medium was replaced with fresh MEM containing 10% FBS at 5 h post-transfection. Approximately 18 h later, cells were treated for 5 h with 50 uM importazole (Calbiochem) or an equivalent volume of ethanol (vehicle control). Cells were fixed in 3.7% formaldehyde, and coverslips were mounted with Fluoro-Gel II containing DAPI (0.5 µg/ml), and then analyzed for the cellular localization of GFP-TRα1 or GFP-TRα1 by fluorescence microscopy.

## *Analysis of nuclear localization by RNA interference (RNAi)*

HeLa cells were seeded on coverslips in 6 well culture dishes at a density of 2.0-2.5 x $10^5$ cells per well. Twenty-four hours post-seeding, cells were cotransfected with 1 µg of the appropriate set of four target-specific or control shRNA expression plasmids and 1 µg GFP-TRα1 expression plasmid using Lipofectamine 2000. The transfection medium was replaced with fresh MEM containing 10% FBS at 8 h post-transfection. At exactly 26

h post-transfection, cells were fixed and analyzed for the cellular localization of GFP-TRα1 by fluorescence microscopy. In pilot studies, a range of post-transfection incubation times (17 h, 24 h, 26 h, and 30 h) were tested. In addition, we varied the amount of Lipofectamine 2000 and the time cells were exposed to the reagent, selected for knockdown cells with puromycin, and varied the shRNA plasmid amounts and combinations. The conditions described above showed high transfection efficiency (50-70% of cells were transfected), reduced the levels of importins in cells, and retained cell viability. Altered conditions either decreased transfection efficiency, decreased knockdown efficiency, or led to increased cell mortality. Cell mortality was assessed by visual inspection of the number of adherent cells before and after transfection, with the standard set at >60% retention.

## *Validation of RNAi by real-time quantitative PCR (RT-qPCR)*

HeLa cells were seeded on 100 mm vented plates at a concentration of 6 x $10^5$ cells per plate in MEM supplemented with 10% FBS. Twenty-four hours post-seeding, each plate was transfected with 10 µg of a set of four target-specific or control shRNA expression plasmids using Lipofectamine 2000. The transfection medium was replaced with fresh MEM containing 10% FBS at 8 h post-transfection. At exactly 26 h post-transfection, total RNA was purified using the AurumTM Total RNA Mini Kit (Bio-Rad, Hercules, CA), following the Spin Protocol for Cultured Mammalian Cells with a 30 min DNase I digestion. Only RNA samples with A260:A280 ratios greater than 2.0 and A260:A230 ratios greater than 1.7 were used. RNA quality and integrity was further analyzed using an RNA 6000 Pico Total RNA Assay and the Agilent 2100 BioAnalyzer's Lab-on-a-Chip technology (Santa Clara, CA).

cDNA was synthesized using SABioscience RT2 First Strand Kit and 0.74 µg total RNA. This amount of total RNA was within the manufacturer's recommended range, and was selected to standardize all cDNA synthesis reactions. Samples for real-time quantitative PCR (RT-qPCR) were set up in a 48-well plate, using RT2 SYBR Green/Fluorescein qPCR Master Mix (SABioscience) and SABioscience validated RT2-qPCR primers specific for importins7, β1, α1, α3, α4, α5, α7, or glyceraldehyde-3-phosphate dehydrogenase (GAPDH) as an internal control. No Template controls and No Reverse Transcription controls also were included for each sample. Plates were centrifuged for 90 sec at 500 xg in a Peqlab PerfectSpin plate spinner (VWR International, Radnor, PA), then analyzed using an Applied Biosystems StepOneTM Real-Time PCR machine (Life Technologies) as follows: 10 min at 95°C, then 40 cycles of 15 sec at 95°C, 35 sec at 55°C, and 30 sec at 72°C. SYBR Green fluorescence was detected and recorded during the annealing step of each cycle. A melting curve analysis was performed as a quality control measure. RT-qPCR data were analyzed by the ΔΔCt (Livak) method (Livak and Schmittgen, 2001) using StepOneTM software, and validated by manual calculation.

## *Validation of RNAi by immunoblotting*

Twenty-six hours' post-transfection, HeLa cell protein lysates were prepared and analyzed by immunoblotting as described (Subramanian et al., 2015). Antibodies were used with the following concentrations: anti-GAPDH (Santa Cruz Biotechnology Inc, Dallas, TX), 1:5000; anti-importinβ1 (Santa Cruz), 1:2000; anti-importin4 (Santa Cruz), 1:333; anti-importin5 (Santa Cruz), 1:10,000; anti-importin7 (Abcam, Cambridge, MA), 1:1000; anti-importin8 (Abcam), 1:250; anti-importin9 (Abcam), 1:250; anti-importin11

(Abcam), 1:333; anti-importin13 (Santa Cruz), 1:100; anti-importinα1 (Santa Cruz), 1:2000; anti-importin α3 (Thermo Scientific), 0.2 µg/ml; horseradish peroxidase (HRP)-conjugated donkey anti-rabbit IgG (GE Healthcare Life Sciences), 1:25,000; HRP-sheep anti-mouse IgG (GE Healthcare Life Sciences), 1:25,000; or HRP-mouse anti-goat IgG (Santa Cruz Biotechnology), 1:25,000. Protein size was confirmed using Pre-Stained Kaleidoscope Protein Standards (Bio-Rad, Hercules, CA). X-ray films were quantified by scanning densitometry using NIH ImageJ software.

## *Cell scoring by fluorescence microscopy and statistical analysis*

For some analyses an inverted Nikon ECLIPSE TE 2000-E fluorescence microscope (Nikon Ultraviolet Excitation: UV-2E/C filter block for DAPI visualization; Blue Excitation: B-2E/C filter block for GFP/ FITC visualization) was used with a Nikon Plan Apo 40x/0.95objective. A CoolSNAP HQ2 CCD camera (Photometrics, Tucson, AZ) and NIS-Elements AR software (Nikon) were used for image capture. For other analyses an Olympus BX60 microscope (U-MNU filter cube for DAPI; Omega Optical XF100-2 for GFP) was used with an Olympus 40xUPlanFL 40x/0.75 objective. A Cooke SenisCamQE camera and IPlab software (BD Biosciences Bioimaging Rockville, MD) were used for image capture. Images were presented using Adobe Photoshop/Illustrator.

For permeabilized cell *in vitro* nuclear import assays, the localization of FITC-GST-TRα1 was scored as “nuclear” when there was a detectable accumulation of fluorescence within the nucleus. FITC-GST-TRα1 that did not accumulate in the nucleus diffused out into the drop of Import Buffer (see Section 2.3), since the cells were permeabilized. Import assays consisted of 4 to 5 independent, biological replicates, with 200 cells scored per

replicate. For RNAi experiments, the localization of GFP-TRα1 was scored in one of three categories: completely nuclear, nuclear and cytoplasmic (with distinct accumulation in the nucleus), or whole cell (with no distinct nuclear accumulation). RNAi experiments consisted of 3 independent, biological replicates, with 100 cells scored per replicate. To ensure consistency in scoring criteria, slides were randomly selected for cross-checking by other lab members. In all experiments, the integrity and morphology of the DAPI-stained nuclei was assessed visually, and only cells with intact nuclei were scored. All cell counts were performed blind, without prior knowledge of the treatment. The slides' original labels were removed and replaced with random numbers by another lab member, who made a key and kept it secure until scoring was completed and data were analyzed. For some RNAi experiments, one lab member set up the transfection and prepared slides, while another lab member scored the slides blind. Data were quantified as the percentage of cells in a given category (e.g., % of cells with a primarily nuclear distribution of TRα1) and presented as bar graphs. Bars indicate the mean percentage of cells in a given category, and error bars indicate plus or minus the standard error of the mean (± SEM). Statistical differences between two groups were determined using an unpaired Student's t test with two-tailed P value. Results were considered significant at $P<0.05$.

## *Luciferase reporter gene assay*

Cells were seeded at $2.0 \times 10^4$ per well in a 96-well plate (PerkinElmer, Waltham, MA). Seventeen hours after seeding, cells were transiently transfected with 100 ng DNA, containing 25 ng each of expression plasmids for GFP-TRα1, TRE (DR+4)-firefly luciferase reporter, Renilla luciferase internal control, scrambled shRNA control or a set of four target-specific shRNAs. Transfection medium was replaced with complete medium

8 h post-transfection. Fourteen hours post-transfection, complete medium was replaced with 100 µl MEM containing 10% charcoal-dextran stripped FBS (Life Technologies), supplemented or not with 100 nM 3,3′,5-triiodo-L-thyronine (T3, Sigma-Aldrich). After an additional 12 h, a Dual-Glo® Luciferase Assay (Promega) was performed, according to the manufacturer's protocol, using 100 µl of reagent per well. Four independent, biologically separate replicate experiments were performed, with 8 wells assayed per treatment. Data were analyzed for statistical significance.

## *GFP-Trap_A coimmunoprecipitation*

HeLa cells were seeded on 100 mm vented plates at a concentration of 9 x $10^5$ cells per plate in MEM supplemented with 10% FBS. Twenty-four hours post-seeding, each plate was transfected with expression plasmids encoding GFP, GFP-TRα1, hTERT-GFP, GST-GFP-NLS, GFP-TRα1, GFP-GST-GFP (G3), G3-A/BD, or G3-Hinge, using Lipofectamine 2000. After 26 h, cells were washed with ice-cold Dulbecco's phosphate-buffered saline (PBS), treated for 3 min with 0.7 ml of 0.25% trypsin (Life Technologies), collected in 1.0 ml MEM supplemented with 10% FBS, then transferred to 2.0 ml microcentrifuge tubes. Cells were washed 2X with Dulbecco's PBS, then lysed in 200 µl of Lysis Buffer (10 mM Tris-HCl, pH 7.2, 150 mM NaCl, 0.5 mM EDTA) containing 0.5% IGEPAL$^R$ (NP-40 equivalent, Sigma-Aldrich) and 1X Halt Protease Inhibitor Cocktail (Thermo Scientific). Cells were incubated for 30 min on ice, with thorough pipetting every 10 min. The lysate was cleared by centrifugation at 4°C, 16,000 x g for 10 min, and the supernatant was transferred to a new tube and diluted with 300 µl of Dilution/Washing Buffer (2 mM Tris-HCl, pH 7.5, 30 mM NaCl, 0.1 mM EDTA), containing 1X Halt Protease Inhibitor Cocktail, to yield a final concentration of 0.2% IGEPAL. GFP-trap agarose beads

(GFP-Trap$^{R}$_A, Chromotek GmbH, Planegg-Martinsried, Germany) were pre-equilibrated by washing 3X with Dilution/Washing Buffer, then 20 µl were added to each diluted supernatant. After 2.5 h of incubation at 4°C with end-over-end rotation, beads were centrifuged at 4°C, 3000 x g for 4 min. A 50 µl sample of the supernatant (unbound proteins) was collected and resuspended with an equal volume of 2X Sample Buffer (2% SDS, 10% glycerol, 250 mM Tris-HCl, pH 6.8, 0.01% bromophenol blue, 20 mM DTT). The beads were washed 3X with 100 µl Dilution/Washing Buffer lacking IGEPAL, then resuspended in 100 µl of 2X Sample Buffer. Samples of unbound and bound proteins (20 ul) were analyzed by immunoblotting (see Section 2.7), using SuperSignal$^{TM}$ West Femto Maximum Sensitivity Substrate (Thermo Scientific). Antibodies were used at the following concentrations: anti-GFP (Santa Cruz), 1:2000; anti-importin4 (Abcam), 1:1250; anti-importin7 (Abcam), 1:1000; anti-importinβ1 (Santa Cruz), 1:1000; anti-importinα1 (Abcam), 1:1000; horseradish peroxidase (HRP)-conjugated donkey anti-rabbit IgG (GE Healthcare Life Sciences), 1: 25,000 or 1: 33,000.

## Results

### TRα1 follows a signal-mediated import pathway in HeLa cells

Our prior studies showed that TRα1 follows both signal-mediated and passive diffusion import pathways in Xenopus oocytes (Bunn et al., 2001). We also showed that there is an energy-requiring step in the nuclear retention or nuclear export process in mammalian cells; however, we did not address the import mechanism in mammalian cells. Given the specialized nature of these amphibian oocytes, it was of interest to

determine whether TRα1 would follow a signal-mediated import pathway in mammalian cells. To this end, permeabilized HeLa (human) cell in vitro nuclear import assays (Adam et al., 1990) were used to address this question.

To test whether soluble factors are required for nuclear entry of TRα1, FITC-labeled recombinant GST-TRα1 was used for import assays in the presence or absence of rabbit reticulocyte lysate (RRL), as a cytosol replacement. In the presence of RRL, TRα1 was able to translocate into the nucleus from its starting point in the cytoplasm. After 30 min incubation at 30°C, on average 61% of cells showed a predominantly nuclear localization of TRα1. In the absence of RRL, TRα1 showed a significantly different localization pattern (Fig. 1, A and B; P=0.00001); the receptor did not accumulate in the nucleus, and formed aggregates or showed fluorescent staining of the nuclear periphery, an indicator of binding at the NPC without subsequent translocation (Newmeyer and Forbes, 1988). On average, TRα1 was only localized to the nucleus in 11% of cells.

Next, we sought to determine whether TRα1 import was temperature-dependent. Chilling has been shown to abolish active transport while only marginally affecting passive transport (Breeuwer and Goldfarb, 1990; Freedman and Yamamoto, 2004). However, given that FITC-GST-TRα1 is 73 kDa in size, this likely would preclude rapid passive diffusion through the NPCs regardless of temperature. Import reactions were incubated at 4°C for 30 min. Nuclear import of FITC-GST-TRα1 was significantly inhibited in chilled cells (Fig. 1, A and B; P=0.007); on average, only 26% of cells showed nuclear accumulation of TRα1. Nuclear import could be fully restored, however, by further incubation at 30°C (P=0.584). Reversible inhibition suggests that chilling blocked TRα1

import by inhibiting specific transport components, rather than by preventing import by way of non-specific cellular damage (Bunn et al., 2001).

To further characterize the energy requirements for nuclear import of TRα1 in permeabilized HeLa cells, the effects of energy depletion were studied by apyrase treatment, which depletes cellular ATP and GTP (Bunn et al., 2001). Import assays were performed in the presence of RRL, as a cytosol replacement, and in the presence of an energy regeneration system or apyrase (Fig. 1, A and B). Incubation at 30ºC for 30 min with apyrase significantly inhibited nuclear accumulation of FITC-GST-TRα1 ($P=0.025$). On average, only 40% of cells showed nuclear localization of TRα1, compared to reactions containing RRL and an energy regeneration system in which TRα1 was localized primarily to the nucleus in 61% of cells. However, TRα1 import in the presence of apyrase was not inhibited to the same extent as import in the absence of RRL, where only 11% of cells showed nuclear accumulation of TRα1.

Soluble factor dependence, chilling inhibition, and energy dependence are commonly used criteria when establishing a signal-mediated import pathway (Carazo et al., 2012; Dhanoya et al., 2013; Umemoto and Fujiki, 2012; Vazquez-Iglesias et al., 2009, 2012), and thus demonstrate a requirement for signal-mediated nuclear import of TRα1 in HeLa cells. To begin to characterize the soluble components required for nuclear localization of TRα1, we turned to an in vivo approach to evaluate the role of a panel of importins in promoting TRα1 nuclear import in HeLa cells.

## Knockdown of importinβ1 and importin7 reduces TRα1 nuclear localization

RNAi is a powerful tool for knockdown of the expression of a specific gene in vivo by targeting its mRNA for degradation. We chose to use importin-specific shRNA expression plasmids, to ensure sustained depletion of protein levels. Since TRα1 is primarily nuclear at steady-state, but shuttles between the nucleus and the cytosol, effective knockdown of an essential import factor would be predicted to result in a shift to a more cytoplasmic distribution of TRα1 over time. It is important to note, however, that it was not expected that cells would ever show a fully cytoplasmic distribution of TRα1 for a number of reasons. First, RNAi leaves a residual portion of target mRNA and protein in cells. Second, a wholly cytoplasmic distribution would depend on the complete export of all nuclear TRα1, which is unlikely as it is strongly retained in the nucleus by interaction with target genes.

Although the classical importinα1/β1 import pathway is widely used by nuclear proteins, and was thus a priority to investigate, other import pathways exist. Of particular interest for this study, importin7 mediates nuclear import of a diversity of cargos including the glucocorticoid receptor (Chook and Suel, 2011; Strom and Weis, 2001). Thus, we also evaluated importin7 for its role in promoting TRα1 nuclear localization. First, shRNA-induced knockdown of importinβ1 and importin7 mRNA was validated by RT-qPCR and protein levels were quantified by immunoblot analysis. Twenty-six hours post-transfection with shRNA expression plasmids, the levels of importinβ1 and importin7 mRNA in HeLa cells were reduced to 21% and 19%, respectively, relative to the control shRNA (set to 100%) (Fig. 2A). Importinβ1 and importin7 protein levels were reduced to 56% and 49%,

respectively, relative to the scrambled control (Fig. 2B), indicating the efficacy of the RNAi system. Control immunoblots also confirmed the specificity of shRNA-mediated knockdown of importin7, importinα1, and importinβ1; shRNA-targeting a particular importin did not exhibit any cross-inhibition of another importin (Fig. 2C).

Next, in a parallel experiment, the effect of importinα1 and importin7 knockdown on the cellular localization of GFP-TRα1 at 26 h post-transfection was assessed by fluorescence microscopy. Knockdown of importinβ1 resulted in a significant shift in localization of TRα1 to a more cytoplasmic distribution (P=0.002); on average only 72% of cells showed TRα1 primarily localized to the nucleus, compared with 86% of cells in the presence of control shRNA (Fig. 3, A and B).

Knockdown of importin7 caused a significant shift in localization of TRα1 to a more cytoplasmic distribution (Fig. 3, A and B; P=0.0001); on average, only 66% of cells showed TRα1 localized to the nucleus, with a concomitant increase in the number of cells with a whole cell distribution of TRα1. In addition, many of these cells were marked by numerous small cytoplasmic or perinuclear aggregates of TRα1. Such an accumulation of foci was typically not observed upon knockdown of the other importins tested. Interestingly, knockdown of importin7 has been shown to alter nucleolar morphology, resulting in a more punctate distribution of fibrillarin (Golomb et al., 2012). Taken together our findings suggest that both importin β1 and importin7 play key roles in promoting nuclear localization of TRα1 in vivo.

## Knockdown of importinα1 reduces TRα1 nuclear localization

In an effort to further characterize additional importins playing a role in the signal-

mediated import pathway, the adaptor importinsα1, α3, α4, α5, and α7 were screened as well. Importinα6 was excluded from the analysis because its expression appears to be limited to the testis (Chook and Suel, 2011). These importins are known to mediate import in conjunction with importinβ1 in the classical nuclear import pathway. We were unable to achieve sufficient knockdown of the levels of importinα5 mRNA; levels only were reduced to 68% relative to the control shRNA with the set of four shRNA expression plasmids used. Thus, further analysis of this adaptor protein was not performed. In contrast, levels of importinα1 mRNA were knocked down to 23% of control levels, while levels of importinα3, α4, and α7 mRNA were knocked down to 5%, 16%, and 8%, respectively (Fig. 4A). Accordingly, levels of importinα1, α3, and α7 proteins were knocked down to 55%, 49%, and 49%, respectively, compared with the scrambled control (Fig. 4B). At the time this study was performed, no antibodies were available for importinα4, so we were only able to assess knockdown via RT-qPCR in this case.

Knockdown of importinα1 resulted in a significant shift of TRα1 towards a more cytoplasmic distribution (Fig. 4, C and D; P=0.025); on average, only 71% of cells showed a primarily nuclear localization of TRα1, compared to 86% of cells in the shRNA control (Fig. 4, C and D). There was no significant change in nuclear localization in cells depleted of importinα3 (P=0.190), importinα4 (P=0.425) and importinα7 (P=0.721) (Fig. 4D), although results with importinα7 were highly variable between replicates. These findings suggest that importinα1 is the main adaptor acting with importinβ1 for nuclear localization of TRα1.

We thought that dual knockdown with combinations of shRNA against importin β1/importinα1 or importin7/importinα1 might have a greater impact than single

knockdowns. However, these combinations did not result in further shifts in the distribution pattern of TRα1, although this could well be due to increased cell mortality. These importins are required for nuclear localization of many other proteins involved in essential cell processes. In addition, since cellular microRNAs (miRNAs) regulate the expression of hundreds of genes, saturation of the RNAi pathway with exogenous shRNA also could contribute to loss of cell viability (Castanotto and Rossi, 2009; Scherr and Eder, 2007). Further, it is likely that the primarily nuclear location of TRα1 at steady-state limits how much the distribution pattern can be altered over the time course of an experiment. We found that extending the time course for knockdown of importins beyond 26 h post-transfection caused a marked decrease in cell viability, in particular for importinβ1. This is consistent with a report that reduced levels of importinβ1 are more harmful to a cell than reduction in the levels of importinβ (Quensel et al., 2004).

## Nuclear import of TRα1 and TRα1 is inhibited by importazole

To provide further evidence that importinβ1 plays a role in mediating TRα1 nuclear localization, we made use of importazole, a small molecule inhibitor of this pathway. Importazole specifically blocks importinβ1-mediated nuclear import, without disrupting transportin-mediated nuclear import or CRM1-mediated nuclear export (Soderholm et al., 2011). Treatment of GFP-TRα1-expressing HeLa cells with importazole resulted in a 16% reduction in nuclear localization of TRα1 compared with cells treated with the vehicle control (P=0.000001) (Fig. 5A), providing further support for a central role of importinβ1 in TRα1 nuclear localization.

The nuclear localization signal, NLS-1, in the hinge domain of TRα1 is conserved in the other major TR subtype, the thyroid hormone receptor β1 (TRβ1); however, NLS-2 in the A/B domain of TRα1 is absent from TR β1 (Mavinakere et al., 2012). TR β1 typically has a small cytosolic population at steady-state, suggesting that its distinct distribution pattern may reflect an altered balance of nuclear import and nuclear export activity, relative to TRα1. We thus included TRβ1 in our analysis to provide a means of teasing apart whether importin7 and the importinβ1/α1 heterodimer interact selectively with one or the other NLS. Treatment of GFP-TRβ1-expressing HeLa cells with importazole resulted in a 12% reduction in nuclear localization of TRβ1 compared with cells treated with the vehicle control (P=0.001) (Fig. 5B), suggesting that importinβ1 plays a role in TR β1 nuclear localization, and that the interaction is mediated by the hinge domain NLS-1.

## Analysis of other import pathways

Having shown that TRα1 localization is influenced by knockdown of importin7, importinα1, and importinβ1, the question still remained of whether additional pathways for nuclear entry are followed by TRα1. To determine whether other importins play a role in TRα1 nuclear localization, we screened the remainder of the well-characterized importins (Chook and Suel, 2011; Kimura and Imamoto, 2014). Given the structural similarity between importin4 and importinβ1 (Pradeepa et al., 2008), and that importin4 mediates import of another member of the nuclear receptor superfamily, the vitamin D receptor (Miyauchi et al., 2005), we predicted that importin4 might also influence TRα1 accumulation. Many cargoes that are primarily imported by importin4 also use importin5 as an alternative pathway (Chook and Suel, 2011). Thus, we predicted that if importin4 was a mediator of TRα1 import, then knockdown of importin5 would have no effect on

TRα1 nuclear localization when importin4 was present in the cell. Importin8 is structurally similar to importin7 (Chook and Suel, 2011; Weinmann et al., 2009), so it was also conceivable that this importin could play a role in TRα1 import. In addition, importin13 has been shown to be one of the importins that mediates glucocorticoid receptor import (Tao et al., 2006), so importin13 also appeared to be a likely candidate. Importin9 imports some ribosomal proteins (Jakel et al., 2002) and nuclear actin (Kimura and Imamoto, 2014), while importin11 imports the ubiquitin-conjugating enzyme, UbcM2 (Plafker and Macara, 2000). No role has yet been reported for these karyopherins, or for transportins1 and 2 (Twyffels et al., 2014), in import of nuclear receptors, so they were considered less likely candidates. In a separate study focused on TRα1 nuclear export pathways, we confirmed that transportins1 and 2 are not involved in nuclear import (or export) of TRα1 (Subramanian et al., 2015).

Efficacy of knockdown was assessed by immunoblotting (Fig. 6A), with levels of knockdown relative to the scrambled control as follows: importin4, 61%; importin5, 63%; importin8, 65%; importin9, 51%, importin11, 55%, and importin13, 59%. There was no significant change in nuclear localization of TRα1 in cells depleted of importin4 (P=0.99), importin5 (P=0.34), importin8 (P=0.60), importin9 (P=0.89), importin11 (P=0.55), and 13 (P=0.70), relative to the scrambled control (Fig. 6, B and C). Taken together, these data indicate that importins4, 5, 8, 9, 11, and 13 either play no role in localizing TR to the nucleus, or are minor, nonessential mediators of nuclear localization, relative to importin7 and the importinβ1/ α1 heterodimer.

Given that TRα1 is a transcription factor that either represses or stimulates expression of T3-responsive genes, we sought to ascertain whether the cytoplasmic shift

in TRα1's distribution resulting from knockdown of importins7, α1, or β1 would reduce TRα1-mediated gene expression to a comparable extent. A firefly luciferase reporter gene under the positive control of a thyroid hormone response element (TRE) was used to examine ligand-dependent transactivation by GFP-TRα1 (Fig. 7), in the presence of shRNAs specific for importin4 (no cytoplasmic shift), importinα1, importin7, or importinβ1. Fold stimulation in the presence of importin-specific shRNAs was not significantly different compared with fold stimulation in the presence of the scrambled shRNA control (importin 4, P=0.62; importinα1, P=0.09; importin7; P=0.24; importinβ1, P=0.27), indicating that under these conditions a reduction in nuclear TRα1 of 14-20% does not have a measurable impact on reporter gene expression. As noted earlier, these importins are required for nuclear localization of many other proteins involved in transcriptional regulation. Importin knockdown is not specific for TRα1 import and, thus, may impact transcriptional output in complex, unanticipated ways.

## Importin7, importinα1, and importinβ1 interact with TRα1

Since knockdown of importin7, importinα1, and importinβ1 leads to a significant shift in TRα1 localization to a more cytoplasmic distribution, we sought to ascertain whether this shift correlates with protein-protein interactions. To confirm that these importins interact with TRα1 in vivo, we performed "GFP-trap" coimmunoprecipitation assays on lysates from HeLa cells that had been transfected with expression plasmids for GFP, GFP-TRα1 or GST-GFP-NLS, a fusion protein containing the classical SV40 NLS (Lange et al., 2010; Walther et al., 2003) (Fig. 8). We confirmed that GFP, GFP-TRα1 and GST-GFP-NLS were all successfully immunoprecipitated by the GFP-trap assay, by immunoblot analysis of immunoprecipitate samples with anti-GFP antibodies

(Fig. 8A). Samples of unbound proteins (immunosupernatant) and bound proteins (immunoprecipitates) were also analyzed for the presence of different importins on separate blots using importin-specific antibodies (Fig. 8B). Endogenous importinα1, importinβ1, and importin7 were coimmunoprecipitated (trapped) with GFP-TRα1, but not with GFP, indicating that these transport factors specifically interact with TRα1 in vivo, either as part of a complex (e.g., importinβ1 via the adaptor importinα1) or separately. In contrast, GST-GFP-NLS trapped importinα1 and importinβ1, but did not interact with importin7 (Fig. 6B). As a positive control for the method we also confirmed that importin7 coimmunoprecipitated with hTERT-GFP (data not shown), as this interaction had been reported previously (Frohnert et al., 2014). Finally, we used importin4 as a negative control, since knockdown of cellular levels of importin4 had no effect on TRα1 localization. As expected, importin4 was not trapped by GFP, GFP-TRα1, or GST-GFP-NLS (Fig. 8B), further validating the RNAi screen as a predictive tool for assessing the role of different importins in mediating nuclear import.

To examine whether importin7 and the importinβ1/ α1 heterodimer interact selectively with NLS-1 (hinge domain) or NLS-2 (A/B domain) in TRα1, we used two different approaches. First, we investigated whether TRα1, which only contains NLS-1, interacts with these importins, using the GFP-trap assay. Samples of unbound proteins (immunosupernatant) from GFP-TRα1-expressing HeLa cell lysates and bound proteins (immunoprecipitates) were analyzed for the presence of “trapped” importins by immunoblotting using importin-specific antibodies (Fig. 8C). Endogenous importinβ1 and the adaptor importinα1 were coimmunoprecipitated with GFP-TRα1, but not with GFP (in some assays there was a trace amount of non-specific trapping of importins by GFP),

indicating that these transport factors specifically interact with TRα1 in vivo. In contrast, importin7 did not show interaction above background levels with GFP-TRα1 (Fig. 8C).

In a second approach, we investigated whether the TRα1 hinge domain or the A/B domain alone, fused with GFP-GST-GFP (G3) interacted with these importins. We have previously shown that G3-Hinge has a predominantly nuclear localization, comparable to full-length TRα1, whereas only around 50% of cells show a predominantly nuclear localization of G3-A/BD (Mavinakere et al., 2012), indicating that NLS-2 is less efficient in facilitating nuclear import in isolation. HeLa cells were transfected with expression plasmids for G3, G3-Hinge, or G3-A/BD and immunoprecipitated by the GFP-trap assay. Samples of unbound proteins and bound proteins were analyzed for the presence of G3 fusion proteins with GFP-specific antibodies (data not shown), and with the different importins on separate blots using importin-specific antibodies (Fig. 8D). Endogenous importinα1 and importinβ1 were coimmunoprecipitated (trapped) with both G3-Hinge and G3-A/BD, indicating that these transport factors specifically interact with NLS-1 and NLS-2 in vivo. In contrast, no consistent interaction above background levels was observed between importin7 and G3-Hinge or G3-A/BD (Fig. 8D).

Taken together, we conclude from these results that TRα1 nuclear import is facilitated by importin7, likely through interactions with NLS-2, and importinβ1 and the adapter importin α1 interacting with NLS-1 and NLS-2, while TRβ1 nuclear import is facilitated by importinβ1/ α1 interacting with NLS-1. Further studies with purified recombinant proteins in vitro will be required to confirm this model, since we were not able to show direct interaction between importin 7 and NLS-2 in this study. When taken

out of the context of the full protein, the A/B domain NLS-2 may not be exposed in a way that promotes stable binding under the conditions of the GFP-trap assay.

## Discussion

Our interest for many years has been in the complex mechanisms regulating the subcellular distribution of TRα1. The emerging picture is one of a finely balanced, dynamic process in which TRα1 shuttles between the nucleus and cytoplasm. Here, we have further investigated the pathway by which TRα1 enters the nucleus, using in vitro nuclear import assays, importin-specific shRNAs and a small molecule inhibitor of importinβ1, in combination with localization assays in transfected cells and coimmunoprecipitation assays to confirm interacting partners. The results of this research show that TRα1 can enter the nucleus by more than one pathway; both IPO7 and the classical IPOβ1/α1 heterodimer mediate TRα1 nuclear import.

The use of more than one pathway by individual cargos is not without precedent. A striking example is the human immunodeficiency virus type 1 Rev protein which binds specifically to importinβ1, transportin1, importin5, and importin7 (Arnold et al., 2006). Importin7 is a notably versatile karyopherin and often plays a shared role with other karypherin-β family members in importing cargo, ranging from ribosomal proteins (Jakel and Gorlich, 1998) and histones (Baake et al., 2001; Muhlhausser et al., 2001) to transcription factors, such as c-Jun (Waldmann et al., 2007) and Smad3 (Chuderland et al., 2008). Adding to its versatility, importin7 can mediate import either as a monomer or as an importin7/importinβ1 heterodimer (Chook and Suel, 2011).

There is ample evidence that other members of the nuclear receptor superfamily are imported via multiple pathways. For example, the glucocorticoid receptor (GR) contains two NLSs, NL1 and NL2, each of which has been shown by in vitro binding assays to interact directly with importin7 and importin8, but only NLS1 was able to bind the importinβ/α heterodimer. Further, only importin7 and the importinβ/α heterodimer were able to import an NL1-containing fragment of GR in an in vitro import assay (Freedman and Yamamoto, 2004). In addition, GST pull-down and coimmunoprecipitation assays have shown that importin13 also binds GR, and silencing of importin13 by RNAi inhibits nuclear import of GR (Tao et al., 2006). The androgen receptor also contains two NLSs and import is mediated via two pathways: one that is dependent on importinα1/β1, and one that is importinα1/β1-independent (Cutress et al., 2008; Kaku et al., 2008).

The six identified mammalian importin α adaptors are ubiquitously expressed, with the exception of testis-specific importinα6 (Kelley et al., 2010; Kohler et al., 1999). Although interchangeable for many substrates in vitro, there are reports of preferential use of specific importinα adapters in vivo; for example, for NF-κB (Fagerlund et al., 2005), STAT3 (Liu et al., 2005), the Ran guanine nucleotide exchange factor, RCC1 (Friedrich et al., 2006; Quensel et al., 2004), and STAT5a (Shin and Reich, 2013). Our findings suggest that only importinα1 plays a key role in mediating import of TRα1, adding to the preferential use of this adaptor in vivo.

The critical role of nuclear import as a control point for modulating thyroid hormone-responsive gene expression is apparent, but the physiological significance of multiple import pathways remains to be determined. Our prior studies have shown that the hinge

region of TRα1 contains NLS-1, a classical, bipartite NLS ($^{130}$KRVAKRKLIEQNRERRRK$^{147}$; Mavinakere et al., 2012). Data presented here indicate that import from this classical NLS is mediated by importinsα1 andβ1 acting together. TRα1 also harbors a second, non-classical NLS, NLS-2, in the N-terminal A/B domain ($^{22}$PDGKRKRK$^{29}$; Mavinakere et al., 2012). TR α1 only harbors NLS-1 (Mavinakere et al., 2012) and, as shown here, does not interact with importin7. By default, this suggests that the novel monopartite NLS-1 in TRα1 provides the signal for use of an alternative pathway for nuclear entry facilitated by importin7, at a different time, or in a cooperative fashion with the classical NLS to enable complete, efficient TRα1 import. Additional analyses of protein-protein interactions by in vitro binding assays with purified proteins should help to identify and clarify whether this NLS interacts directly with an importin7 monomer, or potentially with an importin7/importin β1 heterodimer, and will allow fuller elucidation of how multiple pathways serve to regulate nuclear entry in response to cell-specific signals.

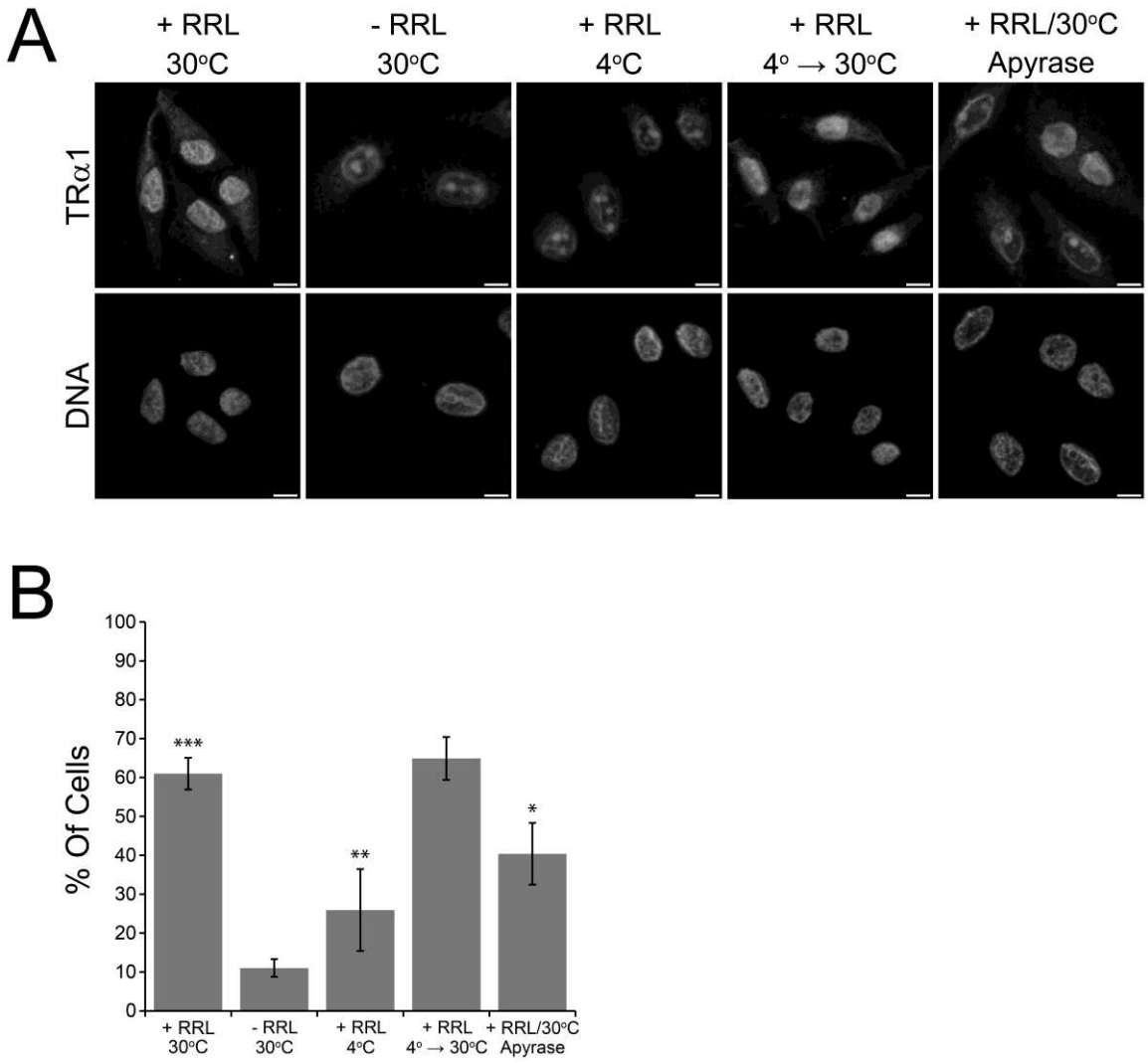


**Fig. 1.** *In vitro* nuclear import of TRα1 requires soluble factors and is temperature and energy-dependent. (A) Digitonin-permeabilized HeLa cells were incubated with import reaction mix containing FITC-GST-TRα1 as substrate, under the conditions indicated: 30ºC or 4ºC followed by 30ºC, with an energy regeneration system or apyrase, and in the presence or absence of rabbit reticulocyte lysate (RRL) as a source of replacement cytosol. After 30 min, samples were fixed, mounted, and viewed by fluorescence microscopy. In the presence of RRL, TRα1 was localized to the nucleus. In the absence of RRL, and in chilled or energy-depleted cells, TRα1 did not accumulate in the nucleus. Scale bar = 10 μm. (B) Quantification of TRα1 nuclear localization. Bars indicate the mean percentage of cells with nuclear accumulation of TRα1 (n=4-5 independent, biologically separate replicate experiments, with 200 cells per replicate) and error bars indicate ± SEM. ***$P$<0.001; **$P$<0.01; *$P$<0.05.

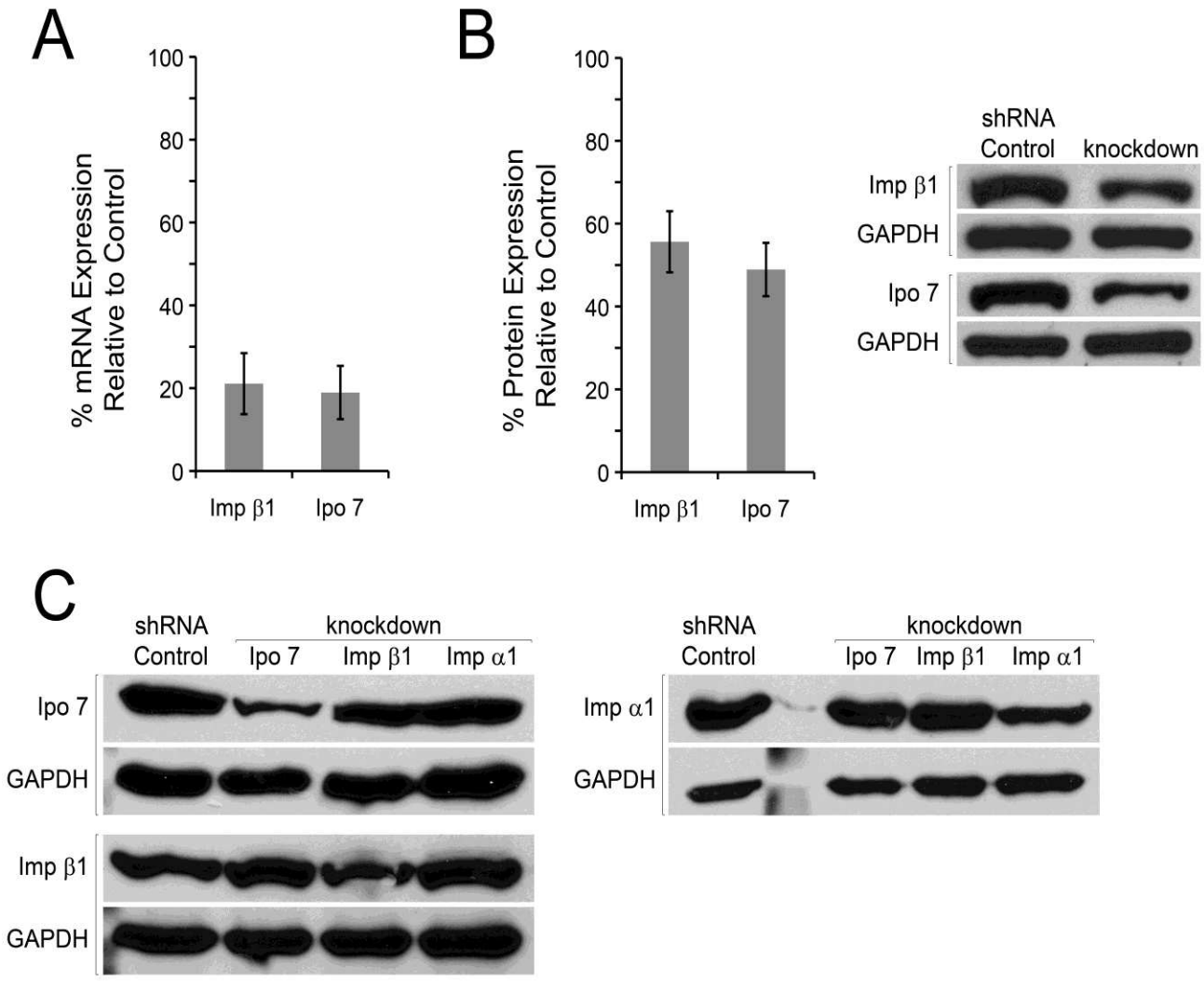


**Fig. 2.** RNAi specifically knocks down selected importins. (A) HeLa cells were transfected with importin-specific shRNA plasmids or a scrambled shRNA plasmid as a control, as indicated. RT-qPCR was used to confirm knockdown of importin mRNA levels. Bars indicate the mean relative expression level of importin mRNA in cells treated with importin-specific shRNA versus control cells, normalized to the levels of the housekeeping mRNA GAPDH. Error bars indicate ±SEM (n=3 independent, biologically separate replicates). (B) Immunoblot analysis was used to confirm knockdown of importin protein levels, as indicated. Bars indicate the mean relative expression level of importin proteins in cells treated with importin-specific shRNA (knockdown) relative to cells treated with the scrambled shRNA control, normalized to levels of GAPDH. Error bars indicate ±SEM (n=3 independent, biologically separate replicates). (C) Knockdown is specific for the selected importin. Immunoblot analysis was used to confirm that knockdown of a target importin with a specific shRNA, as indicated, did not have an effect on expression levels of other importins.

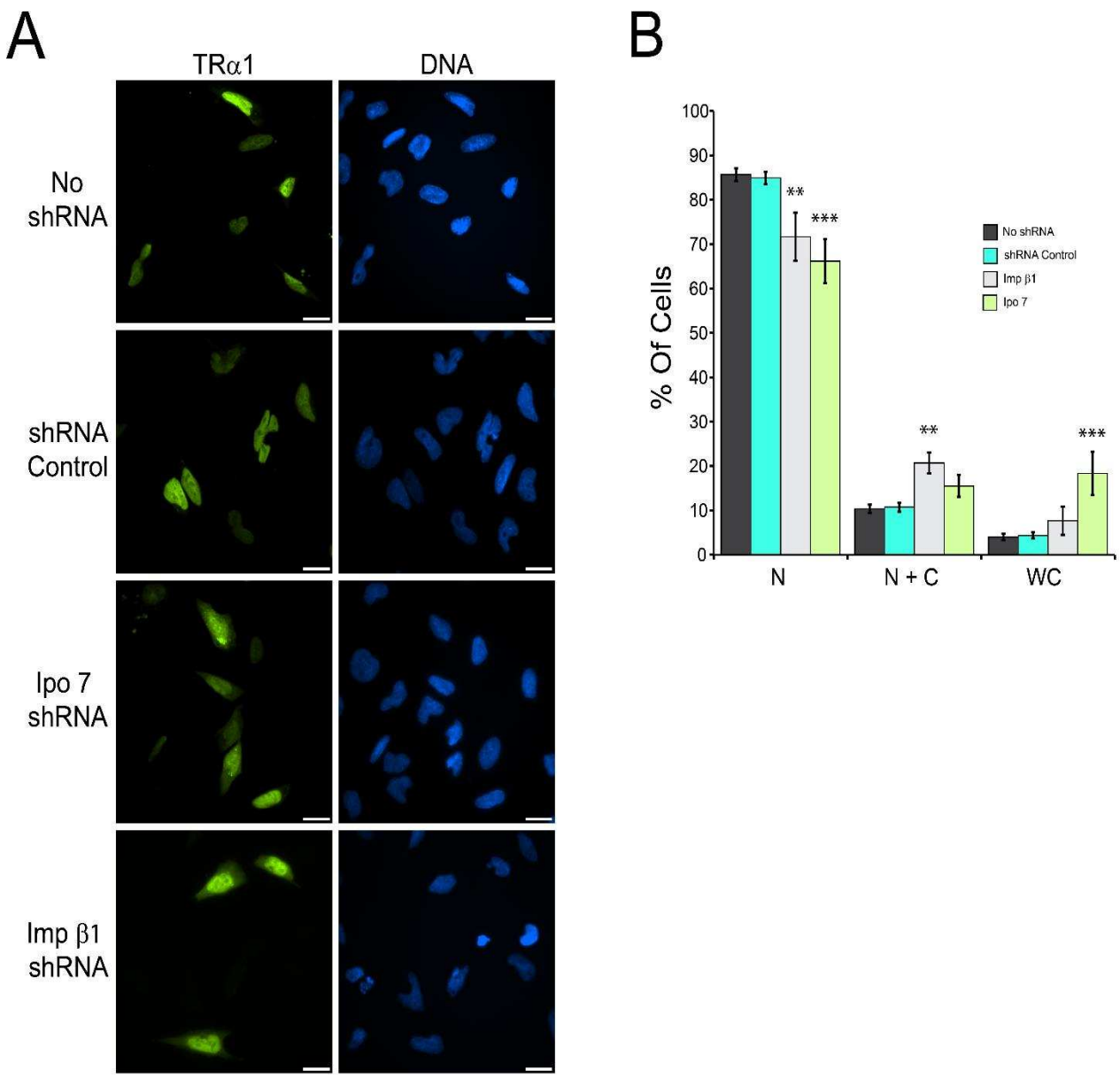


**Fig. 3.** Knockdown of importin β1 (Imp β1) and importin 7 (Ipo 7) by RNAi reduces nuclear accumulation of TRα1. (A) HeLa cells cotransfected with shRNA and GFP-TRα1 expression plasmids, as indicated, were analyzed by fluorescence microscopy after staining with DAPI to visualize the nucleus. Scale bar = 10 μm. (B) HeLa cells cotransfected with shRNA and GFP-TRα1 expression plasmids were fixed and scored for TRα1 localization: N, completely nuclear; N+C, nuclear and cytoplasmic (with distinct nucleus); WC, whole cell (nucleus not distinct). Bars indicate the mean percentage of cells in a given category (n=3 independent, biologically separate replicate experiments, with 100 cells per replicate), and error bars indicate ± SEM. ***$P$<0.001; **$P$<0.01.

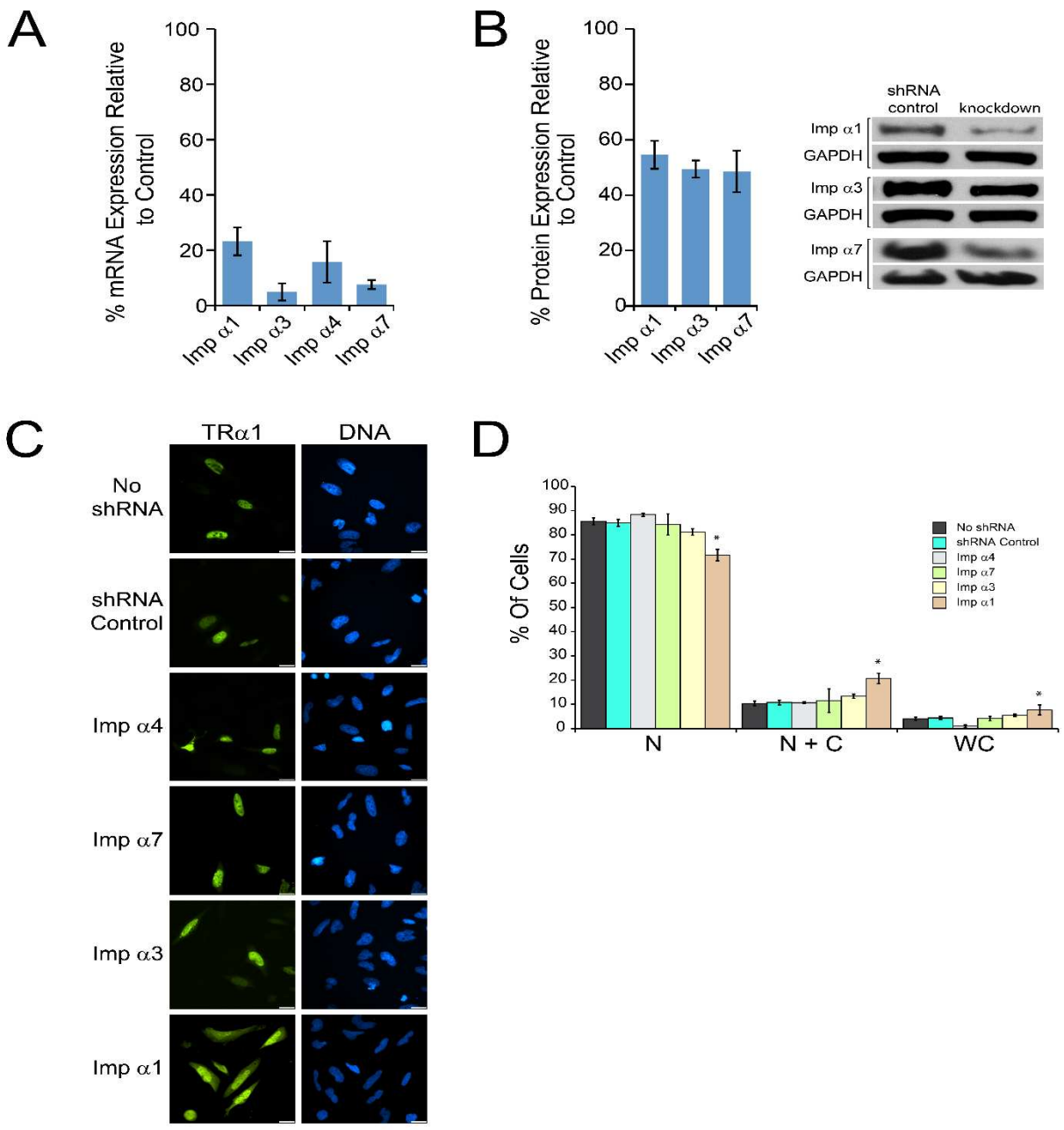


**Fig. 4.** Knockdown of importin α1 (Imp α1) by RNAi reduces nuclear accumulation of TRα1. HeLa cells were transfected with importin-specific shRNA plasmids or a scrambled shRNA plasmid as a control, as indicated. RT-qPCR (A) and immunoblots (B) were used to confirm knockdown of importin mRNA and protein levels, respectively. Error bars indicate ± SEM (n=3 independent, biologically separate replicates). (C) HeLa cells cotransfected with shRNA and GFP-TRα1 expression plasmids, as indicated, were analyzed by fluorescence microscopy. Scale bar = 10 μm. (D) HeLa cells cotransfected with shRNA and GFP-TRα1 expression plasmids were scored for TRα1 localization: N, completely nuclear; N+C, nuclear and cytoplasmic (with distinct nucleus); WC, whole cell (nucleus not distinct). Bars indicate the mean percentage of cells in a given category (n=3 independent, biologically separate replicate experiments, with 100 cells per replicate), and error bars indicate ± SEM. **P*<0.05.

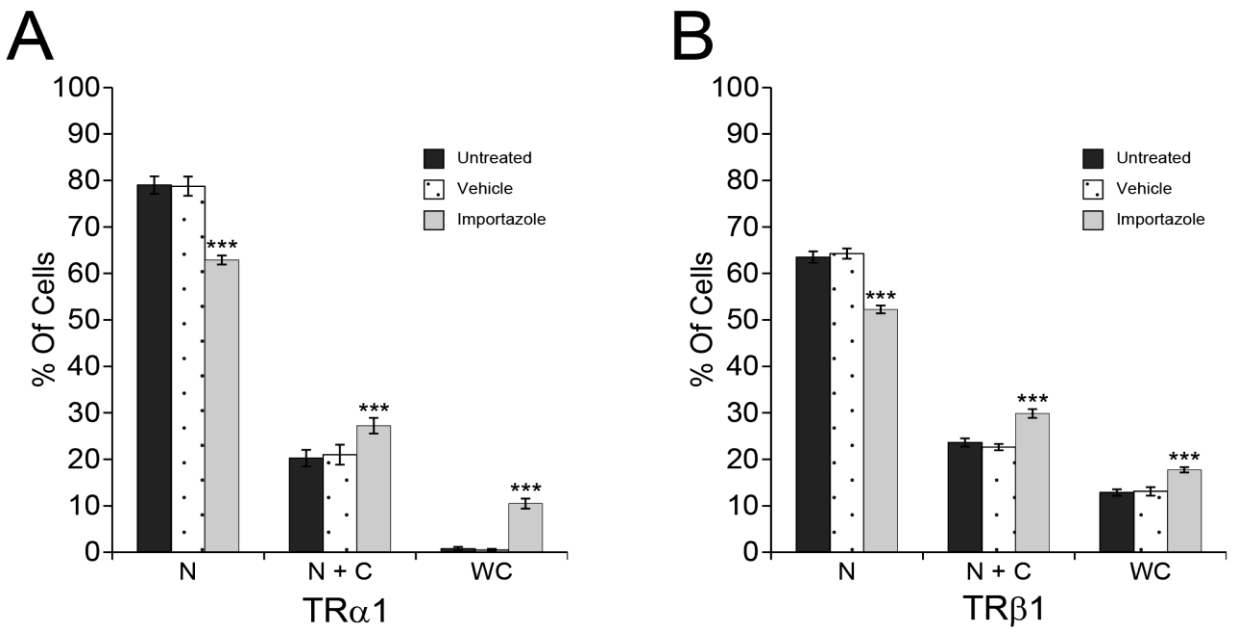


**Fig. 5.** Importazole reduces nuclear localization of TRα1 and TRβ1. HeLa cells were transfected with GFP-TRα1 (A) or GFP-TRβ1 (B) expression plasmids and untreated, treated with vehicle, or treated for 5 h with 50 μM importazole, a small molecule inhibitor of importin β1. Cells were then fixed and scored for localization of TRα1 or TRβ1: N, completely nuclear; N+C, nuclear and cytoplasmic (with distinct nucleus); WC, whole cell (nucleus not distinct). Bars indicate the mean percentage of cells in a given category (n=3 independent, biologically separate replicate experiments, with 200 to 400 cells per replicate), and error bars indicate ± SEM. ***P<0.001.

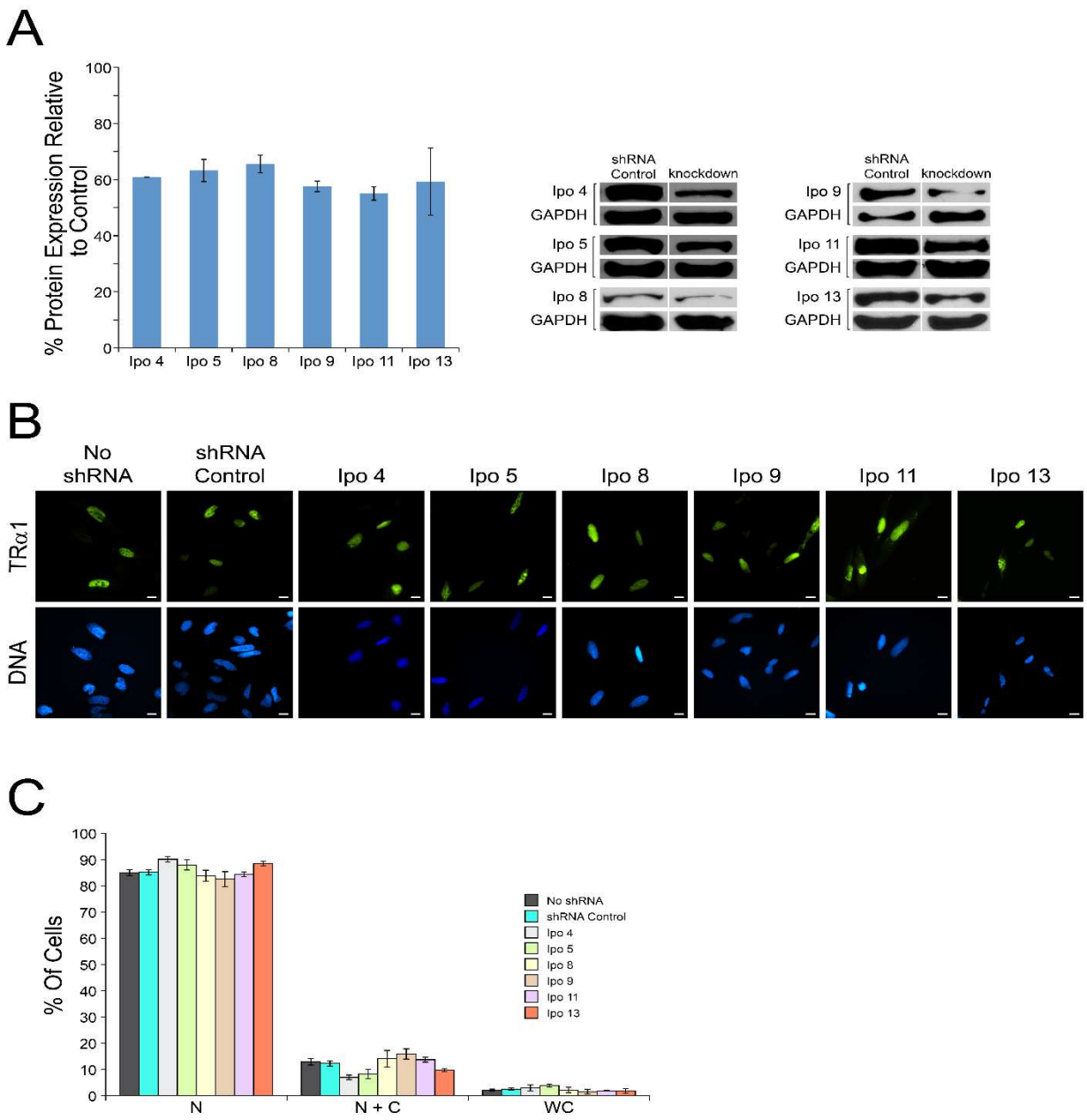


**Fig. 6.** Knockdown of importins 4, 5, 8, 9, 11, and 13 has no effect on nuclear accumulation of TRα1. (A) HeLa cells were transfected with importin (Ipo)-specific shRNA plasmids or a scrambled shRNA plasmid as a control, as indicated, and immunoblot analysis was used to confirm knockdown of importin protein levels. Error bars indicate ± SEM (n=3 independent, biologically separate replicates). (B) HeLa cells cotransfected with shRNA and GFP-TRα1 expression plasmids, as indicated, were analyzed by fluorescence microscopy after staining with DAPI to visualize the nucleus. Scale bar = 10 μm. (C) HeLa cells cotransfected with shRNA and GFP-TRα1 expression plasmids, as indicated, were scored for TRα1 localization: N, completely nuclear; N+C, nuclear and cytoplasmic (with distinct nucleus); WC, whole cell (nucleus not distinct). Bars indicate the mean percentage of cells in a given category (n=3 independent, biologically separate replicate experiments, with 100 cells per replicate), and error bars indicate ± SEM. $P>0.05$.

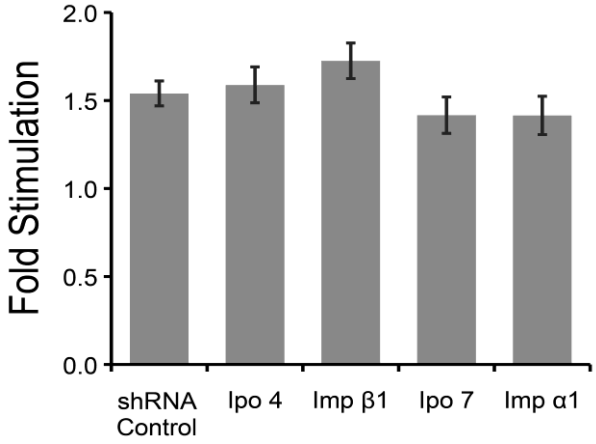


**Fig. 7.** Knockdown of importins 4, β1, 7, and α1 does not significantly alter TRα1-mediated gene expression. HeLa cells were cotransfected with expression plasmids for GFP-TRα1, TRE (DR+4)-firefly luciferase reporter, *Renilla* luciferase internal control, and scrambled shRNA control or a set of four target-specific shRNAs, as indicated. Data are presented as fold stimulation in the presence of $T_3$, relative to luciferase activity (firefly/*Renilla*) in the absence of $T_3$. Error bars indicate ± SEM (n=4 replicates of 8 wells per treatment). *P*>0.05.

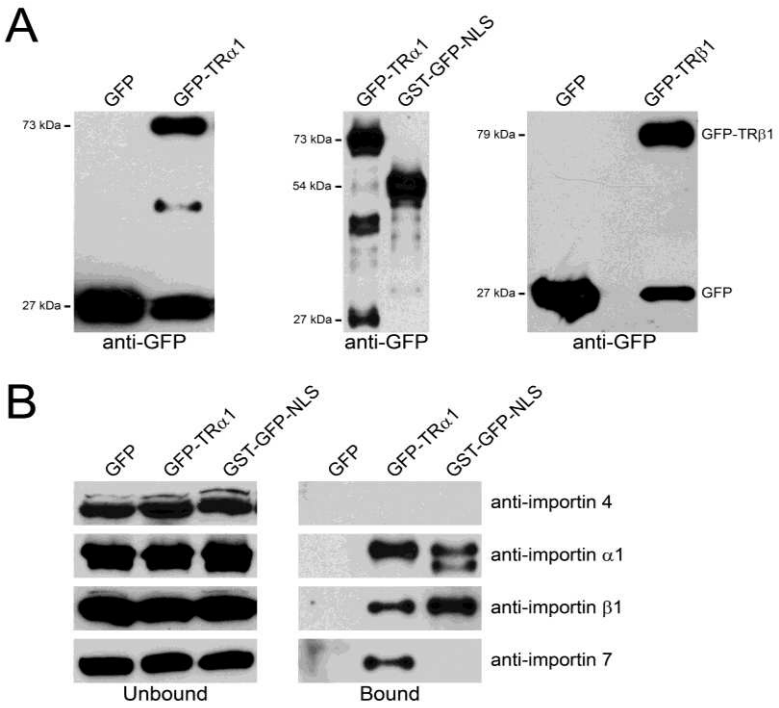


**Fig. 8.** Importin β1, importin α1, and importin 7 coimmunoprecipitate with TRα1. HeLa cells were transfected with expression plasmids encoding GFP (27 kDa), GFP-TRα1 (73 kDa), GST-GFP-NLS (54 kDa), GFP-TRβ1 (79 kDa), GFP-GST-GFP (G3) (80 kDa), G3-A/BD (containing NLS-2) (86 kDa), or G3-Hinge (containing NLS-1) (87 kDa), as indicated. Cell lysates were subjected to coimmunoprecipitation using immobilized anti-GFP-antibodies (GFP-Trap®_A). Representative immunoblots are shown (n=3-5 independent, biologically separate replicate experiments). Protein size was verified using Pre-Stained Kaleidoscope Protein Standards. (A) Trapped GFP-tagged proteins were analyzed by immunoblotting with antibodies specific for GFP. The two lower molecular weight bands in the GFP-TRα1 lane represent specific degradation products.

(B) Immunosupernatants (Unbound) and immunoprecipitates (Bound) from GFP, GFP-TRα1, and GST-GFP-NLS-expressing cell lysates were analyzed on separate immunoblots (using longer exposure times for the immunoprecipitates), with importin-specific antibodies to detect importin 4 (119 kDa), importin α1 (58 kDa), importin β1 (97 kDa), and importin 7 (119 kDa), as indicated. The identity of the ~55 kDa band on the importin α1 immunoblot trapped by GST-GFP-NLS is not known.

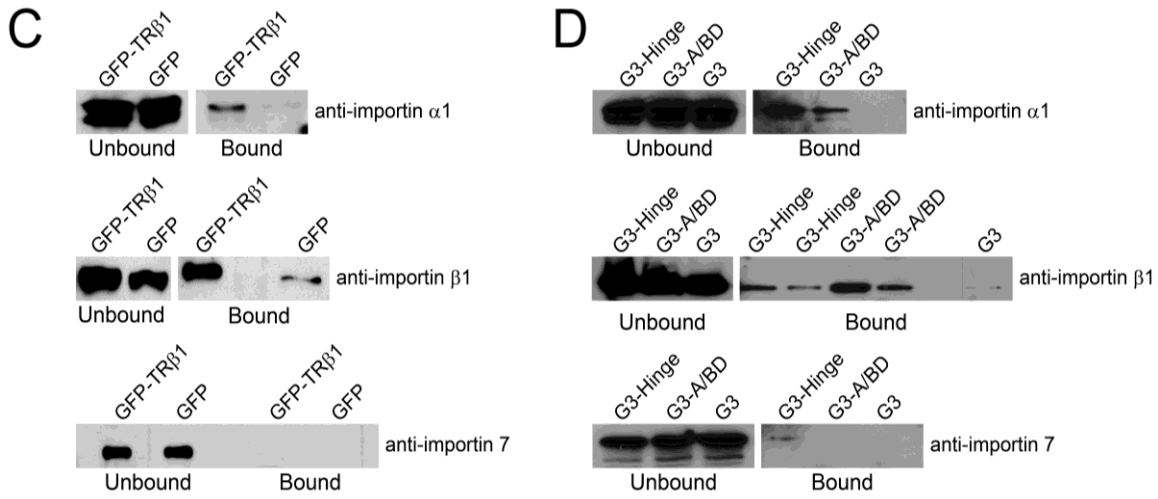


**Fig. 8.** (C) Immunosupernatants (Unbound) and immunoprecipitates (Bound) from GFP and GFP-TRβ1-expressing cell lysates were analyzed by immunoblotting, with importin-specific antibodies, as indicated. (D) Immunosupernatants (Unbound) and immunoprecipitates (Bound) from G3-A/BD and GFP-Hinge-expressing cell lysates were analyzed by immunoblotting, with importin-specific antibodies, as indicated.

## Chapter 4: Discussion and Future Directions

Importins are essential factor in the transports activity of NLS-containing cargo proteins. Although many importins used by NLS-containing proteins have been identified, prior to this thesis research, the question still remained of how many different import pathways are used by TR. Here, we have demonstrated that TRα1 not only uses the classical import pathway directed by IPOβ1/α1 heterodimer but it also uses an IPO7 mediated import pathway. Since our published paper acknowledged the possibility that other importins, whose knockdown didn't effect TRα1 nuclear localization, might still have minor roles in transporting TRα1 into the nucleus, testing their physical interactions with TRα1 using GFP-trap might exclude any doubt.

Another questionable result that needs to be confirmed in the future is the NLS that binds with IPO7. Although performing a IPO7-IPOβ1 double knockdown is unlikely to be achievable, even with a less toxic transfection method, an experiment to observe the impact of removing this heterodimer on TRα1 localization could be very valuable. One way to determine if a cargo is transported either by the IPO7-IPOβ1 heterodimer or individual importins is to measure the cargo's transport rate under conditions in which both are present, both absent, and each individual IPO is present. When a cargo's nuclear import occurs only in the presence of both IPO7 and IPOβ1, it is likely that this cargo is strictly transported by the IPO7-IPOβ1 heterodimer. Wohlwend et al. (2007) used thermodynamic analysis of H1 transport to identify the binding sites on H1 for both IPO7 and IPOβ1. Furthermore, positive cooperation between these two karyopherins in binding H1 was also revealed, indicating that H1 is imported by the heterodimer. In contrast, when

a cargo's import occurs in the presence of one of the two importins but the binding is significantly enhanced by introducing the other importin, it is likely that the cargo's transport is preferably mediated by the heterodimer but individual importins are still capable of doing so. Wodrich and colleagues (2006) reported that the import rate of pVII is increased when both karyopherins are expressed, which puts pVII in the group of cargos that preferably utilize the heterodimer for nuclear import. Finally, when a cargo's transport is not enhanced in the presence of both importins, it can be concluded that the cargo is imported by the importins individually.

On the other hand, many lab members have been working on post-translational modification of TRα1. Knowing how ubiquitination, acetylation, phosphorylation (Nicoll et al., 2003), and sumoylation manipulate TRα1 localization will help to explain the regulation of this *in vivo* transport mechanism. The work conducted by the Allison lab has helped to elucidate TR's nucleocytoplasmic transport. Studying this transport cycle also helps in the understanding of the genetic regulatory mechanisms of TR, in addition to understanding the activity of other members of the nuclear receptor superfamily.

# Chapter 5: Additional Work

The following chapter includes additional work done by the candidate. Data sheets 1-3 show the “trapping” results of replicate experiments with IPOα1, IPOβ1, and IPO7 that also included a positive control for IPO7 interaction, telomerase reverse transcriptase (Tert). This positive control was not included in the published manuscript, because we also found that Tert interacted with IPOβ1, which contradicted the results reported as “data not shown” by the researchers that we obtained the expression vector from. Data sheets 4-7 were collected from the work done for exportin (XPO4, XPO5, XPO6, and XPO7) coimmunoprecipitation with GFP-TRα1. Data show significant protein-protein interactions between TRα1 and XPO4, XPO5, and XPO7, but not XPO6.

## Introduction

As mentioned in the General Introduction (Chapter 1), karyopherins that are in charge of importing cargo into the nucleus are called importins, whereas those that are in charge of exporting cargo back to the cytoplasm are exportins. Since this thesis mainly focused on the study of importin pathways, exportins were only addressed briefly in the General Introduction. A more detailed introduction to exportins in general, and those that are involved in TR nuclear export is provided in this final chapter.

Just like how the gradient of nucleotide-bound Ran influences cargos binding to importins, exportin cargo affinity also depends on the RanGTP/RanGDP ratio. However, in contrast to importins, exportins form stable export complexes with their cargos in the nucleus with a high concentration of RanGTP, whereas their affinity gets lower in a high

concentration of RanGDP. Export complexes, composed of exportin, RanGTP, and cargo dissociate in the cytoplasm by interacting with RanGAP when they pass through the NPC (Lee et al., 2011). The process of cargo export is illustrated in Figure 5 (see Chapter 1). Recall that cargo import is determined by the recognition of NLSs; likewise, exportins bind with specific nuclear export signals (NESs). Among the 20 karyopherins, at least 7 of them in human cells are exportins (Fung and Chook, 2014): CRM1, CAS, exportin-t, exportin 4, exportin 5, exportin 6 and exportin 7.

Although many reports in the literature assert that their cargos of interest utilize a CRM1 (exportin1)-dependent export pathway, due to the fact that CRM1 is the most studied and well characterized exportin, it is still possible that those proteins of interest also might have an unanticipated dependency on other exportin pathways. Indeed, just like how most proteins require more than one importin for efficient transport, exportin pathways are usually shared amongst export cargos. For example, small nuclear RNAs are exported using both exportin 5 and CRM1 (Lee et al., 2011). As for our research on TRα1 nucleocytoplasmic transport, the paper published in 2008 by Grespin and colleagues provided evidence of how TRα1 can utilize a CRM1/calreticulin-dependent export mechanism. Meanwhile, Subramanian et al.'s work in 2015 suggested that TRα1 export is also influenced by exportin 4 (XPO4), exportin 5 (XPO5), and exportin 7 (XPO7). It was not entirely unexpected that an essential hormone receptor like TRα1, which uses multiple importins to enter the nucleus, also would require multiple exportins to get back to the cytoplasm. In this chapter, exportins that are involved in TRα1 nuclear export will be examined.

CRM1, also known as XPO1, was the first exportin discovered in 1989. It was given

the name “Chromosomal Region Maintenance” due to its impact on chromosome structure (Adachi and Yanagida, 1989). In 1997, researchers identified CRM1’s essential role in exporting molecules (Fornerod et al., 1997). Using its natural inhibitor leptomycin B (LMB) to study the pathway, CRM1 has been shown to facilitate the most diverse, yet specific, export pathway (Xu, et al., 2012). Although CRM1 mostly interacts with hydrophobic leucine-rich-NESs (Kosugi et al., 2008), some nuclear receptors, such as TRα1 that have NESs that diverge from this consensus, could still use this export pathway. Up to now, over 300 different cargos have been identified to be exported by CRM1, including several tumor suppressors, cell growth regulators and vitamin receptors (Shen et al., 2009). Overexpression of CRM1 has been confirmed to be a contributing factor in certain diseases such as ovarian cancer (Noske et al., 2008). Meanwhile, CRM1 inhibition has also been shown recently to lead to apoptosis of certain cancer cells by restoring tumor suppressor localization and function (Kojima et al., 2013). The architecture of CRM1 appears to be relatively conserved across different organisms (Berman et al., 2000). The molecular weight of CRM1 is about 120 KDa which is similar to other exportins. CRM1’s full length structure, which contains 21 HEAT repeats, was reported in 2009. Each of the 21 HEAT repeats has specific functions and the cooperation between these repeats directly alters CRM1 activity. When CRM1 interacts with a cargo protein, it adapts its structure to a closed ring shape by connecting the N-terminal HEAT repeats and C-terminal HEAT repeats (Dong et al., 2009). HEAT repeats 11 and 12 form a hydrophobic groove on the surface of CRM1 to bind NESs. Other HEAT repeats, such as 8, 9 and 10 may also contribute to mediating CRM1’s conformation which is crucial for its function (Monecke et al., 2009).

Some exportins are overshadowed by CRM1's influential "reputation." In the early days, CRM1 was assumed to be the carrier of most proteins. But after more exportins were discovered and more research was conducted into the role played by each exportin, scientists found out that credit was given to CRM1 when, in fact, it is not responsible for exporting certain cargos. A perfect example is the cytosolic-localized protein actin. Until 2003, scientists believed that it was CRM1 that exports actin to the cytoplasm and maintains this distribution (Wada et al., 1998). However, it was later reported that CRM1 does not interact with actin directly. XPO6, instead, is considered as the major transporter for actin (Stüven et al., 2003). XPO6 is conserved from amoeba to vertebrates. To date, actin and actin-profilin complexes are the only identified cargos that use the XPO6 pathway (Park et al., 2011). In this thesis research, XPO6 was used as a negative control.

According to Lipowsky et al.'s 2000 research paper, XPO4 does not show obvious orthologues in yeast but seems to be conserved amongst eukaryotes. At that time, the only confirmed cargo of XPO4 was eukaryotic translation initiation factor 5A (eIF-5A). eIF-5A's affinity for XPO4 is at least 1000 times higher than for CRM1, exportin-t, or CAS, indicating its binding specificity. Since 2000, more XPO4 cargos have been discovered. In 2006, Smad3 became the second identified export cargo of XPO4 by Kurisaki and his colleagues. Interestingly, besides exporting Sox9 protein, many studies suggests that XPO4 also imports certain Sox family proteins, such as Sox2 and SRY, into the nucleus in a Ran-independent manner (Gontan et al., 2009). Furthermore, XPO4 is also described as a tumor suppressor gene of hepatocellular carcinoma (HCC), due to the fact that hepatitis B virus (the major cause of HCC) infected patients show a dramatic decrease in

expression of XPO4 (Zhang et al., 2014). XPO4's cargo pool is continuously being extended.

Generally speaking, certain proteins and small double-stranded RNAs like microRNAs are exported by XPO5 (Lee et al., 2011). However, before interacting with any cargo, XPO5 needs to bind RanGTP in the nucleus first. This XPO5-RanGTP complex forms a baseball mitt-like structure to pack the cargo into the inner surface (Okada et al., 2009). Although the physical interaction between XPO5-RanGTP complex and double-stranded RNAs is usually weak, the mitt-like structure acts as a "shield" to not only retain the cargo but also protect it from ribonuclease digestion. The protecting role of XPO5 does not end until the complex locates in the cytoplasm and encounters the enzyme Dicer, meaning that XPO5 perhaps is able to resist RanGAP-mediated cargo release. Therefore, XPO5 is also viewed as a double-stranded RNA stabilizer, which is similar to the protein chaperone activity of IPOβ1. Like CRM1, XPO5 also has 21 HEAT repeats and each one of them influences XPO5's function by altering its conformation. Although XPO5 is known for specifically exporting double-stranded pre-RNAs, it has also been confirmed that proteins such as androgen receptor use XPO5 as their transporters.

XPO7, also known as RanBP16, actively exports numerous proteins including 14-3-3σ and p50RhoGAP to the cytoplasm (Mingot et al., 2004). However, like XPO6, both XPO7 substrates were suggested to be exported by CRM1 at first (Brunet et al., 2002). Due to its diverse cargo pool, the XPO7 pathway was defined as the second general export pathway besides the CRM1 pathway. Compared to CRM1, whose cargos appear to share a common leucine-rich NES, XPO7's cargos don't have any structural or functional similarity. Interestingly, Brunet and colleagues discovered that XPO7 interacts

with 14-3-3σ through a highly charged motif composed of clusters of basic residues. The same result was observed for p50RhoGAP. In both cases, basic residue clusters seem to be important for cargo recognition by XPO7.

## Methods

The work published by Grespin et al. (2008) demonstrated that CRM1 interacts directly with TRα1 and mediates nuclear export in a cooperative manner with calreticulin. Subramanian and colleagues in 2015 then went on to demonstrate that XPO4, XPO5, and XPO7 also influence TRα1 localization, suggesting these exportins are additional candidates for exporting TRα1 back to the cytoplasm through a CRM1-independent pathway. Knocking down any one of these exportins resulted in increased TRα1 nuclear retention and a decrease in nucleocytoplasmic shuttling, whereas overexpression lead to an increased TRα1 cytoplasmic localization pattern. However, without the proof of direct protein-protein interaction, the candidacy of XPO4, XPO5, and XPO7 was only a suggestion. Data sheets 4-7 provided in the next section show western blotting results after coimmunoprecipitation assays for XPO4, XPO5, XPO6 and XPO7. The techniques used are described in detail in Chapter 2 (Materials and Methods). On the data sheets, key information is provided, including primary and secondary antibody dilution, X-ray film exposure time, target protein concentration, target protein size, and number of replicates. “Trapping result” indicates proteins that were coimmunoprecipitated or “trapped”, whereas “unbound result” shows proteins that were left in the supernatant.

## Results

### Data Sheet 1. IPOα1 coimmunoprecipitation result using Tert-GFP as a positive control

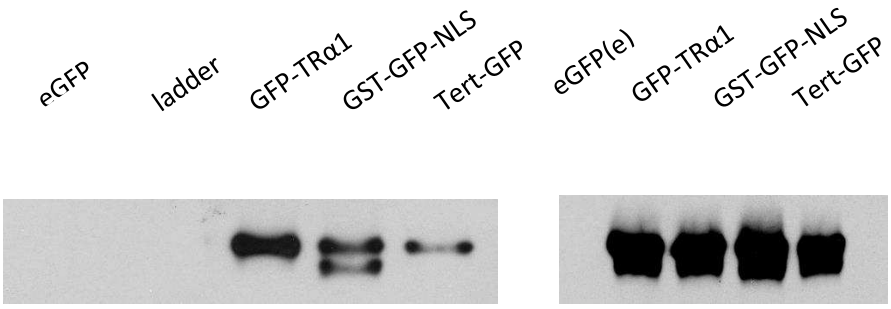


| | |
|---|---|
| **Primary antibody** | 1:1000, rabbit polyclonal (Abcam) |
| **Secondary antibody** | 1:33000, anti-rabbit IgG from donkey (GE Healthcare Life Sciences) |
| **Trapping result exposure time** | 10 sec |
| **Unbound result exposure time** | 1 sec |
| **Replicates** | 4 |
| **Sample loading volume** | 20µl/each wall |
| **IPOα1 size** | 58 kDa |

**Data sheet 1: IPOα1 coimmunoprecipitation result using Tert-GFP as a positive control:** As the blot shows, Tert-GFP interacts with IPOα1 directly. This information was not included in the publication.

## Data Sheet 2. IPOβ1 coimmunoprecipitation result using Tert-GFP as a positive control

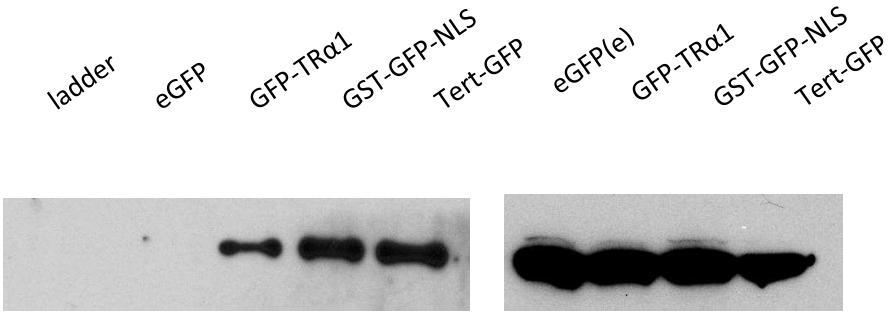


| | |
|---|---|
| **Primary antibody** | **1:1000, rabbit polyclonal (Santa Cruz)** |
| **Secondary antibody** | 1:25000, anti-rabbit IgG from donkey (GE Healthcare Life Sciences) |
| **Trapping result exposure time** | 2 min |
| **Unbound result exposure time** | 5 sec |
| **Replicates** | 4 |
| **Sample loading volume** | 20µl/each wall |
| **IPOβ1 size** | 90 kDa |

**Data sheet 2: IPOβ1 coimmunoprecipitation result using Tert-GFP as a positive control**: As the western blot shows, Tert-GFP also interacts with IPOβ1. Since the result does not agree with what the laboratory that provided us with the protein expression plasmid had published (as data not shown), it was not included in our publication.

## Data Sheet 3. IPO7 coimmunoprecipitation result using Tert-GFP as a positive control

**IPO7 trapping result** **IPO7 unbound result**

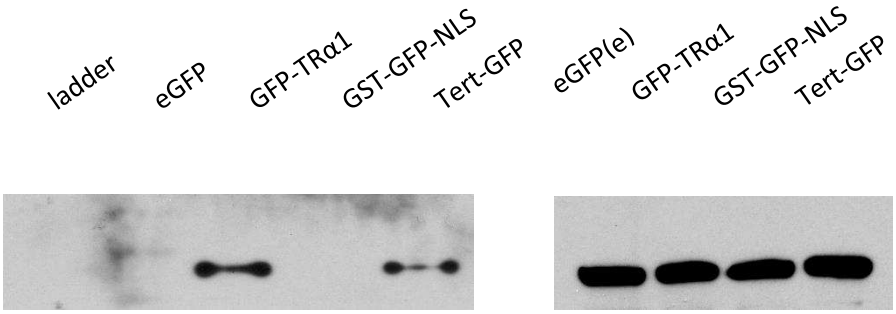


| | |
|---|---|
| **Primary antibody** | 1:1000, rabbit polyclonal (Abcam) |
| **Secondary antibody** | 1:25000, anti-rabbit IgG from donkey (GE Healthcare Life Sciences) |
| **Trapping result exposure time** | 2 min |
| **Unbound result exposure time** | 10 sec |
| **Replicates** | 5 |
| **Sample loading volume** | 20µl/each wall |
| **IPO-7 size** | 120 kDa |

**Data sheet 3: IPO7 coimmunoprecipitation result using Tert-GFP as a positive control**: Western blot shows that Tert-GFP interacts with IPO7 directly. Although these data were not included in our publication, their accuracy was confirmed by the laboratory that provided us with Tert-GFP.

## Data Sheet 4. XPO4 coimmunoprecipitation result

### XPO4 trapping result

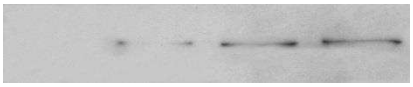


### XPO4 unbound result

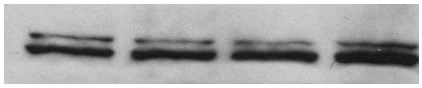


| | |
|---|---|
| **Primary antibody** | 1:500, rabbit monoclonal (Abcam) |
| **Secondary antibody** | 1:25000, anti-rabbit IgG from donkey (GE Healthcare Life Sciences) |
| **Trapping result exposure time** | 2 min |
| **Unbound result exposure time** | 10 sec |
| **Replicates** | 5 |
| **Sample loading volume** | 20µl/each wall |
| **XPO4 size** | 127 kDa |

**Data Sheet 4. XPO4 coimmunoprecipitation result:** Three replicates of GFP-TRα1 were loaded on the same gel. From the “unbound result”, the presence of eGFP or GFP-TRα1 was confirmed. The “trapping result” shows a clear interaction between XPO4 and GFP-TRα1.

## Data Sheet 5. XPO5 coimmunoprecipitation result

**XPO5 trapping result** **XPO5 unbound result**

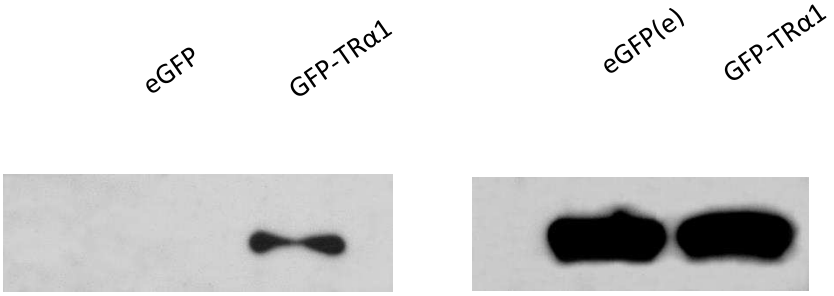


| | |
|---|---|
| **Primary antibody** | 1:2000, rabbit polyclonal (Abcam) |
| **Secondary antibody** | 1:25000, anti-rabbit IgG from donkey (GE Healthcare Life Sciences) |
| **Trapping result exposure time** | 10 sec |
| **Unbound result exposure time** | 1 sec |
| **Replicates** | 8 |
| **Sample loading volume** | 20µl/each wall |
| **XPO5 size** | 136 kDa |

**Data Sheet 5. XPO5 coimmunoprecipitation result:** One replicate of GFP-TRα1 was loaded on the gel. From the “unbound result”, the presence of eGFP or GFP-TRα1 was confirmed. The “trapping result” shows a clear interaction between XPO5 and GFP-TRα1.

## Data Sheet 6. XPO6 coimmunoprecipitation result

**XPO6 trapping result** **XPO6 unbound result**

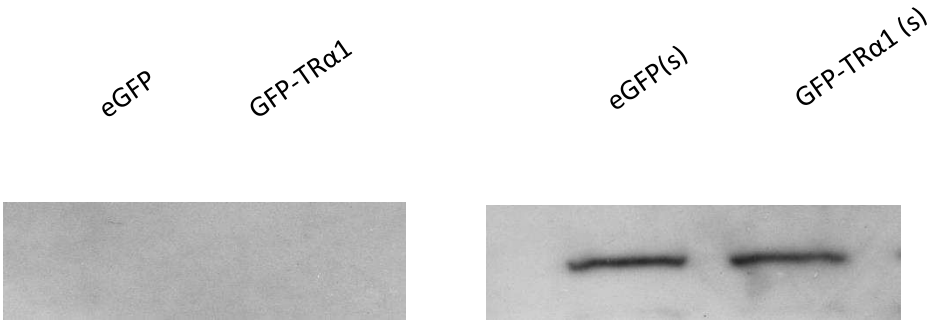


| | |
|---|---|
| **Primary antibody** | 1:1000, rabbit polyclonal (Abcam) |
| **Secondary antibody** | 1:25000, anti-rabbit IgG from donkey (GE Healthcare Life Sciences) |
| **Trapping result exposure time** | 2 min |
| **Unbound result exposure time** | 2 min |
| **Replicates** | 6 |
| **Sample loading volume** | 20µl/each wall |
| **XPO6 size** | 129 kDa |

**Data Sheet 6. XPO6 coimmunoprecipitation result:** One replicate of GFP-TRα1 was loaded on the gel. From the “unbound result”, the presence of eGFP or GFP-TRα1 was confirmed. The “trapping result” shows no interaction between XPO6 and GFP-TRα1.

## Data Sheet 7. XPO7 coimmunoprecipitation result

**XPO7 trapping result**

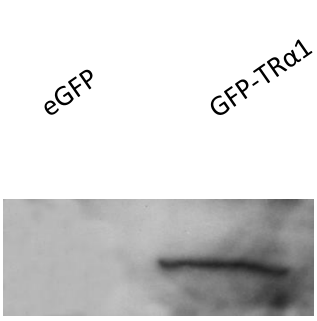


**XPO7 unbound result**

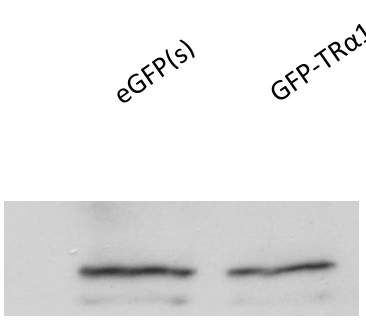


| | |
|---|---|
| **Primary antibody** | 1:1000, goat polyclonal (Abcam) |
| **Secondary antibody** | 1:25000, anti-goat IgG from mouse (Santa Cruz) |
| **Trapping result exposure time** | 1 min |
| **Unbound result exposure time** | 10 sec |
| **Replicates** | 8 |
| **Sample loading volume** | 20µl/each wall |
| **XPO7 size** | 110 kDa |

**Data Sheet 7. XPO7 coimmunoprecipitation result:** One replicate of GFP-TRα1 was loaded on the gel. From the “unbound result”, the presence of eGFP or GFP-TRα1 was confirmed. The “trapping result” shows a clear interaction between XPO7 and GFP-TRα1.

## Conclusion

Years of effort have been dedicated to mapping the cycle of the dynamic and precisely balanced process of TRα1 nucleocytoplasmic transport. Previous chapters of this thesis discussed the importins that are involved in TRα1 nuclear import. In this final chapter, potential exportins that were believed to influence TRα1 cytoplasmic localization were further investigated by using coimmunoprecipitation assays and western blot analyses. The results presented here confirm that XPO4, XPO5 and XPO7 have direct protein-protein interactions with TRα1, meaning that besides CRM1, TRα1 also uses XPO4, XPO5 and XPO7 pathways to translocate back to the cytoplasm. As a negative control, XPO6 was also tested along with the other exportins and the results indicate no interaction between TRα1 and XPO6. To date, all karyopherins that mediate TRα1 nucleocytoplasmic shuttling have been identified. The IPOβ1/α1 complex and IPO7 are the main importins that carry TRα1 into the nucleus, whereas CRM1, XPO4, XPO5, and XPO7 are the exportins that transport TRα1 back to the cytoplasm. The question of which importin recognizes which TRα1 NLS was addressed in the publication included in this thesis (Roggero et al., 2016); however, the same question remains to be answered for the exportins. So far, we know that TRα1 has three CRM1-independent NESs located in the ligand binding domain. The next step will be to test which exportins interact directly with each of these NESs in TRα1.

## References


1 Adachi, Y., & Yanagida, M. (1989). Higher order chromosome structure is affected by cold-sensitive mutations in a Schizosaccharomyces pombe gene crm1+ which encodes a 115-kD protein preferentially localized in the nucleus and its periphery. The Journal of Cell Biology, 108(4), 1195-1207.

2 Algenäs, C., Agaton, C., Fagerberg, L., Asplund, A., Björling, L., Björling, E., . . . Hober, S. (2014). Antibody performance in western blot applications is context-dependent. Biotechnology Journal, 9(3), 435-445.

3 Aranda, A., & Pascual, A. (2001). Nuclear hormone receptors and gene expression. Physiological Reviews, 81(3), 1269-1304.

4 Askjaer, P., Bachi, A., Wilm, M., Bischoff, F. R., Weeks, D. L., Ogniewski, V., … Fornerod, M. (1999). RanGTP-Regulated Interactions of CRM1 with Nucleoporins and a Shuttling DEAD-Box Helicase. Molecular and Cellular Biology, 19(9), 6276–6285.

5 Baake, M., Bäuerle, M., Doenecke, D., & Albig, W. (2001). Core histones and linker histones are imported into the nucleus by different pathways. European Journal of Cell Biology, 80(11), 669-677.

6 Baniahmad, A., Köhne, A.C., & Renkawitz, R. (1992). A transferable silencing domain is present in the thyroid hormone receptor, in the v-erbA oncogene product and in the retinoic acid receptor. The EMBO Journal, 11(3), 1015-1023.

7 Baniahmad, A., Leng, X., Burris, T. P., Tsai, S. Y., Tsai, M. J., & O'Malley,B.W. (1995). The tau 4 activation domain of the thyroid hormone receptor is required for release of a putative corepressor(s) necessary for transcriptional silencing. Molecular and Cellular Biology, 15(1), 76-86.

8 Bassett, J. H. D., Harvey, C. B., & Williams, G. R. (2003). Mechanisms of thyroid hormone receptor-specific nuclear and extra nuclear actions. Molecular and Cellular Endocrinology, 213(1), 1-11.

9 Baumann, C. T., Maruvada, P., Hager, G. L., & Yen, P. M. (2001). Nuclear cytoplasmic shuttling by thyroid hormone receptors. multiple protein interactions are required for nuclear retention. The Journal of Biological Chemistry, 276(14), 11237-11245.

10 Bergh, J. J., Lin, H., Lansing, L., Mohamed, S. N., Davis, F. B., Mousa, S., & Davis, P. J. (2005). Integrin alphaVbeta3 contains a cell surface receptor site for thyroid hormone that is linked to activation of mitogen-activated protein kinase and induction of angiogenesis. Endocrinology, 146(7), 2864-2871.

11 Berman, H. M., Westbrook, J., Feng, Z., Gilliland, G., Bhat, T. N., Weissig, H., . . . Bourne, P. E. (2000). The protein data bank. Nucleic Acids Research, 28(1), 235-242.

12 Bianco, A. C. (2011). Minireview: Cracking the metabolic code for thyroid hormone signaling. Endocrinology, 152(9), 3306-3311.

13 Bianco, A. C., Salvatore, D., Gereben, B., Berry, M. J., & Larsen, P. R. (2002). Biochemistry, cellular and molecular biology, and physiological roles of the iodothyronine selenodeiodinases. Endocrine Reviews, 23(1), 38-89.
14 Birmingham, A., Anderson, E. M., Reynolds, A., Ilsley-Tyree, D., Leake, D., Fedorov, Y., . . . Khvorova, A. (2006). 3' UTR seed matches, but not overall identity, are associated with RNAi off-targets. Nature Methods, 3(3), 199-204.
15 Bonifaci, N., Moroianu, J., Radu, A., & Blobel, G. (1997). Karyopherin beta2 mediates nuclear import of a mRNA binding protein. Proceedings of the National Academy of Sciences of the United States of America, 94(10), 5055-5060.
16 Bono, F., Cook, A. G., Grünwald, M., Ebert, J., & Conti, E. (2010). Nuclear import mechanism of the EJC component mago-Y14 revealed by structural studies of importin 13. Molecular Cell, 37(2), 211-222.
17 Braverman, L. E., Ingbar, S. H., & Sterling, K. (1970). Conversion of Thyroxine (T4) to triiodothyronine (T3) in athyreotic human subjects. Journal of Clinical Investigation, 49(5), 855–864.
18 Brent GA. (1994). The molecular basis of thyroid hormone action. N Engl J Med. 331(13):847– 853.
19 Brunet, A., Kanai, F., Stehn, J., Xu, J., Sarbassova, D., Frangioni, J. V., . . . Yaffe, M. B. (2002). 14-3-3 transits to the nucleus and participates in dynamic nucleocytoplasmic transport. The Journal of Cell Biology, 156(5), 817-828.
20 Bunn, C.F., Neidig, J.A., Freidinger, K.E., Stankiewicz, T.A., Weaver, B.S., McGrew, J., Allison, L.A. (2001) Nucleocytoplasmic shuttling of the thyroid hormone receptor a. Molecular Endocrinology.
21 Burke B. and Stewart C. L. (2002) Life at the edge: the nuclear envelope and human disease. Nat. Rev. Mol. Cell Biol. 3: 575–585.
22 Bustamante, J. O. (1993). Restricted ion flow at the nuclear envelope of cardiac myocytes. Biophysical Journal, 64(6), 1735–1749.
23 Cansizoglu, A. E., Lee, B. J., Zhang, Z. C., Fontoura, B. M. A., & Chook, Y. M. (2007). Structure-based design of a pathway-specific nuclear import inhibitor. Nature Structural & Molecular Biology, 14(5), 452-454.
24 Cavazza, T., & Vernos, I. (2015). The RanGTP pathway: From nucleo-cytoplasmic transport to spindle assembly and beyond. Frontiers in Cell and Developmental Biology, 3, 82.
25 Chachami, G., Paraskeva, E., Mingot, J., Braliou, G. G., Görlich, D., & Simos, G. (2009). Transport of hypoxia-inducible factor HIF-1alpha into the nucleus involves importins 4 and 7. Biochemical and Biophysical Research Communications, 390(2), 235-240.
26 Chachami, G., Paraskeva, E., Mingot, J., Braliou, G. G., Görlich, D., & Simos, G. (2009). Transport of hypoxia-inducible factor HIF-1alpha into the nucleus involves importins 4 and 7. Biochemical and Biophysical Research Communications, 390(2), 235-240.

27 Chassande, O. (2003). Do unliganded thyroid hormone receptors have physiological functions? Journal of Molecular Endocrinology, 31(1), 9-20.
28 Chavez E, Franco M, Reyes-Vivas H, Zazueta C, Ramirez J, Carrillo R. (1998). Hypothyroidism renders liver mitochondria resistant to the opening of membrane permeability transition pore. Biochim Biophys Acta. 1407(3):243–248.
29 Chen JD, Evans RM. 1995. A transcriptional co-repressor that interacts with nuclear hormone receptors. Nature 377: 454 –457.
30 Chen, Y., & Young, M. A. (2010). Structure of a thyroid hormone receptor DNA-binding domain homodimer bound to an inverted palindrome DNA response element. Molecular Endocrinology (Baltimore, Md.), 24(8), 1650-1664.
31 Cheng, S., Leonard, J. L., & Davis, P. J. (2010). Molecular aspects of thyroid hormone actions. Endocrine Reviews, 31(2), 139-170.
32 Chook, Y. M., & Blobel, G. (2001). Karyopherins and nuclear import. Current Opinion in Structural Biology, 11(6), 703-715.
33 Chook, Y. M., & Süel, K., E. (2011). Nuclear import by karyopherin-βs: Recognition and inhibition. Biochimica Et Biophysica Acta, 1813(9), 1593-1606.
34 Chuderland, D., Konson, A., & Seger, R. (2008). Identification and characterization of a general nuclear translocation signal in signaling proteins. Molecular Cell, 31(6), 850-861.
35 Clemens, J. C., Worby, C. A., Simonson-Leff, N., Muda, M., Maehama, T., Hemmings, B. A., & Dixon, J. E. (2000). Use of double-stranded RNA interference in drosophila cell lines to dissect signal transduction pathways. Proceedings of the National Academy of Sciences of the United States of America, 97(12), 6499-6503.
36 Conti, E., Uy, M., Leighton, L., Blobel, G., & Kuriyan, J. (1998). Crystallographic analysis of the recognition of a nuclear localization signal by the nuclear import factor karyopherin alpha. Cell, 94(2), 193-204.
37 Cooper GM, (2000). The Cell: A Molecular Approach. 2nd edition. Sunderland (MA): Sinauer Associates; The Nuclear Envelope and Traffic between the Nucleus and Cytoplasm.
38 Cronshaw, J. M., Krutchinsky, A. N., Zhang, W., Chait, B. T., & Matunis, M. J. (2002). Proteomic analysis of the mammalian nuclear pore complex. The Journal of Cell Biology, 158(5), 915–927.
39 D'angelo, M.A., & Hetzer, M. W. (2006). The role of the nuclear envelope in cellular organization. Cellular and Molecular Life Sciences, 63(3), 316-32.
40 Dahl K.N., Kahn S. M., Wilson K. L. and Discher D. E. (2004) The nuclear envelope lamina network has elasticity and a compressibility limit suggestive of a molecular shock absorber. J. Cell. Sci. 117: 4779–4786.
41 D'Angelo, M. A., & Hetzer, M. W. (2006). The role of the nuclear envelope in cellular organization. Cellular & Molecular Life Sciences, 63(3), 316-332.

42 D'Angelo, M.A., & Hetzer, M. W. (2006). The role of the nuclear envelope in cellular organization. Cellular and Molecular Life Sciences: CMLS, 63(3), 316-332.
43 D'Arezzo, S., Incerpi, S., Davis, F. B., Acconcia, F., Marino, M., Farias, R. N., & Davis, P. J. (2004). Rapid nongenomic effects of 3,5,3'-triiodo-L-thyronine on the intracellular pH of L-6 myoblasts are mediated by intracellular calcium mobilization and kinase pathways. Endocrinology, 145(12), 5694-5703.
44 Davis, P. J., Davis, F. B., & Cody, V. (2005). Membrane receptors mediating thyroid hormone action. Trends in Endocrinology and Metabolism: TEM, 16(9), 429-435.
45 Dean, K. A., von Ahsen, O., Görlich, D., & Fried, H. M. (2001). Signal recognition particle protein 19 is imported into the nucleus by importin 8 (RanBP8) and transportin.
46 Dhanoya, A., Wang, T., Keshavarz-Moore, E., Fassati, A., & Chain, B. M. (2013). Importin-7 mediates nuclear trafficking of DNA in mammalian cells. Traffic (Copenhagen, Denmark), 14(2), 165-175.
47 Dong, X., Biswas, A., Süel, K.,E., Jackson, L. K., Martinez, R., Gu, H., & Chook, Y. M. (2009). Structural basis for leucine-rich nuclear export signal recognition by CRM1. Nature, 458(7242), 1136-1141.
48 Dunn, J. T., & Dunn, A. D. (2001). Update on intrathyroidal iodine metabolism. Thyroid: Official Journal of the American Thyroid Association, 11(5), 407-414.
49 Echeverria, P. C., & Picard, D. (2010). Molecular chaperones, essential partners of steroid hormone receptors for activity and mobility. Biochimica Et Biophysica Acta, 1803(6), 641-649.
50 Elbashir, S. M., Harborth, J., Lendeckel, W., Yalcin, A., Weber, K., & Tuschl, T. (2001). Duplexes of 21-nucleotide RNAs mediate RNA interference in cultured mammalian cells. Nature, 411(6836), 494-498.
51 Fagerlund, R., Kinnunen, L., Köhler, M., Julkunen, I., & Melén, K. (2005). NF-{kappa}B is transported into the nucleus by importin {alpha}3 and importin {alpha}4. The Journal of Biological Chemistry, 280(16), 15942-15951.
52 Fanara, P., Hodel, M. R., Corbett, A. H., & Hodel, A. E. (2000). Quantitative analysis of nuclear localization signal (NLS)-importin alpha interaction through fluorescence depolarization. evidence for auto-inhibitory regulation of NLS binding. The Journal of Biological Chemistry, 275(28), 21218-21223.
53 Feng, X., Jiang, Y., Meltzer, P., & Yen, P. M. (2000). Thyroid hormone regulation of hepatic genes in vivo detected by complementary DNA microarray. Molecular Endocrinology (Baltimore, Md.), 14(7), 947-955.
54 Fire, A., Xu, S., Montgomery, M. K., Kostas, S. A., Driver, S. E., & Mello, C. C. (1998). Potent and specific genetic interference by double-stranded RNA in Caenorhabditis elegans. Nature, 391(6669), 806-811.
55 Fondell, J. D., Guermah, M., Malik, S., & Roeder, R. G. (1999). Thyroid hormone receptor-associated proteins and general positive cofactors mediate thyroid hormone receptor function in the absence of the TATA box-binding

protein-associated factors of TFIID. Proceedings of the National Academy of Sciences of the United States of America, 96(5), 1959-1964.
56 Fornerod, M., Ohno, M., Yoshida, M., & Mattaj, I. W. (1997). CRM1 is an export receptor for leucine-rich nuclear export signals. Cell, 90(6), 1051-1060.
57 Fung, H. Y. J., & Chook, Y. M. (2014). Atomic basis of CRM1-cargo recognition, release and inhibition. Seminars in Cancer Biology, 27, 52-61.
58 Fung, H. Y. J., & Chook, Y. M. (2014). Atomic basis of CRM1-cargo recognition, release and inhibition. Seminars in Cancer Biology, 27, 52-61.
59 Furumoto, H., Ying, H., Chandramouli, G. V. R., Zhao, L., Walker, R. L., Meltzer, P. S., . . . Cheng, S. (2005). An unliganded thyroid hormone beta receptor activates the cyclin D1/cyclin-dependent kinase/retinoblastoma /E2F pathway and induces pituitary tumorigenesis. Molecular and Cellular Biology, 25(1), 124-135.
60 Gerace L. and Burke B. (1988) Functional organization of the nuclear envelope. Annu. Rev. Cell. Biol. 4: 335–374.
61 Gereben B, Zavacki AM, Ribich S, Kim BW, Huang SA, Simonides WS, Zeöld A, Bianco AC. 2008. Cellular and molecular basis of deiodinase-regulated thyroid hormone signaling. Endocr Rev 29:898–938
62 Glass CK, Rosenfeld MG. 2000. The coregulator exchange in transcriptional functions of nuclear receptors. Genes Dev 14: 121–141.
63 Gontan, C., Güttler, T., Engelen, E., Demmers, J., Fornerod, M., Grosveld, F. G., . . . Rottier, R. J. (2009). Exportin 4 mediates a novel nuclear import pathway for sox family transcription factors. The Journal of Cell Biology, 185(1), 27-34.
64 Görlich, D., Seewald, M. J., & Ribbeck, K. (2003). Characterization of ran-driven cargo transport and the RanGTPase system by kinetic measurements and computer simulation. The EMBO Journal, 22(5), 1088-1100.
65 Grespin, M. E., Bonamy, G. M. C., Roggero, V. R., Cameron, N. G., Adam, L. E., Atchison, A. P., . . . Allison, L. A. (2008). Thyroid hormone receptor alpha1 follows a cooperative CRM1/calreticulin-mediated nuclear export pathway. The Journal of Biological Chemistry, 283(37), 25576-25588.
66 Grimm, D. (2009). Small silencing RNAs: State-of-the-art. Advanced Drug Delivery Reviews, 61(9), 672-703.
67 Gronemeyer H, Moras D. (1995). Nuclear receptors. How to finger DNA. Nature 375:190 –191.
68 Grünwald, M., Lazzaretti, D., & Bono, F. (2013). Structural basis for the nuclear export activity of Importin13. The EMBO Journal, 32(6), 899-913.
69 Gruss, O. J., Carazo-Salas, R., Schatz, C. A., Guarguaglini, G., Kast, J., Wilm, M., . . . Mattaj, I. W. (2001). Ran induces spindle assembly by reversing the inhibitory effect of importin alpha on TPX2 activity. Cell, 104(1), 83-93.
70 Gudleski, N., Flanagan, J. M., Ryan, E. P., Bewley, M. C., & Parent, L. J. (2010). Directionality of nucleocytoplasmic transport of the retroviral gag protein depends on sequential binding of karyopherins and viral RNA.

Proceedings of the National Academy of Sciences of the United States of America, 107(20), 9358-9363.
71 Haddow, J. E., Cleary-Goldman, J., McClain, M. R., Palomaki, G. E., Neveux, L. M., Lambert-Messerlian, G., . . . First- and Second-Trimester Risk of Aneuploidy (FaSTER), Research Consortium. (2010). Thyroperoxidase and thyroglobulin antibodies in early pregnancy and preterm delivery. Obstetrics and Gynecology, 116(1), 58-62.
72 Hahm, J. B., Schroeder, A. C., & Privalsky, M. L. (2014). The two major isoforms of thyroid hormone receptor, TRα1 and TRβ1, preferentially partner with distinct panels of auxiliary proteins. Molecular and Cellular Endocrinology, 383(1-2), 80-95.
73 Hall, R. A. (2005). Co-immunoprecipitation as a strategy to evaluate receptor-receptor or receptor-protein interactions. G protein coupled receptor–protein interactions. Wiley, New Jersey, USA, 165-178.
74 Hartong R, wang N, Kurokawa R, Lazar MA, Glass CK, Apriletti Jw, Dillmann wH (1994) Delineation of three different thyroid hormone-response elements in promoter of rat sarcoplasmic reticulum Ca2 + ATPase gene. Demonstration that retinoid X receptor binds 5 to thyroid hormone receptor in response element 1. J Biol Chem 269(17):13021–13029.
75 Heese, K., Yamada, T., Akatsu, H., Yamamoto, T., Kosaka, K., Nagai, Y., & Sawada, T. (2004). Characterizing the new transcription regulator protein p60TRP. Journal of Cellular Biochemistry, 91(5), 1030-1042.
76 Henikoff, S., & Henikoff, J. G. (1992). Amino acid substitution matrices from protein blocks. Proceedings of the National Academy of Sciences of the United States of America, 89(22), 10915-10919.
77 Herold, A., Truant, R., Wiegand, H., & Cullen, B. R. (1998). Determination of the functional domain organization of the importin alpha nuclear import factor. The Journal of Cell Biology, 143(2), 309-318.
78 Hikunguwo, S., Brethauer, S., Nirujogi, V., Pitt, T., Udomsawaengsup, S., Chand, B., & Schauer, P. (2007). Influence of obesity and surgical weight loss on thyroid hormone levels. Surgery for Obesity and Related Diseases : Official Journal of the American Society for Bariatric Surgery, 3(6), 631-5.
79 Hochstrasser M., Mathog D., Gruenbaum Y., Saumweber H. and Sedat J.W. (1986) Spatial organization of chromosomes in the salivary gland nuclei of Drosophila melanogaster. J. Cell Biol. 102: 112–123.
80 Holaska J. M., Wilson K. L. and Mansharamani M. (2002) The nuclear envelope, lamins and nuclear assembly. Curr. Opin. Cell Biol. 14: 357–364.
81 Horlein, A.J., Naar, A.M., Heinzel, T., Torchia, J., Gloss, B., Kurokawa, R., Ryan, A., Kamei, Y., Soderstrom, M., Glass, C.K., et al., (1995). Ligand-independent repression by the thyroid hormone receptor mediated by a nuclear receptor co-repressor. Nature 377, 397–404.
82 Hu, X., Lazar, M.A., (1999). The CoRNR motif controls the recruitmentof corepressors by nuclear hormone receptors. Nature 402, 93–96.

83 Huber, B. R., Desclozeaux, M., West, B. L., Cunha-Lima, S., Nguyen, H. T., Baxter, J. D., . . . Fletterick, R. J. (2003). Thyroid hormone receptor-beta mutations conferring hormone resistance and reduced corepressor release exhibit decreased stability in the N-terminal ligand-binding domain. Molecular Endocrinology (Baltimore, Md.), 17(1), 107-116.
84 Hutchison, C. J., Alvarez-Reyes, M., & Vaughan, O. A. (2001). Lamins in disease: Why do ubiquitously expressed nuclear envelope proteins give rise to tissue-specific disease phenotypes? Journal of Cell Science, 114, 9-19.
85 Hutvagner, G., & Simard, M. J. (2008). Argonaute proteins: Key players in RNA silencing. Nature Reviews.Molecular Cell Biology, 9(1), 22-32.
86 Incerpi, S., De Vito, P., Luly, P., Spagnuolo, S., & Leoni, S. (2002). Short-term effects of thyroid hormones and 3,5-diiodothyronine on membrane transport systems in chick embryo hepatocytes. Endocrinology, 143(5), 1660-1668.
87 Jackson, R. J., Hellen, C. U. T., & Pestova, T. V. (2010). The mechanism of eukaryotic translation initiation and principles of its regulation. Nature Reviews.Molecular Cell Biology, 11(2), 113-127.
88 Jäkel, S., & Görlich, D. (1998). Importin beta, transportin, RanBP5 and RanBP7 mediate nuclear import of ribosomal proteins in mammalian cells. The EMBO Journal, 17(15), 4491-4502.
89 Jäkel, S., Mingot, J., Schwarzmaier, P., Hartmann, E., & Görlich, D. (2002). Importins fulfil a dual function as nuclear import receptors and cytoplasmic chaperones for exposed basic domains. The EMBO Journal, 21(3), 377-386.
90 Jäkel, S., Mingot, J., Schwarzmaier, P., Hartmann, E., & Görlich, D. (2002). Importins fulfil a dual function as nuclear import receptors and cytoplasmic chaperones for exposed basic domains. The EMBO Journal, 21(3), 377-386.
91 Jäkel, S., Mingot, J., Schwarzmaier, P., Hartmann, E., & Görlich, D. (2002). Importins fulfil a dual function as nuclear import receptors and cytoplasmic chaperones for exposed basic domains. The EMBO Journal, 21(3), 377-386.
92 Kelley, J. B., Talley, A. M., Spencer, A., Gioeli, D., & Paschal, B. M. (2010). Karyopherin alpha7 (KPNA7), a divergent member of the importin alpha family of nuclear import receptors. BMC Cell Biology, 11, 63.
93 Kim, Y., Geiger, J. H., Hahn, S., & Sigler, P. B. (1993). Crystal structure of a yeast TBP/TATA-box complex. Nature, 365(6446), 512-520.
94 Klieverik, L. P., Janssen, S. F., van Riel, A., Foppen, E., Bisschop, P. H., Serlie, M. J., . . . Kalsbeek, A. (2009). Thyroid hormone modulates glucose production via a sympathetic pathway from the hypothalamic paraventricular nucleus to the liver. Proceedings of the National Academy of Sciences of the United States of America, 106(14), 5966-5971.
95 Kobe, B. (1999). Autoinhibition by an internal nuclear localization signal revealed by the crystal structure of mammalian importin alpha. Nature Structural Biology, 6(4), 388-397.
96 Köhler, M., Ansieau, S., Prehn, S., Leutz, A., Haller, H., & Hartmann, E. (1997). Cloning of two novel human importin-alpha subunits and analysis of the

expression pattern of the importin-alpha protein family. FEBS Letters, 417(1), 104-108.

97 Köhler, M., Speck, C., Christiansen, M., Bischoff, F. R., Prehn, S., Haller, H., . . . Hartmann, E. (1999). Evidence for distinct substrate specificities of importin alpha family members in nuclear protein import. Molecular and Cellular Biology, 19(11), 7782-7791.

98 Kojima, K., Kornblau, S. M., Ruvolo, V., Dilip, A., Duvvuri, S., Davis, R. E., . . . Andreeff, M. (2013). Prognostic impact and targeting of CRM1 in acute myeloid leukemia. Blood, 121(20), 4166-4174.

99 Kortvely, E., Burkovics, P., Varszegi, S., & Gulya, K. (2005). Cloning and characterization of rat importin 9: Implication for its neuronal function. Brain Research.Molecular Brain Research, 139(1), 103-114.

100 Kosugi, S., Hasebe, M., Tomita, M., & Yanagawa, H. (2008). Nuclear export signal consensus sequences defined using a localization-based yeast selection system. Traffic (Copenhagen, Denmark), 9(12), 2053-2062.

101 Kurisaki, A., Kurisaki, K., Kowanetz, M., Sugino, H., Yoneda, Y., Heldin, C., & Moustakas, A. (2006). The mechanism of nuclear export of Smad3 involves exportin 4 and ran. Molecular and Cellular Biology, 26(4), 1318-1332.

102 Kutay, U., Bischoff, F. R., Kostka, S., Kraft, R., & Görlich, D. (1997). Export of importin alpha from the nucleus is mediated by a specific nuclear transport factor. Cell, 90(6), 1061-1071.

103 Laurila, E., Vuorinen, E., Savinainen, K., Rauhala, H., & Kallioniemi, A. (2014). KPNA7, a nuclear transport receptor, promotes malignant properties of pancreatic cancer cells in vitro. Experimental Cell Research, 322(1), 159-167.

104 Lazar MA. (1993). Thyroid hormone receptors: multiple forms, multiple possibilities. Endocr Rev.;14(2):184 –193.

105 Lee MS, Kliewer SA, Provencal J, Wright PE, Evans RM. (1993). Structure of the retinoid X receptor alpha DNA binding domain: a helix required for homodimeric DNA binding. Science 260:1117–1121.

106 Lee, B. J., Cansizoglu, A. E., Süel, K., E., Louis, T. H., Zhang, Z., & Chook, Y. M. (2006). Rules for nuclear localization sequence recognition by karyopherin beta 2. Cell, 126(3), 543-558.

107 Lee, K. C., Li, J., Cole, P. A., Wong, J., & Kraus, W. L. (2003). Transcriptional activation by thyroid hormone receptor-beta involves chromatin remodeling, histone acetylation, and synergistic stimulation by p300 and steroid receptor coactivators. Molecular Endocrinology (Baltimore, Md.), 17(5), 908-922.

108 Lee, S. J., Jiko, C., Yamashita, E., & Tsukihara, T. (2011). Selective nuclear export mechanism of small RNAs. Current Opinion in Structural Biology, 21(1), 101-108.

109 Leonard, J. L., & Farwell, A. P. (1997). Thyroid hormone-regulated actin polymerization in brain. Thyroid: Official Journal of the American Thyroid Association, 7(1), 147-151.

110 Leslie, D. M., Zhang, W., Timney, B. L., Chait, B. T., Rout, M. P., Wozniak, R. W., & Aitchison, J. D. (2004). Characterization of karyopherin cargoes reveals unique mechanisms of Kap121p-mediated nuclear import. Molecular and Cellular Biology, 24(19), 8487-8503.

111 Lin, D. H., Stuwe, T., Schilbach, S., Rundlet, E. J., Perriches, T., Mobbs, G., . . . Hoelz, A. (2016). Architecture of the symmetric core of the nuclear pore. Science (New York, N.Y.), 352(6283), 1.

112 Lin, H., Cody, V., Davis, F. B., Hercbergs, A. A., Luidens, M. K., Mousa, S. A., & Davis, P. J. (2011). Identification and functions of the plasma membrane receptor for thyroid hormone analogues. Discovery Medicine, 11(59), 337-347.

113 Lin, K.H., Parkison, C., McPhie, P., Cheng, S.Y., (1991). An essential role of domain D in the hormone-binding activity of human beta 1 thyroid hormone nuclear receptor. Mol. Endocrinol. 5, 485–492.

114 Lin, W., Ye, W., Cai, L., Meng, X., Ke, G., Huang, C., . . . Tao, T. (2009). The roles of multiple importins for nuclear import of murine aristaless-related homeobox protein. The Journal of Biological Chemistry, 284(30), 20428-20439.

115 Linke, M., Jordans, S., Mach, L., Herzog, V., & Brix, K. (2002). Thyroid stimulating hormone upregulates secretion of cathepsin B from thyroid epithelial cells. Biological Chemistry, 383(5), 773-784.

116 Lipowsky, G., Bischoff, F. R., Schwarzmaier, P., Kraft, R., Kostka, S., Hartmann, E., . . . Görlich, D. (2000). Exportin 4: A mediator of a novel nuclear export pathway in higher eukaryotes. The EMBO Journal, 19(16), 4362-4371.

117 Liu, J., Carmell, M. A., Rivas, F. V., Marsden, C. G., Thomson, J. M., Song, J., . . . Hannon, G. J. (2004). Argonaute2 is the catalytic engine of mammalian RNAi. Science (New York, N.Y.), 305(5689), 1437-1441.

118 Liu, X., Bushnell, D. A., Wang, D., Calero, G., & Kornberg, R. D. (2010). Structure of an RNA polymerase II-TFIIB complex and the transcription initiation mechanism. Science (New York, N.Y.), 327(5962), 206-209.

119 Lubert, E. J., & Sarge, K. D. (2003). Interaction between protein phosphatase 2A and members of the importin beta superfamily. Biochemical and Biophysical Research Communications, 303(3), 908-913.

120 Mangelsdorf DJ, Thummel C, Beato M, Herrlich P, Schutz G, Umesono K, Blumberg B, Kastner P, Mark M, Chambon P, et al. 1995. The nuclear receptor superfamily: The second decade. Cell 83: 835–839.

121 Mansourian, A. R. (2011). Metabolic pathways of tetraidothyronine and triidothyronine production by thyroid gland: A review of articles. Pakistan Journal of Biological Sciences: PJBS, 14(1), 1-12.

122 Marshall W.F. (2002) Order and disorder in the nucleus. Curr. Biol. 12: R185–R192.

123 Mason, D. A., Stage, D. E., & Goldfarb, D. S. (2009). Evolution of the metazoan-specific importin alpha gene family. Journal of Molecular Evolution, 68(4), 351-365.

124 Mavinakere, M. S., Powers, J. M., Subramanian, K. S., Roggero, V. R., & Allison, L. A. (2012). Multiple novel signals mediate thyroid hormone receptor nuclear import and export. The Journal of Biological Chemistry, 287(37), 31280-31297.

125 McDonnell, J. M., Fushman, D., Cahill, S. M., Zhou, W., Wolven, A., Wilson, C. B., . . . Cowburn, D. (1998). Solution structure and dynamics of the bioactive retroviral M domain from Rous sarcoma virus. Journal of Molecular Biology, 279(4), 921-928.

126 Mingot, J. M., Kostka, S., Kraft, R., Hartmann, E., & Görlich, D. (2001). Importin 13: A novel mediator of nuclear import and export. The EMBO Journal, 20(14), 3685-3694.

127 Mingot, J., Bohnsack, M. T., Jäkle, U., & Görlich, D. (2004). Exportin 7 defines a novel general nuclear export pathway. The EMBO Journal, 23(16), 3227-3236.

128 Monecke, T., Güttler, T., Neumann, P., Dickmanns, A., Görlich, D., & Ficner, R. (2009). Crystal structure of the nuclear export receptor CRM1 in complex with Snurportin1 and RanGTP. Science (New York, N.Y.), 324(5930), 1087-1091.

129 Moore, M. S., & Blobel, G. (1993). The GTP-binding protein Ran/TC4 is required for protein import into the nucleus. Nature, 365(6447), 661-663.

130 Moran, C., Agostini, M., Visser, W. E., Schoenmakers, E., Schoenmakers, N., Offiah, A. C., . . . Chatterjee, K. K. (2014). Resistance to thyroid hormone caused by a mutation in thyroid hormone receptor (TR)α1 and TRα2: Clinical, biochemical, and genetic analyses of three related patients. The Lancet.Diabetes & Endocrinology, 2(8), 619-626.

131 Moroianu, J., Blobel, G., & Radu, A. (1996). The binding site of karyopherin alpha for karyopherin beta overlaps with a nuclear localization sequence. Proceedings of the National Academy of Sciences of the United States of America, 93(13), 6572-6576.

132 Mosammaparast, N., Del Rosario, B., C., & Pemberton, L. F. (2005). Modulation of histone deposition by the karyopherin kap114. Molecular and Cellular Biology, 25(5), 1764-1778.

133 Mühlhäusser, P., Müller, E.C., Otto, A., & Kutay, U. (2001). Multiple pathways contribute to nuclear import of core histones. EMBO Reports, 2(8), 690-696.

134 Mühlhäusser, P., Müller, E.C., Otto, A., & Kutay, U. (2001). Multiple pathways contribute to nuclear import of core histones. EMBO Reports, 2(8), 690-696.

135 Murray, A. B., & Davies, H. G. (1979). Three-dimensional reconstruction of the chromatin bodies in the nuclei of mature erythrocytes from the newt Triturus cristatus: The number of nuclear envelope-attachment sites. Journal of Cell Science, 35, 59-66.

136 Nachury, M. V., Maresca, T. J., Salmon, W. C., Waterman-Storer, C., Heald, R., & Weis, K. (2001). Importin beta is a mitotic target of the small GTPase ran in spindle assembly. Cell, 104(1), 95-106.
137 Nakai, K., & Horton, P. (1999). PSORT: A program for detecting sorting signals in proteins and predicting their subcellular localization. Trends in Biochemical Sciences, 24(1), 34-36.
138 Nakamura, T., Arai, Y., Umehara, H., Masuhara, M., Kimura, T., Taniguchi, H., . . . Nakano, T. (2007). PGC7/Stella protects against DNA demethylation in early embryogenesis. Nature Cell Biology, 9(1), 64-71.
139 Nascimento, A. S., Dias, S. M. G., Nunes, F., Aparício, R., Ambrosio, A. L. B., Bleicher, L., . . . Polikarpov, I. (2006). Structural rearrangements in the thyroid hormone receptor hinge domain and their putative role in the receptor function. Journal of Molecular Biology, 360(3), 586-598.
140 Navarrete-Ramírez, P., Luna, M., Valverde-R, C., & Orozco, A. (2014). 3,5-di-iodothyronine stimulates tilapia growth through an alternate isoform of thyroid hormone receptor β1. Journal of Molecular Endocrinology, 52(1), 1-9.
141 Nicoll, J. B., Gwinn, B. L., Iwig, J. S., Garcia, P. P., Bunn, C. F., & Allison, L. A. (2003). Compartment-specific phosphorylation of rat thyroid hormone receptor alpha1 regulates nuclear localization and retention. Molecular and Cellular Endocrinology, 205(1-2), 65-77.
142 Noske, A., Weichert, W., Niesporek, S., Röske, A., Buckendahl, A., Koch, I., . . . Denkert, C. (2008). Expression of the nuclear export protein chromosomal region maintenance/exportin 1/Xpo1 is a prognostic factor in human ovarian cancer. Cancer, 112(8), 1733-1743.
143 Oetting, A., & Yen, P. M. (2007). New insights into thyroid hormone action. Best Practice & Research.Clinical Endocrinology & Metabolism, 21(2), 193-208.
144 Okada, C., Yamashita, E., Lee, S. J., Shibata, S., Katahira, J., Nakagawa, A., . . . Tsukihara, T. (2009). A high-resolution structure of the pre-microRNA nuclear export machinery. Science (New York, N.Y.), 326(5957), 1275-1279.
145 Okada, N., Ishigami, Y., Suzuki, T., Kaneko, A., Yasui, K., Fukutomi, R., & Isemura, M. (2008). Importins and exportins in cellular differentiation. Journal of Cellular and Molecular Medicine, 12(5), 1863-1871.
146 Onde, I., Paniagua, R., Zamora, J., Blánquez, M.J., Fraile, B., Ruiz, A., & Arenas, M. I. (2006). Influence of thyroid hormone receptors on breast cancer cell proliferation. Annals of Oncology: Official Journal of the European Society for Medical Oncology / ESMO, 17(1), 60-64.
147 O'Reilly, A., J., Dacks, J. B., & Field, M. C. (2011). Evolution of the karyopherin-β family of nucleocytoplasmic transport factors; ancient origins and continued specialization. PloS One, 6(4), 1.
148 Padmakumar, V. C., Abraham, S., Braune, S., Noegel, A. A., Tunggal, B., Karakesisoglou, I., & Korenbaum, E. (2004). Enaptin, a giant actin-binding

protein, is an element of the nuclear membrane and the actin cytoskeleton. Experimental Cell Research, 295(2), 330-339.

149 Panté, N., & Kann, M. (2002). Nuclear pore complex is able to transport macromolecules with diameters of about 39 nm. Molecular Biology of the Cell, 13(2), 425-434.

150 Pappa, T., Ferrara, A. M., & Refetoff, S. (2015). Inherited defects of thyroxine-binding proteins. Best Practice & Research. Clinical Endocrinology & Metabolism, 29(5), 735-747.

151 Park, S. H., Park, T. J., & Lim, I. K. (2011). Reduction of exportin 6 activity leads to actin accumulation via failure of RanGTP restoration and NTF2 sequestration in the nuclei of senescent cells. Experimental Cell Research, 317(7), 941-954.

152 Pascual A, Aranda A. (2013). Thyroid hormone receptors, cell growth and differentiation. Biochim Biophys Acta. 1830(7):3908 –3916.

153 Pawson, T., & Nash, P. (2003). Assembly of cell regulatory systems through protein interaction domains. Science (New York, N.Y.), 300(5618), 445-452.

154 Pemberton, L. F., Blobel, G., & Rosenblum, J. S. (1998). Transport routes through the nuclear pore complex. Current Opinion in Cell Biology, 10(3), 392-399.

155 Picard, D., & Yamamoto, K. R. (1987). Two signals mediate hormone-dependent nuclear localization of the glucocorticoid receptor. The EMBO Journal, 6(11), 3333-3340.

156 Pilo, A., Iervasi, G., Vitek, F., Ferdeghini, M., Cazzuola, F., & Bianchi, R. (1990). Thyroidal and peripheral production of 3,5,3'-triiodothyronine in humans by multicompartmental analysis. The American Journal of Physiology, 258(4), E715-E726.

157 Plafker, S. M., & Macara, I. G. (2002). Ribosomal protein L12 uses a distinct nuclear import pathway mediated by importin 11. Molecular and Cellular Biology, 22(4), 1266-1275.

158 Plafker, S. M., Plafker, K. S., Weissman, A. M., & Macara, I. G. (2004). Ubiquitin charging of human class III ubiquitin-conjugating enzymes triggers their nuclear import. The Journal of Cell Biology, 167(4), 649-659.

159 Ploski, J. E., Shamsher, M. K., & Radu, A. (2004). Paired-type homeodomain transcription factors are imported into the nucleus by karyopherin 13. Molecular and Cellular Biology, 24(11), 4824-4834.

160 Ploski, J. E., Shamsher, M. K., & Radu, A. (2004). Paired-type homeodomain transcription factors are imported into the nucleus by karyopherin 13. Molecular and Cellular Biology, 24(11), 4824-4834.

161 Pumroy, R. A., & Cingolani, G. (2015). Diversification of importin-α isoforms in cellular trafficking and disease states. The Biochemical Journal.

162 Pumroy, R. A., Ke, S., Hart, D. J., Zachariae, U., & Cingolani, G. (2015). Molecular determinants for nuclear import of influenza A PB2 by importin α isoforms 3 and 7. Structure (London, England: 1993), 23(2), 374-384.

163 Purves D, Augustine GJ, Fitzpatrick D, et al., (2001). editors. Neuroscience. 2nd edition. Sunderland (MA): Sinauer Associates; Receptor Types.

164 Quan, Y., Ji, Z., Wang, X., Tartakoff, A. M., & Tao, T. (2008). Evolutionary and transcriptional analysis of karyopherin beta superfamily proteins. Molecular & Cellular Proteomics: MCP, 7(7), 1254-1269.

165 Rastinejad F, Perlmann T, Evans RM, Sigler PB. (1995). Structural determinants of nuclear receptor assembly on DNA direct repeats. Nature 375:203–211.

166 Razin S.V., Petrov A., Hair A. and Vassetzky Y. S. (2004) Chromatin domains and territories: flexibly rigid. Crit. Rev. Eukaryot. Gene Expr. 14: 79–88.

167 Ribeiro MO, Carvalho SD, Schultz JJ, Chiellini G, Scanlan TS, Bianco AC, Brent GA (2001) Thyroid hormone–sympathetic interaction and adaptive thermogenesis are thyroid hormone receptor isoform-specific. J Clin Invest 108: 97–105.

168 Roggero, V. R., Zhang, J., Parente, L. E., Doshi, Y., Dziedzic, R. C., McGregor, E. L., Allison, L. A. (2016). Nuclear import of the thyroid hormone receptor α1 is mediated by importin 7, importin β1, and adaptor importin α1. Molecular and Cellular Endocrinology, 419, 185-197.

169 Rosenfeld, M.G., Glass, C.K., (2001). Coregulator codes of transcriptionalregulation by nuclear receptors. J. Biol. Chem. 276, 36865–36868.

170 Rout M. P. and Aitchison J. D. (2001) The nuclear pore complex as a transport machine. J. Biol. Chem. 276: 16593–16596.

171 Rout, M. P., & Aitchison, J. D. (2001). The nuclear pore complex as a transport machine. The Journal of Biological Chemistry, 276(20), 16593-16596.

172 Sadow, P. M., Chassande, O., Koo, E. K., Gauthier, K., Samarut, J., Xu, J., . . . Weiss, R. E. (2003). Regulation of expression of thyroid hormone receptor isoforms and coactivators in liver and heart by thyroid hormone. Molecular and Cellular Endocrinology, 203(1-2), 65-75.

173 Saijou, E., Itoh, T., Kim, K., Iemura, S., Natsume, T., & Miyajima, A. (2007). Nucleocytoplasmic shuttling of the zinc finger protein EZI is mediated by importin-7-dependent nuclear import and CRM1-independent export mechanisms. The Journal of Biological Chemistry, 282(44), 32327-32337.

174 Schapira, M., Raaka, B. M., Das, S., Fan, L., Totrov, M., Zhou, Z., . . . Samuels, H. H. (2003). Discovery of diverse thyroid hormone receptor antagonists by high-throughput docking. Proceedings of the National Academy of Sciences of the United States of America, 100(12), 7354-7359.

175 Sekimoto, T., Imamoto, N., Nakajima, K., Hirano, T., & Yoneda, Y. (1997). Extracellular signal-dependent nuclear import of Stat1 is mediated by nuclear pore-targeting complex formation with NPI-1, but not Rch1. The EMBO Journal, 16(23), 7067-7077.

176 Senese, R., Cioffi, F., de Lange, P., Goglia, F., & Lanni, A. (2014). Thyroid: Biological actions of 'nonclassical' thyroid hormones. The Journal of Endocrinology, 221(2).
177 Sever, R., & Glass, C. K. (2013). Signaling by nuclear receptors. Cold Spring Harbor Perspectives in Biology, 5(3), 1.
178 Shen, A., Wang, Y., Zhao, Y., Zou, L., Sun, L., & Cheng, C. (2009). Expression of CRM1 in human gliomas and its significance in p27 expression and clinical prognosis. Neurosurgery, 65(1), 153-9; discussion 159-60.
179 Siebrasse, J. P., & Peters, R. (2002). Rapid translocation of NTF2 through the nuclear pore of isolated nuclei and nuclear envelopes. EMBO Reports, 3(9), 887-92.
180 Song, J., Smith, S. K., Hannon, G. J., & Joshua-Tor, L. (2004). Crystal structure of argonaute and its implications for RISC slicer activity. Science (New York, N.Y.), 305(5689), 1434-1437.
181 Soniat, M., & Chook, Y. M. (2015). Nuclear localization signals for four distinct karyopherin-β nuclear import systems. The Biochemical Journal, 468(3), 353-362.
182 Sorokin, A. V., Kim, E. R., & Ovchinnikov, L. P. (2007). Nucleocytoplasmic transport of proteins. Biochemistry.Biokhimiia, 72(13), 1439-1457.
183 Stark, G. R., Kerr, I. M., Williams, B. R., Silverman, R. H., & Schreiber, R. D. (1998). How cells respond to interferons. Annual Review of Biochemistry, 67, 227-264.
184 Stewart, M. (2007). Molecular mechanism of the nuclear protein import cycle. Nature Reviews.Molecular Cell Biology, 8(3), 195-208.
185 Structural, G. C., China Structural, G. C., Northeast Structural, G. C., Gräslund, S., Nordlund, P., Weigelt, J., . . . Gunsalus, K. C. (2008). Protein production and purification. Nature Methods, 5(2), 135-146.
186 Stüven, T., Hartmann, E., & Görlich, D. (2003). Exportin 6: A novel nuclear export receptor that is specific for profilin. actin complexes. The EMBO Journal, 22(21), 5928-5940.
187 Subramanian, K. S., Dziedzic, R. C., Nelson, H. N., Stern, M. E., Roggero, V. R., Bondzi, C., & Allison, L. A. (2015). Multiple exportins influence thyroid hormone receptor localization. Molecular & Cellular Endocrinology, 411: 86-96.
188 Suntharalingam, M., & Wente, S. R. (2003). Peering through the pore: Nuclear pore complex structure, assembly, and function. Developmental Cell, 4(6), 775-789.
189 Tagami T, Kopp P, Johnson W, Arseven OK, Jameson JL. (1998). The thyroid hormone receptor variant 2 is a weak antagonist becauseitis deficientininteractionswith nuclear receptor corepressors. Endocrinology. 139(5):2535–2544.
190 Takeda, S., Fujiwara, T., Shimizu, F., Kawai, A., Shinomiya, K., Okuno, S., . . . Hirai, Y. (1997). Isolation and mapping of karyopherin alpha 3 (KPNA3), a human gene that is highly homologous to genes encoding xenopus importin,

yeast SRP1 and human RCH1. Cytogenetics and Cell Genetics, 76(1-2), 87-93.

191 Tao, T., Lan, J., Lukacs, G. L., Haché, R., J.G., & Kaplan, F. (2006). Importin 13 regulates nuclear import of the glucocorticoid receptor in airway epithelial cells. American Journal of Respiratory Cell and Molecular Biology, 35(6), 668-680.

192 Taylor, S. C., Berkelman, T., Yadav, G., & Hammond, M. (2013). A defined methodology for reliable quantification of western blot data. Molecular Biotechnology, 55(3), 217-226.Thuestad, G., Kraus, I., Apriletti, J., & Saatcioglu, F. (2000). The N-terminal domain of thyroid hormone receptor-alpha is required for its biological activities. DNA and Cell Biology, 19(7), 389-399.

193 Tian, H., Mahajan, M. A., Wong, C. T., Habeos, I., & Samuels, H. H. (2006). The N-terminal A/B domain of the thyroid hormone receptor-beta2 isoform influences ligand-dependent recruitment of coactivators to the ligand-binding domain. Molecular Endocrinology (Baltimore, Md.), 20(9), 2036-2051.

194 Tinnikov A, Nordstrom K, Thoren P, Kindblom JM, Malin S, Rozell B, Adams M, Rajanayagam O, Pettersson S, Ohlsson C, Chatterjee K, Vennstrom B (2002) Retardation of post-natal development caused by a negatively acting thyroid hormone receptor alpha1. EMBO J 21: 5079–5087.

195 Towbin, H., Staehelin, T., & Gordon, J. (1979). Electrophoretic transfer of proteins from polyacrylamide gels to nitrocellulose sheets: procedure and some applications. Proceedings of the National Academy of Sciences of the United States of America, 76(9), 4350–4354.

196 Van, D. G. (2014). Analysis of protein-protein interactions by coimmunoprecipitation. Methods in Enzymology, 541, 35-47.

197 Wada, A., Fukuda, M., Mishima, M., & Nishida, E. (1998). Nuclear export of actin: A novel mechanism regulating the subcellular localization of a major cytoskeletal protein. The EMBO Journal, 17(6), 1635-1641.

198 Wagner, R. L., Apriletti, J. W., McGrath, M. E., West, B. L., Baxter, J. D., & Fletterick, R. J. (1995). A structural role for hormone in the thyroid hormone receptor. Nature, 378(6558), 690-697.

199 Waldmann, I., Wälde, S., & Kehlenbach, R. H. (2007). Nuclear import of c-jun is mediated by multiple transport receptors. The Journal of Biological Chemistry, 282(38), 27685-27692.

200 Wang, Z., Rao, D. D., Senzer, N., & Nemunaitis, J. (2011). RNA interference and cancer therapy. Pharmaceutical Research, 28(12), 2983-2995.

201 Wawrzynska, L., Sakowicz, A., Rudzinski, P., Langfort, R., & Kurzyna, M. (2003). The conversion of thyroxine to triiodothyronine in the lung: Comparison of activity of type I iodothyronine 5' deiodinase in lung cancer with peripheral lung tissues. Monaldi Archives for Chest Disease = Archivio Monaldi Per Le Malattie Del Torace / Fondazione Clinica Del Lavoro, IRCCS [and] Istituto Di

Clinica Tisiologica e Malattie Apparato Respiratorio, Università Di Napoli, Secondo Ateneo, 59(2), 140-145.

202 Weinmann, L., Höck, J., Ivacevic, T., Ohrt, T., Mütze, J., Schwille, P., . . . Meister, G. (2009). Importin 8 is a gene silencing factor that targets argonaute proteins to distinct mRNAs. Cell, 136(3), 496-507.

203 Weis K. (2002) Nucleocytoplasmic transport: cargo trafficking across the border. Curr. Opin. Cell Biol. 14: 328–335.

204 Weis, K., Mattaj, I. W., & Lamond, A. I. (1995). Identification of hSRP1 alpha as a functional receptor for nuclear localization sequences. Science (New York, N.Y.), 268(5213), 1049-1053.

205 Wiese, C., Wilde, A., Moore, M. S., Adam, S. A., Merdes, A., & Zheng, Y. (2001). Role of importin-beta in coupling ran to downstream targets in microtubule assembly. Science (New York, N.Y.), 291(5504), 653-656.

206 Wikstrom L, Johansson C, Salto C, Barlow C, Campos BA, Baas F, Forrest D, Thoren P, Vennstrom B (1998) Abnormal heart rate and body temperature in mice lacking thyroid hormone receptor alpha 1. EMBO J 17: 455–461.

207 Williams GR. (2000). Cloning and characterization of two novel thyroid hormone receptor β isoforms. Mol Cell Biol. 20(22):8329 – 8342.

208 Wodrich, H., Cassany, A., D'Angelo, M., A., Guan, T., Nemerow, G., & Gerace, L. (2006). Adenovirus core protein pVII is translocated into the nucleus by multiple import receptor pathways. Journal of Virology, 80(19), 9608-9618.

209 Wohlwend, D., Strasser, A., Dickmanns, A., Doenecke, D., & Ficner, R. (2007). Thermodynamic analysis of H1 nuclear import: Receptor tuning of importinbeta/importin7. The Journal of Biological Chemistry, 282(14), 10707-10719.

210 Wolf, G. (2002). The regulation of the thyroid-stimulating hormone of the anterior pituitary gland by thyroid hormone and by 9-cis-retinoic acid. Nutrition Reviews, 60(11), 374-377.

211 Wu, Y., & Koenig, R. J. (2000). Gene regulation by thyroid hormone. Trends in Endocrinology and Metabolism: TEM, 11(6), 207-211.

212 Wurtz, J. M., Bourguet, W., Renaud, J. P., Vivat, V., Chambon, P., Moras, D., & Gronemeyer, H. (1996). A canonical structure for the ligand-binding domain of nuclear receptors.

213 Xu, D., Farmer, A., & Chook, Y. M. (2010). Recognition of nuclear targeting signals by karyopherin-β proteins. Current Opinion in Structural Biology, 20(6), 782-790.

214 Xu, D., Grishin, N. V., & Chook, Y. M. (2012). NESdb: A database of NES-containing CRM1 cargoes. Molecular Biology of the Cell, 23(18), 3673-3676.

215 Yehuda-Shnaidman, E., Kalderon, B., & Bar-Tana, J. (2014). Thyroid hormone, thyromimetics, and metabolic efficiency. Endocrine Reviews, 35(1), 35-58.

216 Yen PM, Ando S, Feng X, Liu Y, Maruvada P, Xia X (2006) Thyroid hormone action at the cellular, genomic and target gene levels. Mol Cell Endocrinol 246(1–2):121–127

217 Yen, P.M. (2001) Physiological and molecular basis of thyroid hormone action. Physiol. Rev. 81, 1097–1142.

218 Zaitseva, L., Cherepanov, P., Leyens, L., Wilson, S. J., Rasaiyaah, J., & Fassati, A. (2009). HIV-1 exploits importin 7 to maximize nuclear import of its DNA genome. Retrovirology, 6, 11.

219 Zamore, P. D., Tuschl, T., Sharp, P. A., & Bartel, D. P. (2000). RNAi: Double-stranded RNA directs the ATP-dependent cleavage of mRNA at 21 to 23 nucleotide intervals. Cell, 101(1), 25-33.

220 Zhang, F., Fan, Y., Mu, N., Zhao, J., Sun, F., Zhao, Z., . . . Wang, K. (2014). Exportin 4 gene expression and DNA promoter methylation status in chronic hepatitis B virus infection. Journal of Viral Hepatitis, 21(4), 241-250.

221 Zilliacus J, Wright AP, Carlstedt-Duke J, Gustafsson JA. (1995). Structural determinants of DNA-binding specificity by steroid receptors. Mol Endocrinol 9:389 – 400.